Sequence Stratigraphy, Provenance, Isotopic Composition, and Regional Correlation of the Upper Hornby Bay and Lower Dismal Lakes Groups, NWT and Nunavut

Katherine Hahn

A thesis submitted to the Faculty of Graduate and Postdoctoral Affairs in partial fulfillment of the requirements for the degree of

Master

In

Earth Sciences

Carleton University
Ottawa, Ontario

Your file Votre référence
ISBN: 978-0-494-79605-4
Our file Notre référence
ISBN: 978-0-494-79605-4

Abstract

Late Paleoproterozoic uraniferous basins of Canada's north including the Thelon, Athabasca, and Hornby Bay, can be broadly correlated based on similarities in age, sequence stratigraphy, paleocurrents and detrital zircon provenance. In this-drill core based study, detailed sequence stratigraphy was analyzed in the upper Hornby Bay (UHG) to lower Dismal Lakes groups (LDG) (Hornby Bay Basin, Nunavut). Sedimentary provenance was examined using Sm-Nd isotopes from siliciclastic mudstones and stable C and O isotopes were analyzed on carbonates within the Hornby Bay Group. Sequence stratigraphy identified a major unconformity between the Hornby Bay and Dismal Lakes Groups. Results from Sm-Nd analyses identified two important sources for sediment, the Thelon-Taltson Magmatic Zone (TMZ) and the Great Bear Magmatic Zone (GMZ). Stable isotopes are in the range of $\delta^{13}C$ between -1.5 ‰ and 0.5 ‰ VPDB, and were interpreted to represent a primary seawater value. Results from this study support the correlation of the Hornby Bay Basin with other Proterozoic basins within Canada. In particular, the Wernecke Supergroup of the Wernecke Mountains, Yukon is identified as the distal equivalent of the UHG and together they comprise a westward deepening intracratonic basin.

Acknowledgements

This thesis would not have been possible without the guidance and support of my supervisor Dr.Robert Rainbird. He has patiently helped me grow and develop as a researcher since the challenging days of my undergrad writing experience. I'd also like to thank him for accepting me back on as a M.Sc. student so that I could continue the research I began during my B.Sc. Financial support from an NSERC discovery grant awarded to Rob Rainbird made this research possible. I'd also like to thank Triex Minerals Corp. for their overwhelming support in providing me with samples for this project and summer employment. Without the help of Triex, the data could not have been obtained. I'd also like to thank Dr. Brian Cousens for helping me negotiate my way through two years at Carleton as my onsite supervisor and giving me a crash course in geochemistry. I could not have completed all of my lab work without the patient supervision and guidance provided by the staff at the G.G. Hatch Stable Isotope lab at the University of Ottawa. I must specifically thank Lizzy-Ann Spencer for all of her help during my Sm-Nd analyses. I'm very thankful to Dr. George Dix who provided me with insightful conversation and helped steer me in the right direction with my research. I could not have completed this thesis without the help and support from my fellow graduate students at Carleton University. Finally, I must mention my friends and family who provided me with much needed encouragement and support during my more stressful days.

Table of Contents

List of Tables

List of Figures

1.0 General Introduction

This research was undertaken with support from the Geological Survey of Canada's Geoscience for Energy and Minerals (GEM) Energy program. The purpose of the GEM project is to provide public geological information that will encourage exploration for minerals and energy in northern Canada. Rationale for this project was the general lack of useful geological information in Canada's north, specifically in the territories where adequate knowledge only exists for about one third of Nunavut. In the Hornby Bay Basin, Nunavut, renewed interest in uranium led to increased activity by the mineral exploration industry. The last major study completed on the basin involved detailed mapping by Ross and Kerans (1989), followed by a few smaller studies. The GEM program identified the Hornby Bay Basin, host to the Mountain Lake uranium deposit, as a good candidate for further research in the field of uranium mineralization and it became a component of the program.

Late Paleoproterozoic basins of Canada's north including the Thelon, Athabasca, and Hornby Bay, all host to uranium deposits, can be broadly correlated based on similarities in age, sequence stratigraphy, paleocurrents and detrital zircon provenance (Figure 1). This study is one of several ongoing GEM Energy projects designed to better understand the occurrence of uranium in Canadian Proterozoic basins (Jefferson, et al., 2009). This study contributes to the ongoing uranium exploration by: (i) providing the age and depositional setting of the uraniferous Hornby Bay Basin and (ii) correlating the Hornby Bay Basin with other Paleoproterozoic basins within Canada.

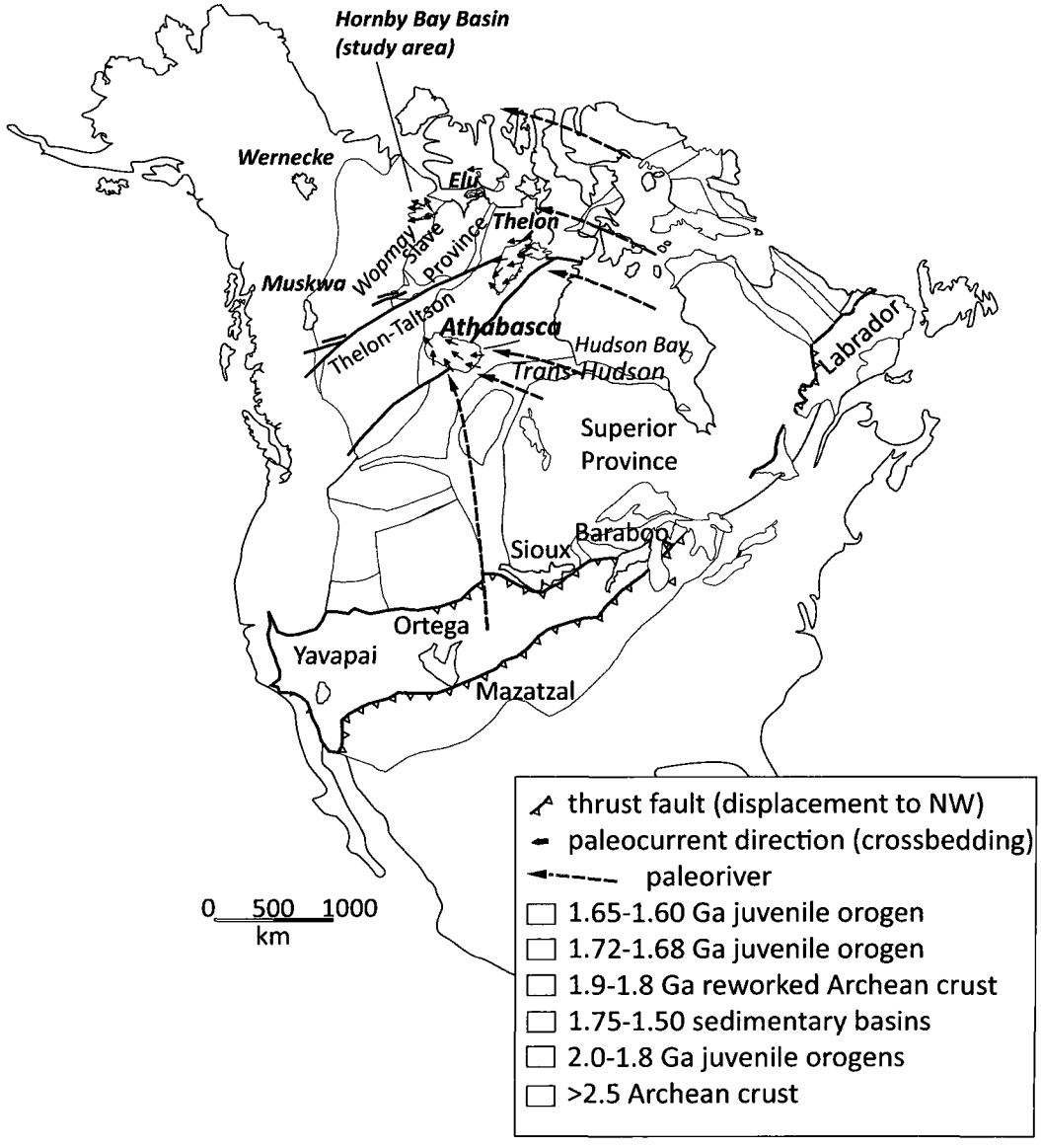

Figure 1.1: Modified from Rainbird and Young (2009). Generalized map of North America illustrating the extent of Laurentia and corresponding Paleoproterozoic basins

The Hornby Bay Basin is located along the Nunavut-Northwest Territories border north of Great Bear Lake (Figures 1 and 2). This basin contains two siliciclastic to carbonate sequences, the Hornby Bay Group and the Dismal Lakes Group, which are overlain by the laterally extensive Coppermine Flood Basalts (Figures 2 and 3). Detailed mapping by Ross and Kerans (1989) provided the stratigraphic and sedimentologic framework that forms the basis for this study, which focused on the upper Hornby Bay Group and the lower Dismal Lakes Group.

Fraser et al. (1970) and Young et al. (1979) suggested that the Wernecke Supergroup of the Wernecke Mountains, Yukon, may represent the distal, fine-grained deep-marine equivalent of the shallow-marine to terrestrial Hornby Bay strata by placing both groups within Proterozoic sequence A (~1.7 G.a. to ~ 1.2 Ga.). This relationship was further investigated and refined by Maclean and Cook (2004) through the interpretation of seismic data from the interior plains regions of northwestern Canada. The results of Maclean and Cook (2004) supported the original hypothesis of Young et al. (1979) but subdivided sequence A into subsequences (A1, A2, A3, A4), specifically linking subsequence A1 in the Hornby Bay Group to the Wernecke Supergroup of the northern Cordillera (Figure 1). Recent detrital zircon ages from the Wernecke Supergroup (Furlanetto et al., 2008) indicate that the age of the Wernecke Supergroup is close to 100 m.y. younger than previously hypothesized. Maclean and Cook (2004) used in the older age in their study, and one aim of this study is to re-examine the age connection between the two basins.

This study was centered around the Mountain Lake uranium deposit, located approximately 15 kms southwest of the southern arm of Dismal Lakes, Nunavut (Figure 2). Results are based on observations and samples from exploratory diamond drill holes drilled by Triex Minerals Corp. during the summer field seasons of 2007 and 2008. Detailed sequence stratigraphy in the Hornby Bay Basin was evaluated to be used in age comparisons and regional sequence correlations with other Proterozoic basins in Canada. U-Pb dating on detrital zircon from sandstones of the Hornby Bay Group was recently completed (Rainbird and Davis, 2009, unpublished). U-Pb dating on detrital zircon specifically records the felsic component of provenance. In this project, Sm-Nd was analyzed on mudrocks to evaluate both the mafic and felsic components of sediment, or average source region composition. Both methods of examining sediment provenance were used in a comparison with sediment provenance from the Wernecke Supergroup as a way to test the link between the two basins. The justification for this is that if there was a paleogeographic link at the time of deposition, then both areas could have received detrital material from common source regions. As a secondary test to the correlation of the two basins, stable C and O isotopes were measured on carbonate units within each basin based on the theory that carbonate precipitated from a common oceanic source will exhibit similar stable isotopic ratios.

2.0 Geologic Setting

Stratigraphy of the Hornby Bay Basin includes the Hornby Bay Group, Dismal Lakes Group, and Coppermine River Group, which unconformably overlie deformed

magmatic and supracrustal rocks of the Wopmay Orogen (Figure 1; Bowring and Grotzinger, 1992).

The Wopmay Orogen is Paleoproterozoic (~1.85 Ga) in age and consists of three tectonic elements; the Hottah Terrane, the Coronation Margin, and the Great Bear Magmatic Zone. Each of these terranes represent individual magmatic arcs accreted to the western margin of the Slave Craton (Bowring and Grotzinger, 1992). The orogen trends north and is cut by northwest- and northeast-trending faults that were later reactivated during deposition of the Hornby Bay Group. The Hornby Bay Basin mainly overlies the northern margin of the Great Bear Magmatic Zone, which contributed significant amounts of detritus to lower Hornby Bay Group (Ross, 1983).

The Leith Line is a north-south trending syndepositional structural hinge across which sedimentary units thicken to the west. It became active mid-way through deposition of the Hornby Bay Group and remained so during deposition of the unconformably overlying Dismal Lakes Group (Kerans, 1981). Ross (1983) noted that the location of the Leith Line corresponds with the western edge of the Great Bear Magmatic Zone and may represent a buried tectonic boundary within the Wopmay Orogen.

The Hornby Bay Group is approximately 3 km thick and directly overlies rocks of the Wopmay Orogen. The Hornby Bay Goup is composed of fluvial and eolian sandstones of the Big Bear and Fault River formations, passing up-section to shallow marine siliciclastic rocks (Lady Nye Formation), carbonate rocks (East River Formation), and deltaic mudrocks (Kaertok Formation) (Ross, 1983; refer to Figure 3). The Hornby

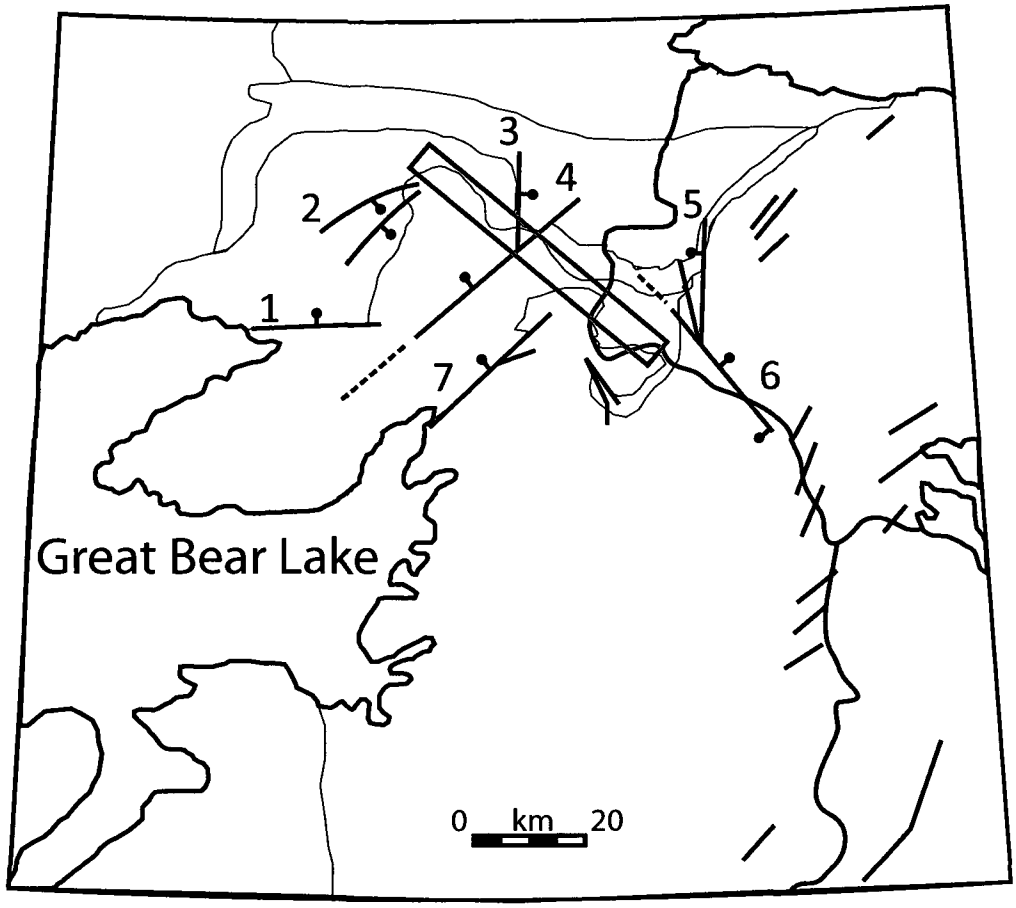

- Paleozoic Cover
- Neoproterozoic Rae Group
- Coppermine River Group
- Dismal Lakes Group
- Hornby Bay Group
- Great Bear Magmatic Zone
- Study Area

1. East River Fault Zone
2. Falcon Lake Fault
3. Herb Dixon Fault
4. Teshierpi Fault
5. Canoe Lake Fault
6. Sinister Fault
7. Fault River Fault

Figure 2: Location map showing general geology and study area. Modified from (Ross and Kerans, 1989)

Bay Group was subsequently uplifted and deformed during the Forward Orogeny before deposition of the Dismal Lakes Group (Cook and MacLean 1995).

The Dismal Lakes Group unconformably overlies the Hornby Bay Group and consists of terrestrial to shallow-marine siliciclastic rocks (LeRoux, Fort Confidence formations) which pass up-section into deeper water carbonate rocks (Dease Lake, Kendall River, Sulky, Greenhorn Lakes formations) (Kerans, 1981; Figure 3). The Hornby Bay and Dismal Lakes groups are intruded by diabase dykes, part of the Mackenzie Dyke Swarm (~1270 Ma) of the Mackenzie large igneous province. Thermal doming during emplacement of the Muskox Intrusion uplifted carbonates of the Dismal Lakes Group and caused the development of a karst which was buried by further carbonates, before the eruptive Coppermine Flood Basalts (~1270 Ma) ended deposition of the Dismal Lakes Group (Kerans, 1983).

3.0 Previous Work

3.1 Geochronology

The Hornby Bay Basin was previously broadly mapped by Donaldson (1969), Baragar and Donaldson (1973), and Cook and Aitken (1971) which produced two maps at 1: 250 000 scale. Ross (1983) and Kerans (1983) mapped the region in detail at variable scale, from 1:50 000 and 1:100 000 to 1:5000 in areas of good outcrop exposure (Ross and Kerans, 1989). They also defined the current formational names that this study is based on.

The age of the Hornby Bay basin is constrained by the Narakay Volcanic Complex, which occurs toward the top of the Hornby Bay Group, dated at approximately 1663 Ma (Bowring and Ross, 1985), and the Coppermine Flood Basalts at the top of the Dismal Lakes Group which has been dated at 1270 Ma (Baragar et al, 1996). The Western Channel Diabase, which cuts the Hornby Bay Group but is not present in the Dismal Lakes Group, is ~1590 Ma (Hamilton and Buchan 2010) and the Cleaver Dykes which only cut the lowermost Hornby Bay Group strata are ~1740 Ma (Irving and Hamilton, 2004). Recent U-Pb ages of detrital zircons are summarized in Figure 3.

The most recent work on Hornby Bay stratigraphy was completed by Cook and Maclean (1995) and Maclean and Cook (2004) who interpreted petroleum industry seismic profiles throughout north-western Canada, including strata of the Hornby Bay Group and their relationship to potentially correlative strata in the northern Cordillera. Maclean and Cook (2004) concluded that an unconformity between the Hornby Bay Group and Dismal Lakes Group should be placed between the LeRoux and Fort Confidence formations, contrary to Ross and Kerans (1989) who placed it between the Kaertok and LeRoux Formations. The location of this unconformity is important to understand the regional stratigraphy as the Mountain Lake Uranium deposit is hosted within the LeRoux Formation above the unconformity.

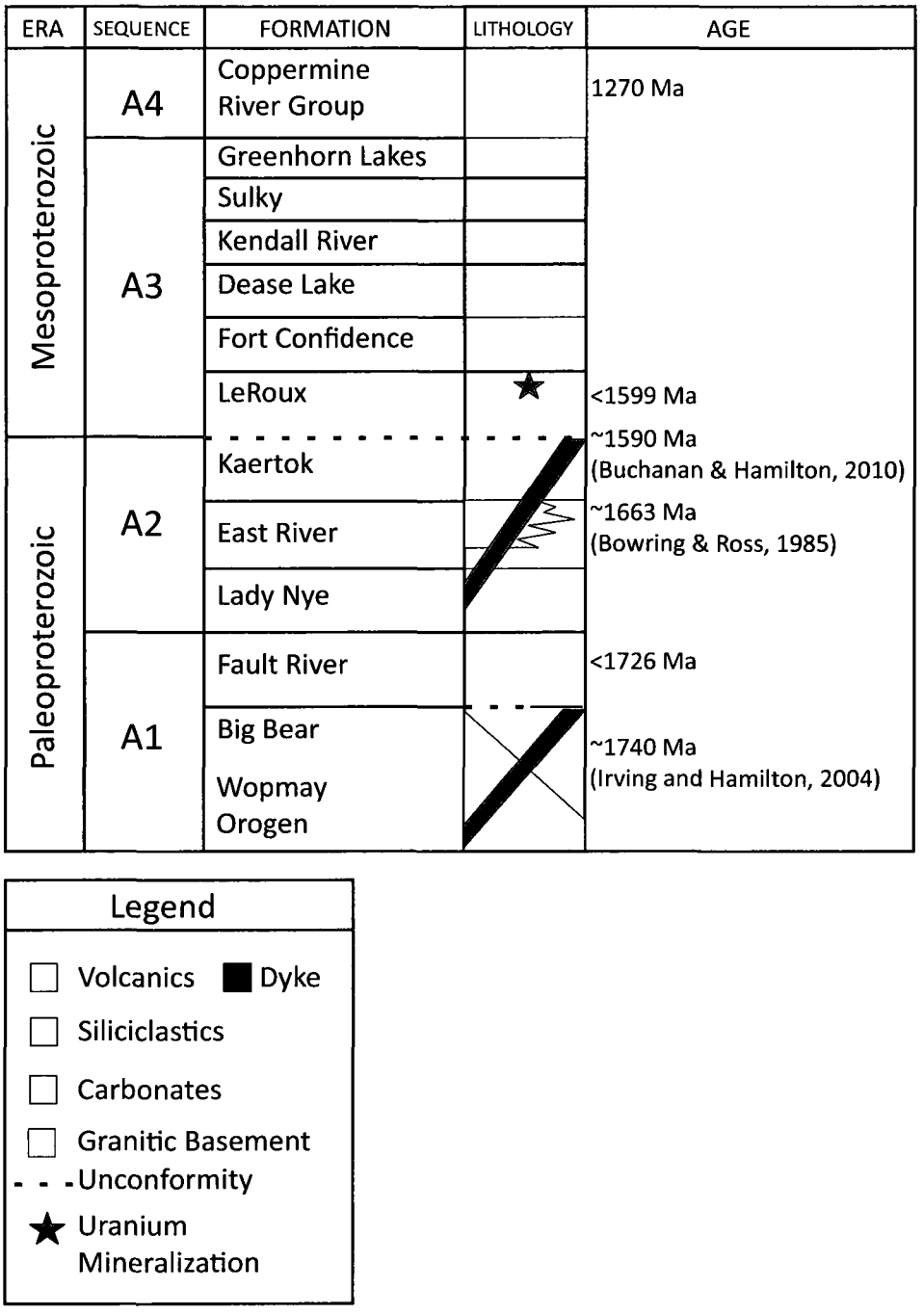

Figure 3: Stratigraphy and ages of the Hornby Bay Basin.

3.2 Lithostratigraphy of the Study Area

This study deals exclusively with the Upper Hornby Bay Group and Lower Dismal Lakes Group due to the availability and depth of penetration of exploration drill cores in the vicinity of the Mountain Lake Uranium deposit.

The lowermost strata observed are from the Lady Nye Formation, which conformably to unconformably overlies the Fault River and Big Bear formations (Figure 3), however this boundary was never intersected in drill core. It consists dominantly of arenite with minor conglomerate and mudstone and is up to 500m thick in some sections. Strata are interpreted to be generally fluvial sandstone at the base and shallow marine-deltaic at the top (Ross, 1983).

The East River Formation is dominantly dolostone with minor siliciclastic intervals and overlies the Lady Nye Formation and records a gradual marine transgression of a storm-dominated carbonate platform. It ranges in thickness from 100 to 200m (Ross, 1983).

The Kaertok Formation overlies the East River Formation and ranges in thickness from 0 to >400 m. It comprises mudstone to cross-bedded arenite recording development of a delta, with its geometry largely controlled by faulting (Ross, 1983).

The LeRoux Formation unconformably overlies the Kaertok Formation and other strata of the Hornby Bay Group where an angular unconformity is present. It ranges in thickness from 10 to >150 m and is dominantly composed of white quartz arenite. It records deposition in a fluvial to shallow-marine setting (Kerans, 1983).

The Fort Confidence Formation conformably overlies the LeRoux Formation and the full thickness was never intersected in drill core, however Kerans (1983) made an estimate of >200m based on outcrop. It is composed of interbedded wavy and lenticular-bedded sandstone and carbonaceous mudstones, which are interpreted to represent extensive tidal flat deposits.

4.0 Objectives

Within the current literature for the Hornby Bay Basin several outstanding questions exist and have been addressed in this study. Regarding the nature of the unconformity between the Hornby Bay Group and Dismal Lake Group, there are discrepancies concerning the type of boundary, where the boundary lies, and the length of the hiatus (Maclean and Cook, 2004; Ross and Kerans, 1989), and so sequence stratigraphy was used as a tool to interpret nature of the unconformity. Sequence stratigraphy is a useful correlation tool and was used to interpret regional depositional trends. The Mountain Lake uranium deposit is strata-bound at the contact between the Hornby Bay and Dismal Lakes groups so local interpretations of sequence stratigraphy may provide useful information for further uranium exploration within the basin. Deformation during deposition of the Hornby Bay Group and the LeRoux Formation is likely related to a regional orogenic event, the Forward Orogeny, which is proposed to be an extension of the Racklan Orogeny of the Wernecke Mountains (Cook and Maclean, 1995), but due to age discrepancies this relationship has not been confirmed. U-Pb ages from detrital zircon have helped refine depositional ages within the basin and

it, along with the Sm-Nd composition on interbedded mudrocks will constrain sediment provenance. There has been no stable (C and O) isotope study completed on the East River Formation so a detailed study has been completed as a means of chemostratigraphic correlation with the Wernecke Supergroup.

5.0 Depositional Setting

The following lithofacies interpretations are based on observations logs from drill core, limited outcrop mapping, and limited outcrop photos, provided by G.M. Ross.

5.1 Facies Association 1: Sand-bed Braided Stream

Lithofacies Description

Fine- to coarse-grained, trough cross-stratified sandstone occurs in bedsets ranging between 0.5-10 m thick. Beds of disperssed pebbly sandstones, up to 10 cm thick, and mudrock clasts are common at the base of cross-stratified units and upward-fining bedsets. Cross-bedding is common, but bedding is commonly obscured by leisegang bands (Figure 4a) in thick intervals (>10 m), which are also interpreted to be cross-bedded based on similarities in grain size. Mud clasts and pebbly layers are present throughout these intervals.

Medium-grained, ripple cross-laminated sandstone was observed at a single locale and overlies trough cross-bedded sandstone (Figure 4b).

Mudstone beds are parallel-laminated or massive and occur at the top of upward-fining successions and range in thickness from 5-10 cm (Figure 4c). Parallel-

bedded, fine- to medium-grained sandstone is associated with trough crossbedded facies.

Rare interbeds, <1m thick, of massive, clast-supported conglomerate are present in beds <1m thick (Figure 4d). Clasts within conglomerate include rounded quartz cobbles or rounded sandstone boulders, on average 10cm in diameter. Conglomerates of the sand-bed braided stream facies association were not observed in outcrop and lateral continuity could not be established in drill core.

Facies Association	Formation	Lithofacies Present
1. Braided Stream	Lady Nye LeRoux	Trough cross-stratified sandstone Medium-grained ripple cross-stratified sandstone Parallel laminated and massive mudstone
2. Shallow Carbonate Platform	East River	Massive/parallel bedded siliciclastic and dolo-mudstone Massive/microbially laminated dolo-mudstone Packstone Grainstone Rudstone/Floatstone
3. Fluvial-dominated Delta	Kaertok	Trough cross-stratified sandstone Ripple-cross stratified sandstone Interstratified Mudrock/Siltstone
4. Alluvial Fan	LeRoux	Oligomict boulder conglomerate Monomict gravel conglomerate Coarse-grained sandstone Siliciclastic Mudstone
5. Lower to Upper Shoreface	LeRoux	Trough cross-stratified and parallel bedded fine- to coarse-grained sandstone
6. Tidal Flat	Fort Confidence	Interstratified mudrock/siltstone/fine-grained sandstone Trough cross-stratified sandstone

Table 1: Summary of facies associations and associated lithofacies

Figure 4: Outcrop and core photos of the braided fluvial and the platformal carbonate facies associations. a) Core photo showing pebble lag at the based of a fining-up sequence in the braided fluvial facies association, as well as leisegang banding, obscuring primary bedding features. Top to the left b) Current-ripples in fine-grained sadstone.

Figure 4 (continued): c) Mudrock interbed within the braided fluvial facies association, top to left. d) Basal conglomerate of braided fluvial facies association resting directly on granite of the Great Bear Magmatic Zone, top to left.

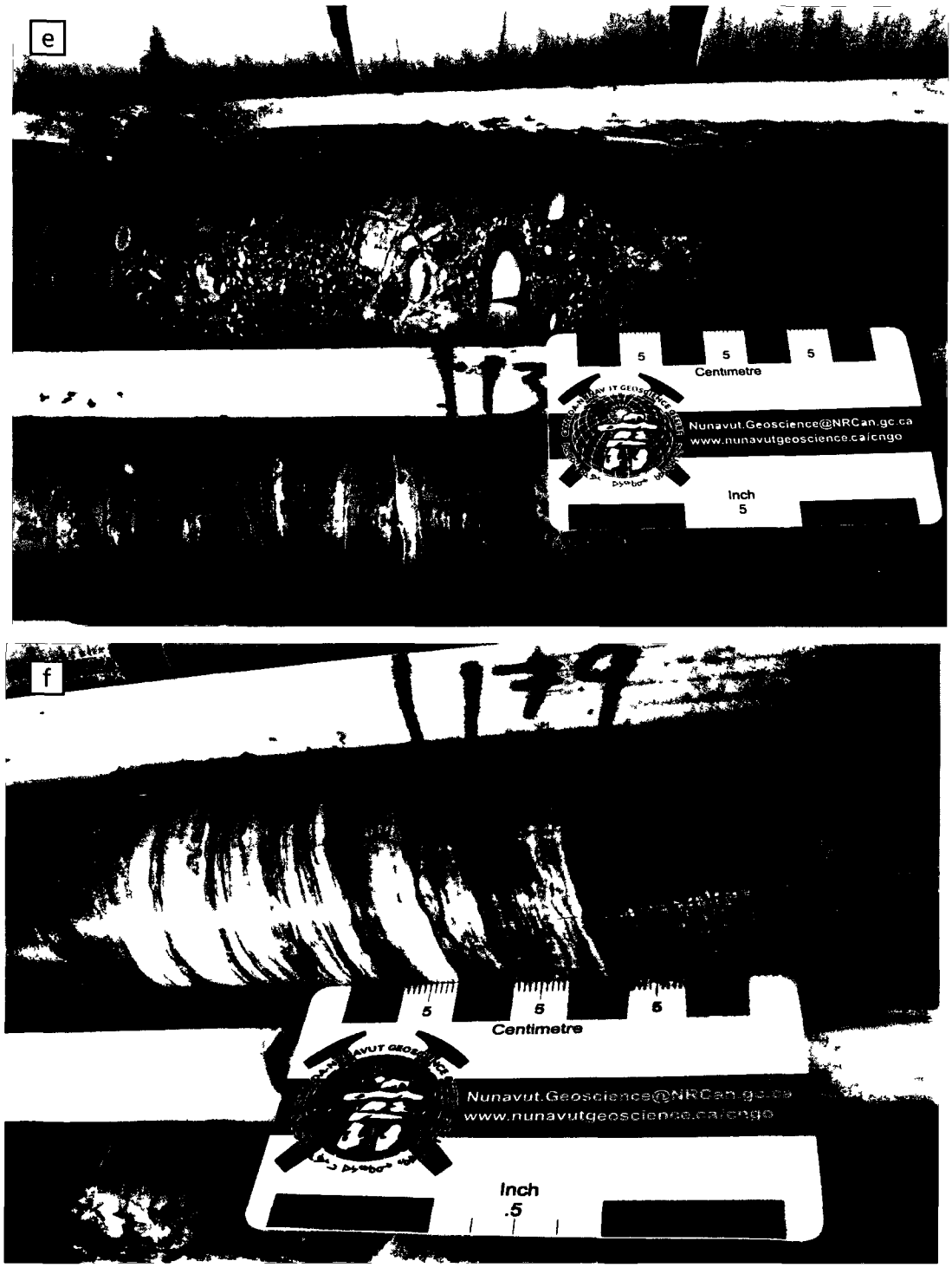

Figure 4 (continued): e) Intraclastic rudstone with a grainstone matrix within the platformal carbonate facies association, top to left. f) Microbiallly laminated dolo-mudstone within the platformal carbonate facies association, top to left.

Facies Successions

Upward-fining bedsets (0.5-10 m thick) are characterized by pebble lags and mud clasts at the base gradationally overlain by trough cross-stratified sandstone. Thick units of trough cross-stratified sandstone are commonly interstratified with parallel-bedded sandstone in sequences on the order of decimeters thick. Lateral facies associations were not established based on wide spacing of drill holes. Mud beds are associated with upward-fining sequences and lower flow regime deposits such as ripples and lower plane beds (Figure 8).

Lithofacies Interpretation

Trough cross-bedded sandstone represents deposition from migrating 3D subaqueous dunes (Ashley, 1990). Parallel-bedded sandstone is a common feature of sedimentation during upper-flow regime conditions although not exclusive to these conditions. Other sedimentary structures formed during upper-flow regime conditions such as current lineation was not observed in outcrop due to poor exposure and extensive lichen cover. The abundance of trough cross-stratified sandstone and parallel-bedded sandstone represent deposition in migrating channels in a braided-stream environment (Cant and Walker, 1978). Conglomerate and pebbly sandstone beds may represent deposition of a coarser sediment load at the bottom of a high-energy channel (Cant and Walker, 1978). Conglomerate-rich beds deposited at the base of high-energy

channels are inferred to grade laterally to sand-bed channels as stream energy decreases.

Mudstone beds represent deposition from suspension due to channel abandonment or and upward-fining bedsets represent deposition during waning flood flows. Mud clasts are characteristic of channel formation across previously deposited mud beds (Cant and Walker, 1978) (Refer to Figure 12a).

5.2 Facies Association 2: Shallow Carbonate Platform

Lithofacies Description

Massive to parallel-bedded mudrock is present in 5-50 cm thick beds, commonly interstratified with massive dolo-mudstone and locally interstratified with microbially laminated dolo-mudstone (Figure 4f). Thin (<1 cm) beds of fine-grained quartz arenite are present within some dolo-mudstone bedsets and are associated with overall higher detrital quartz contents within individual dolo-mudstone beds. Salt casts, mud cracks and fenestral porosity are rarely present in dolo-mudstone. Relict gypsum laths are locally observed.

Ooid packstones and grainstones (Figure 5a) are present in bedsets ranging from 1-10 m in thickness and commonly coarsen upwards into intraclastic rudstone and floatstone (Figure 9). Rudstone and floatstone are dominantly composed of sub-angular to sub-rounded clasts of micrite with an ooid grainstone matrix (Figure 4e). Rudstone and floatstone also contain a slightly higher siliciclastic component (up to 15%), which includes detrital quartz, muscovite, and zircon.

Authigenic chert is common throughout all lithofacies as void-fill cement, and as a recrystallization of primary framework components (mostly ooids). Partially intact stromatolites and oncoids are present in >1 m -thick beds. Laminated, domal, and digitate stomatolites were reported in outcrop by Ross (1983), in drill core stomatolite morphologies were difficult to distinguish (Figure 5b).

This facies association is described as syndepositional to the Narakay Volcanic Complex, interpreted as rhyolite domes and shallow marine tuff cones and localized tuff beds (<4 cm thick) were observed in drill core (Ross 1986).

Facies Successions

Dolomitic mudstones and siltstones are intimately associated as are grainstone and rudstone/floatstone. These typically occur as 1 m- to 10 m-thick packages interbedded with 1 m- to 10 m-thick packages of dolo-mudstone, representing alternating periods of low and high energy. High energy facies represent landward migration of seawater during storm surges, while low energy facies represent quiet water deposition where wave energy was greatly reduced due to the low angle of slope. Stromatolites are most common at the base of the observed sections and pass up-section into mudstones. Refer to Figure 9 for representative stratigraphic section.

Lithofacies Interpretation

Mudrocks and dolomudstones are interpreted to represent shallow-water, peritidal deposition along a broad, very gently sloping carbonate shelf. The presence of

salt casts and mudcracks indicate that this environment was periodically exposed and subject to evaporation. Rarely, greater influxes of siliciclastic material deposited mud, silt, and fine-grained sand in the quiet water environment. This material may have originated during periods of increased erosion, such as during particularly wet climatic conditions (Haines, 1988). Small asymmetric ripples observed in sand may represent uni-directional currents generated within small, low-energy tidal channels. Ooid grainstones were formed in the high-energy subtidal zone where wave action was strong. Intraclastic floatstone and rudstones represent tempestites, formed when storm surges ripped up the rapidly lithifying sea-floor and carried this material shore-ward (Scholle, 1983). Alternatively, intraclastic floatstone and rudstone may have been deposited as lags in the troughs of migrating ooid shoals, similar to modern processes occuring in the Bahamas (Dill, 1988). Regardless of the mechanism of deposition, the intraclastic floatstone and rudstone are of clear energetic subtidal origin. Digitate stromatolite bioherms observed by Ross (1983) suggest a clear subtidal origin while parallel-laminated stomatolites suggest an intertidal to supratidal origin (Figures 12c and 13a).

5.3 Facies Association 3: Fluvial-dominated Delta

Lithofacies Description

Red and green mudrock and siltstone are present in beds < 2 cm thick and are interstratified with beds of fine-grained sandstone > 5 cm thick, present in packages up to 10 m thick (Figure 5c). Mudrock commonly displays polygonal mud cracks and is

parallel bedded. Rare, < 5 cm thick, beds of fining up-sequences from medium-grained sandstone to mudrock were observed. In drill core rare ptygmatically folded, intersecting silty dikelets were observed in mudrock. Starved ripples and lenticular sandstone beds are common in outcrop. Lenticular, fine-grained sandstone beds commonly have scoured bases with abundant mud clasts at the base and are uncommonly normally graded.

Medium-grained sandstone is present in thicker beds (up to 1m) that are trough cross-stratified and interbedded with parallel-bedded, medium-grained sandstone (Figure 5d and 5e). Cross-bedsets range in size from 10-75 cm thick and display roughly west-directed orientations with high variance. Medium-grained sandstone commonly contains abundant clay matrix with a high percentage of angular grains. Poorly sorted, pebbly intervals occur sporadically, <15 cm thick, at the base of cross-bedded intervals.

Facies Successions

Interstratified siltstone, mudrock, and fine-grained sandstone occur together in thick (>10 m) packages. These are gradationally overlain by sandier intervals, where interstratified siltstone/mudrock/fine-grained sandstone packages gradually decrease in thickness to ~ 3m, and are capped by thick deposits of trough cross-stratified and parallel-bedded sandstone. This represents an upward-coarsening sequence on the scale of decameters (~40 m), which is repetitive throughout the facies association (Figure 5f). Lateral variation of this facies association is unknown due to limited drill

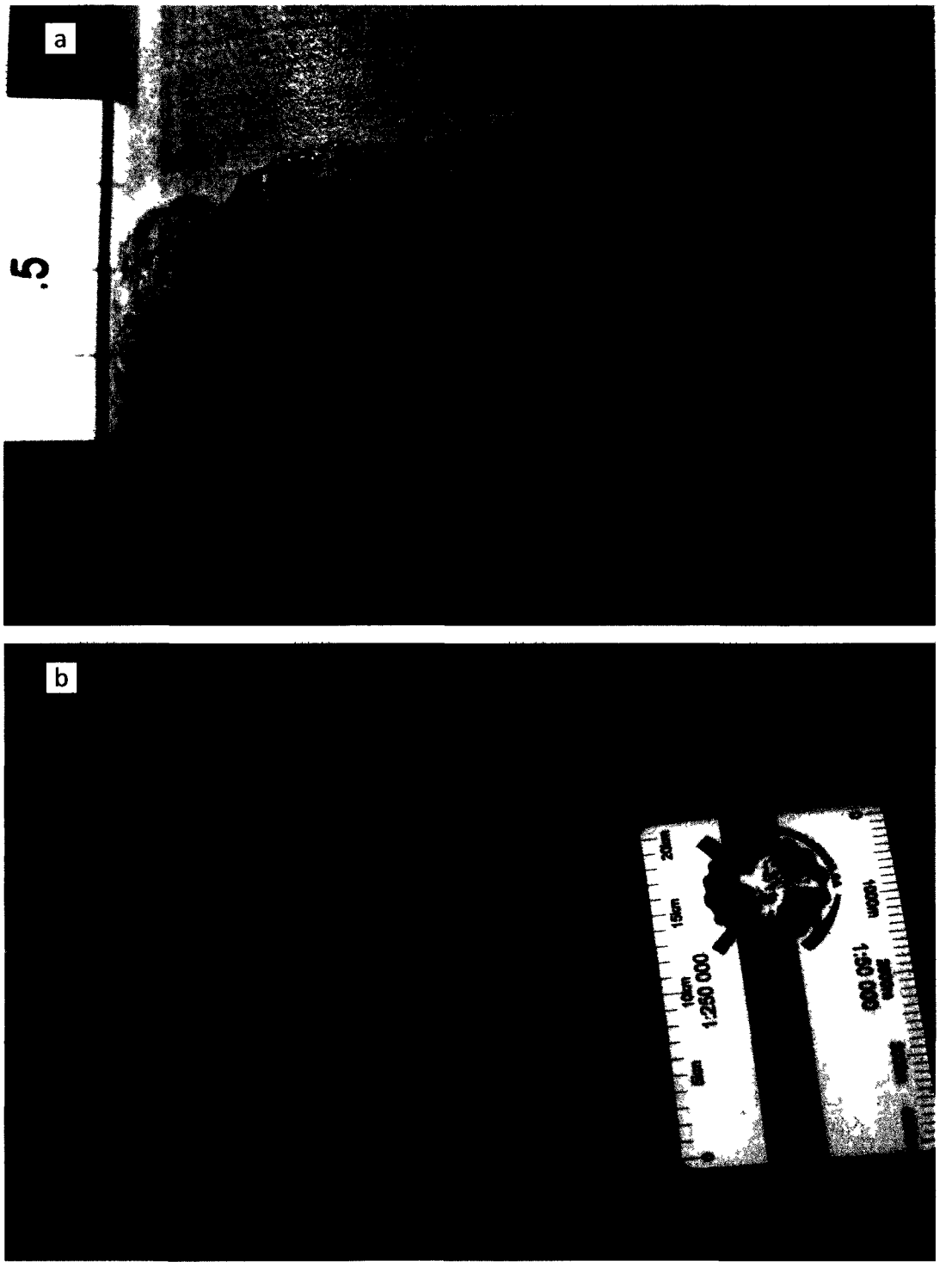

Figure 5: Outcrop and core photos of the East River and Kaertok formations. a) Ood grainstone, partially phosphatized, within the platformal carbonate facies association. b) Stromatolites in dolo-mudstone within the platformal carbonate facies association, top to the left.

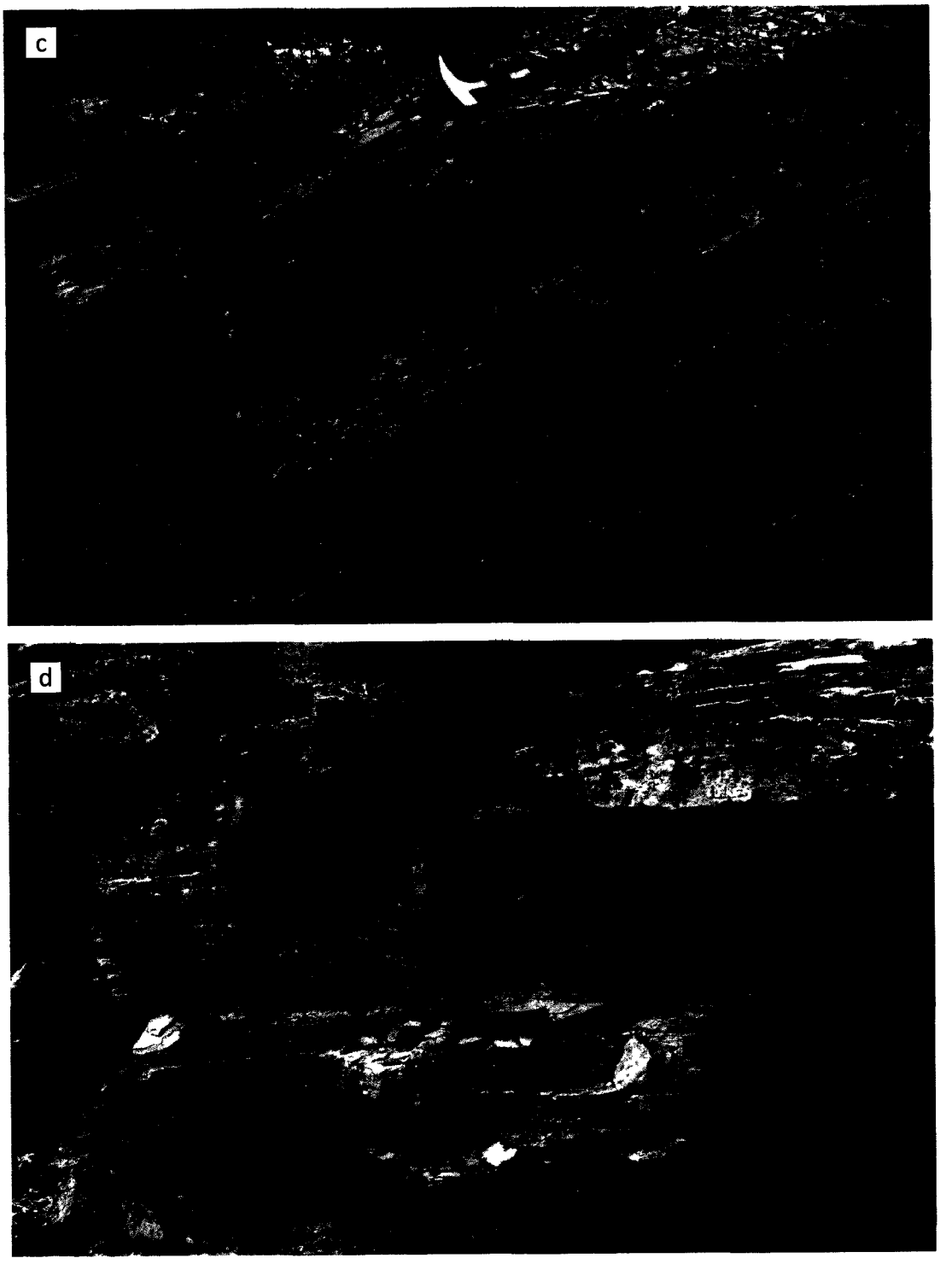

Figure 5 (continued): c) Lenticular bedded fine-grained sandstone interbedded with mudrock/siltstone of the fluvial-dominated delta facies association, hammer for scale. d) Parallel bedded medium-grained sandstone of the fluvial-dominated delta facies association, hammer for scale.

f

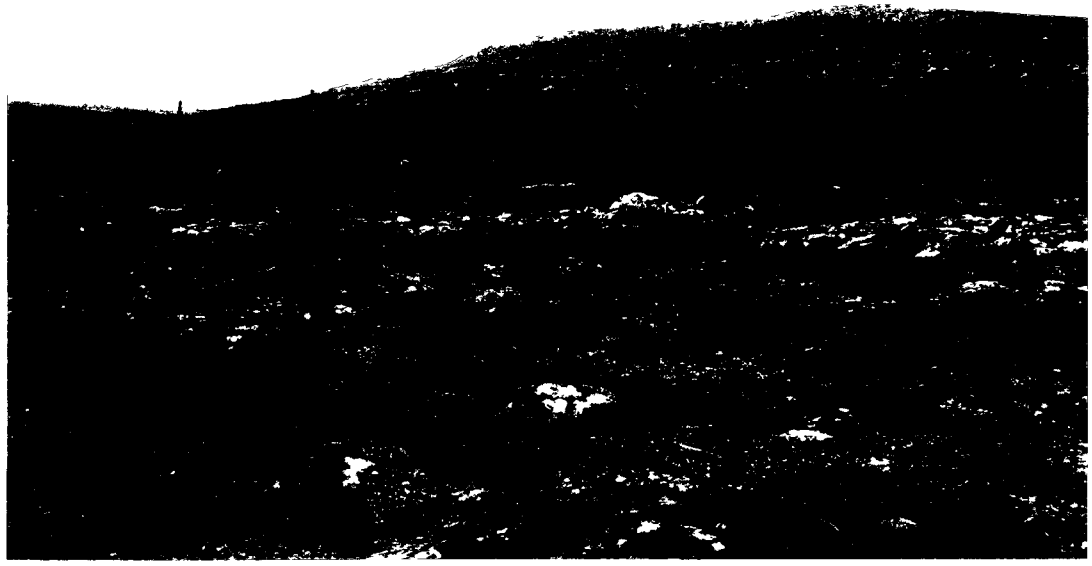

Figure 5 (continued): e) Trough cross-stratified sandstone in the fluvial-dominated delta facies association, hammer for scale (upper right). f) Two coarsening up sequences in outcrop with preferential weathering of fine-grained material in the fluvial-dominated delta facies association, small trees in background (upper left) for scale.

core availability and the facies association was only observed west of the Teshierpi fault zone (Figure 15) (Refer to Figure 10 for representative stratigraphic section).

Lithofacies Interpretation

Interstratified mudrock and siltstone with fine-grained sandstone represent alternating periods of suspension and traction deposition. Polygonal, vertically oriented mud cracks indicate a subaerial origin through desiccation. Ptygmatically folded dikelets are interpreted to be syneresis cracks of subaqueous origin (Gostin and Plummer, 1981). Mud cracks, lenticular bedding and starved ripples all suggest a tidally influenced environment (Dalrymple et al, 1990).

Medium-grained, trough cross-stratified sandstone represents deposition due to the migration of 3D dunes in a uni-directional flow (Ashley, 1990). Parallel-bedded sandstone may represent deposition during upper flow regime conditions, although current lineations were not observed.

The decameter-scale upward coarsening successions observed in this facies association are characteristic of a deltaic environment (Galloway, 1975). The fine-grained facies were deposited on the quiet water delta-plain, and thicker cross-bedded sandstone units were deposited within distributary channels, migrating throughout the delta. Upward coarsening packages record individual cycles of progradation and abandonment of a delta lobe (Galloway, 1975).

Ross (1983) noted a thin-bedded arenite facies, dominated by cross-bedded sandstone at the top of coarsening up sequences, which was interpreted to represent

reworked fluvial deposits following channel abandonment. Paleocurrents in this facies were strongly uni-modal broadly towards the east and originated via onshore-directed currents. Tidal-structures such as herringbone cross-stratification and lenticular and flaser bedding were observed by Ross (1983) in this facies, which indicates that onshore-directed currents may have been influenced by tidal-action.

The tidal-influenced nature of Ross's thin-bedded arenite facies overlying the distributary channel facies indicates that this delta was, in part, a tidally-influenced. The precense of massive beds of mudrock and siltstones, graded bedding, and the abundance of cross-bedding suggest a significant fluvial influnence on the delta as well (Galloway, 1975) (see Figure 13). A wave-dominated delta would include more wave-influenced sedimentary structures such as hummocky-cross stratification and would be more sand- than mud-rich (Galloway, 1975). The combination of fluvial-formed structures as well as rare tidal-formed structures suggests a characterization of the delta as a fluvial-dominated delta with minor tidal influence. A tide-dominated delta would exhibit a stronger facies association of tidally formed sedimentary structures such as tidal rhythmites and abundant flaser bedding (Galloway, 1975).

5.4 Facies Association 4: Alluvial Fan

Lithofacies Description

Oligomict, framework-supported, poorly to weakly sorted conglomerate contains boulder-sized, sub angular to sub-rounded clasts of sandstone and fault breccias (Figure 6a and 6b). Sheets of conglomerate were deposited along an angular unconformity in

weakly organized beds up to 5m thick that are laterally continuous for 10s to 100s of meters. Horizontal stratification is weakly developed in some conglomerate zones, but they are otherwise massive. Monomict, framework-supported, conglomerate is parallel-bedded and composed of quartz pebbles. Parallel-bedded, coarse-grained sandstone is present in beds up to 1 m thick. Thin, laterally discontinuous beds of mud-cracked mudstone are rarely present sharply above the boulder conglomerate facies.

Facies Successions

Beds of sandstone and gravel conglomerate commonly overlie and intertongue with one another and are closely associated with boulder conglomerate, which is regionally restricted to locations close to faults, presumed to be active during deposition. These deposits directly overlie a major erosional angular unconformity (Figure 15). In the vicinity of the Mountain Lake uranium deposit, boulder conglomerate was observed to grade laterally to very coarse-grained sandstone over a distance of ~1km. Conglomerate occurs in drill core but far spacing between drill holes does not allow sufficient resolution for correlation of individual beds (Figure 8). Mud-cracked mudrock was present in one locale directly overlying boulder conglomerate.

Lithofacies Interpretation

The clast-supported, poorly to weakly sorted sediment, and weakly stratified nature of the boulder conglomerate facies suggests a streamflow origin rather than a debris flow origin (Blair, 1999). Hadlari et al. (2000) describe a similar facies, interpreted

to have been deposited by unconfined, high-magnitude stream-flood flows. The weak stratification, lack of inverse grading, and erosional lower contacts of the boulder conglomerate facies are considered by Jo et al. (1997) to be streamflow characteristics which supports this interpretation.

Parallel-bedded, gravel conglomerate and coarse-grained sandstone are interpreted as lower energy streamflow deposits, either deposited in lower engery events, or as more distal deposits (Blair et al, 1999). Mud-cracked beds are of dessication origin and were deposited from suspension during waning-flow.

The combination of poorly-sorted boulder conglomerate, coarse-grained sandstone, and mud-cracked beds are similar to associations described by Blair et al. (2000) in various alluvial fans in Death Valley. One other environmental interpretation which fits closely with the facies association is that of a gravel-bed braided stream, however the lack of significant clast imbrications and poor sorting of the conglomerate, and the lack of significant fining up sequences supports the alluvial fan interpretation (Miall, 1977). Refer to Figure 13c for schematic block diagram.

5.5 Facies Association 5: Shoreface to Foreshore

Lithofacies Description

In drill core, medium to fine-grained, quartz arenite is massive with nearly all primary bedding features obscured due to pervasive silicification. Rarely, faint parallel bedding and cross bedding are preserved. In outcrop, multidirectional tabular and low-angle wedge sets of trough cross-bedding occur in beds up to 1 m thick. Outcrops show

a broad range in bedforms from symmetrical ripples, superposed ripples, horizontal lamination, and tabular and trough cross-stratification (Figure 6c to 6f). In one outcrop low domes (>50 cm in height, ~ 1m diameter) of supermature white quartz arenite were observed in plan view, internal stratification was not observed.

Facies Successions

Tabular cross beds, trough cross beds, and planar-laminated beds are interstratified in outcrop. In drill core, heavy silicification obscures almost all primary bedding features, however low-angle cross-bedding and parallel lamination are most prevalent. Parallel lamination is most abundant towards the top of the association. Refer to Figure 11 for representative stratigraphic section.

Lithofacies Interpretation

Symmetrical ripples are interpreted to have formed by oscillatory wave action. Large-scale trough-cross stratification represents migrating 3D dunes (Ashley, 1990). The strong multi-directional nature of the dunes represents multiple flow directions formed by wave action and wind-induced currents, interacting with fluvial currents at the mouth of braided streams. Parallel bedding can represent deposition in both the upper and lower flow regimes. The relationship with other high energy bedforms such as 3D dunes suggests that parallel bedding was deposited in the upper flow regime. Low sandstone domes may represent plan-view of hummocky cross-stratification (Walker and Plint, 1992).

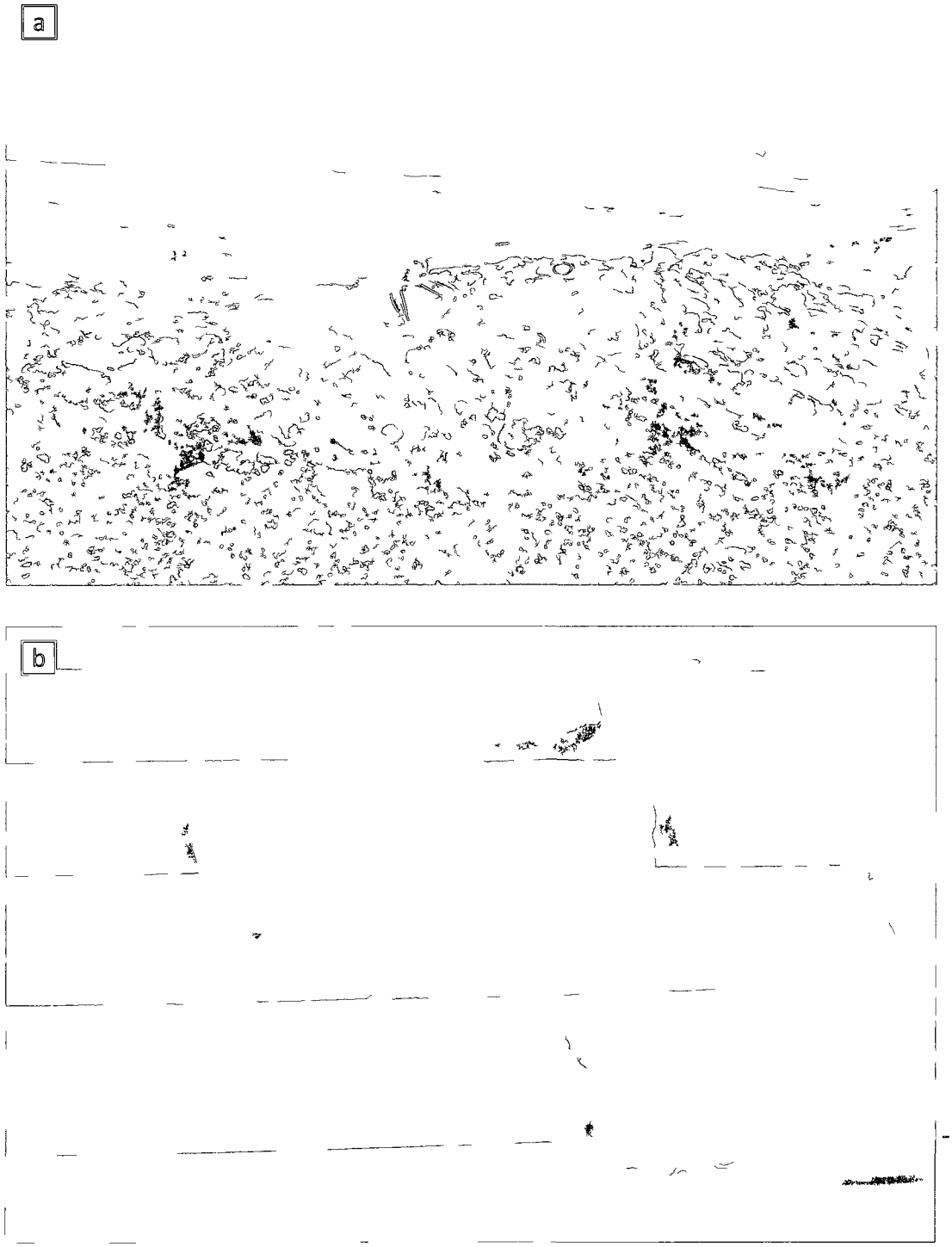

Figure 6: Outcrop and core photos of the LeRoux Formation. Photo credits for c-f, G.M. Ross. a) Polymict conglomerate of the alluvial fan facies association, compass for scale. d) Core photo of conglomerate above sub-aerial unconformity, interpreted alluvial fan facies association, top to the left.

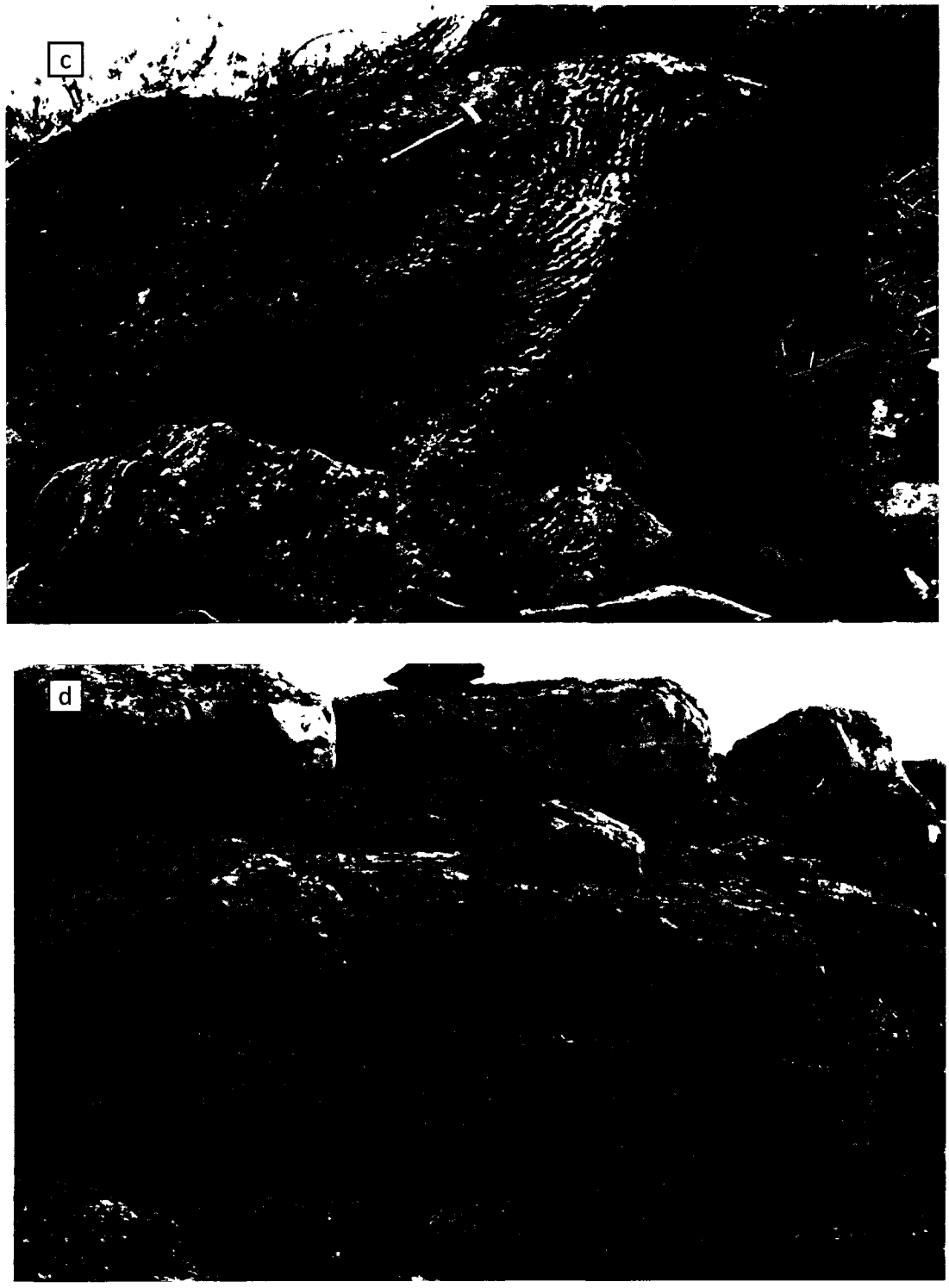

Figure 6 (continued): c) Interference wave ripples on frost heaved block of the LeRoux Formation, interpretted upper shoreface/foreshore facies association. Hammer for scale. d) Low-angle cross stratification in quartz arenite, upper shoreface facies association.

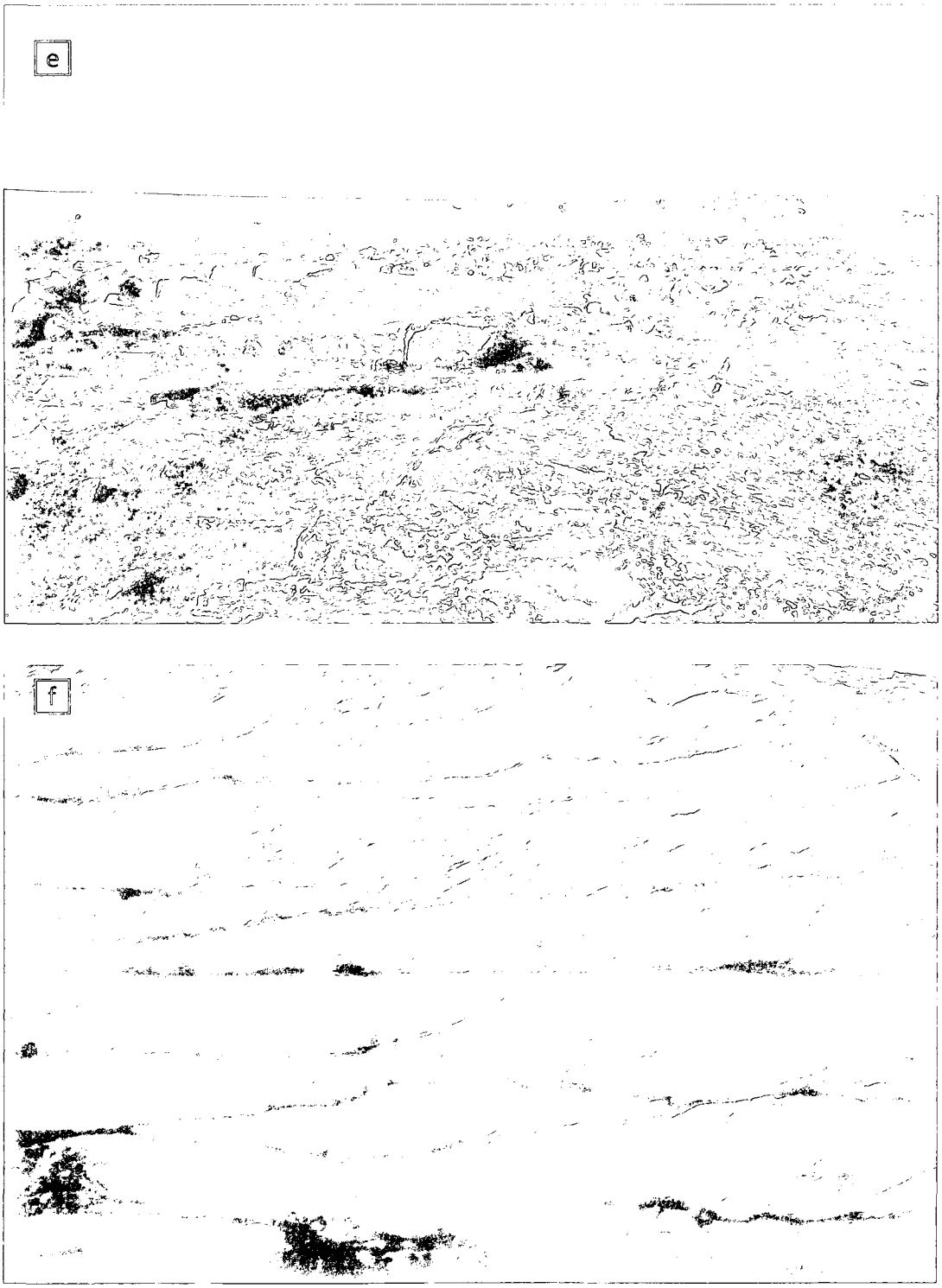

Figure 6 (continued): e) Large domes in heavily silicified quartz arenite, LeRoux Formation. Interpreted upper shoreface facies association. Potentially hummocky cross-stratification. f) Stacked cross-bed sets in the LeRoux Formation. Braided fluvial, or upper shoreface facies association. Pen cap for scale.

The combination of wave-formed ripples, multi-directional 3D dunes, and the presence of hummocky cross-stratification suggest deposition in a nearshore-marine environment. The super-mature nature of this sediment also supports a wave-dominated coastline where extensive re-working has occurred.

It is reasonable to state that this facies association covers a broad range from the lower shoreface to the foreshore. The presence of one locale where possible hummocky cross stratification was observed indicates that this sandy environment may have extended into lower shoreface (Walker and Plint, 1992). Refer to Figure 14a for schematic block diagram.

5.6 Facies Association 6: Tidal Flat

Lithofacies Description

Weakly carbonaceous mudrock is present in massive and parallel laminated layers ranging from < 1 cm to 5 cm thick (thick laminated to thin bedded). Ptygmatically folded shrinkage cracks are abundant throughout this lithology but are not always present (Figure 7b). Kerans (1983) noted the presence of polygonal mud cracks with curled edges. Slightly carbonaceous mudrock also is present as wispy laminations interstratified with fine-grained, grey quartz arenite and dark grey siltstone varying from flaser bedded to lenticular bedded (Figure 7d).

Light grey quartz arenite is fine-grained and is present in beds < 1cm to > 1 m in thickness. It is commonly parallel laminated but small-scale cross lamination is also

observed (Figure 7c). Mud rip-ups are dispersed throughout the quartz arenite. Dark grey siltstone is parallel laminated and present in beds from 1 cm to 5 cm thick.

Thicker units (> 1 m) of trough cross-stratified, medium-grained, bleached sandstone occur in intervals where overall sand:shale ratios are higher.

Facies Successions

Thick, sand-dominated intervals occur on a gradational scale with mud and silt dominated intervals and are more common towards the base of the facies association. Kerans (1983) noted that intervals of thinly interstratified mud, silt, and fine sand interfinger both laterally and vertically with thicker sand-dominated intervals. Coarser-grained sand beds are present in intervals throughout the facies association and Kerans (1983) noted that they pinch out laterally over 700-1000 m. These coarser-grained sandstones occur as lenses which are scour based and fine upwards. Refer to Figure 11 for representative stratigraphic section.

Lithofacies Interpretation

Interstratification of mud and sand with silt represent alternating periods of suspension and traction deposition, respectively (Quaresma et al, 2007). This type of stratification is common in tidal environments where sand is deposited during tidal ebb and flood events and mud and silt are deposited during slack water periods. Shrinkage cracks may have originated in two ways; as dessication cracks during periodic exposure, or subtidally as syneresis cracks. Keran's (1983) noted the presence of polygonal mud

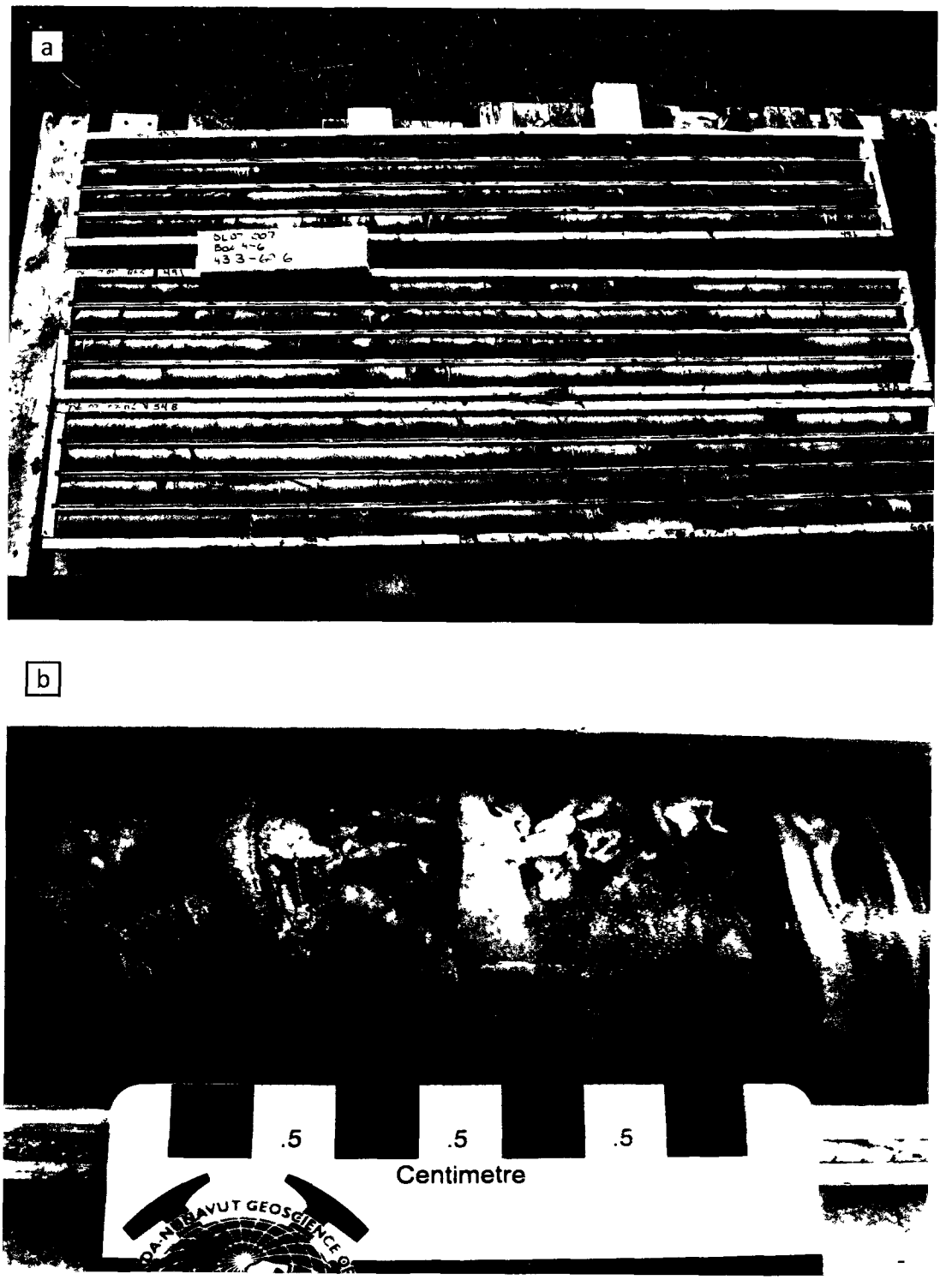

Figure 7: Outcrop and core photos of the tidal flat facies association. a) Gradational contact between the shoreface/foreshore facies association and the tidal flat facies association. Top to the left. b) Ptygmatically folded syneresis cracks in interstratified fine-grained sandstone and mudrock/siltstone of the tidal flat facies association.

Figure 7 (continued): c) Small-scale cross-stratification in fine-grained sandstone in the tidal flat facies association, top to the left. d) Lenticular and flaser bedded fine-grained sandstone in black mudrock of the tidal flat facies association.

cracks displaying mud curls, which must have originated through dessication. The syneresis cracks originated subtidally below the sediment-water interface as earthquake-induced dikelets (Pratt, 1998). The sandstone dikelets are highly deformed and were injected into surrounding mudrock both upwards and downwards and differentiates syneresis cracks from dessication cracks. The close association of flaser and lenticular bedding with dessication cracks is indicative of an environment heavily influenced by tidal activity (Dalrymple, 1990). Decimeter-thick cross-bedded sandstone with mud clasts are considered to be migrating tidal channels, inferred have scoured into underlying strata. Contacts in drill core were sharp-based, contacts may have been scoured but this was not evident in drill core. Another origin for the beds may be storm deposits (Dalrymple, 1990).

This facies association was deposited in an extensive tidal flat environment. The interpretation of an intertidal coastal depositional environment rather than an offshore environment is heavily influenced by the presence of exposure features such as mud cracks. This depositional system overlies and interfingers with the sand-rich shoreface to foreshore facies association. The tidal flat facies association extends further to the East (onshore-direction) than the underlying shorface facies association and is associated with a rise in sea-level. The development of the tidal flat facies association marks the transition from an energetic sand-dominated coastline to a quiet-water mud-dominated environment. Kerans (1983) interpreted the depositional environment most analogous to a delta emptying into a shallow epicontinental sea. The formation of deltaic facies associations such as coarsening up sequences were inhibited by the

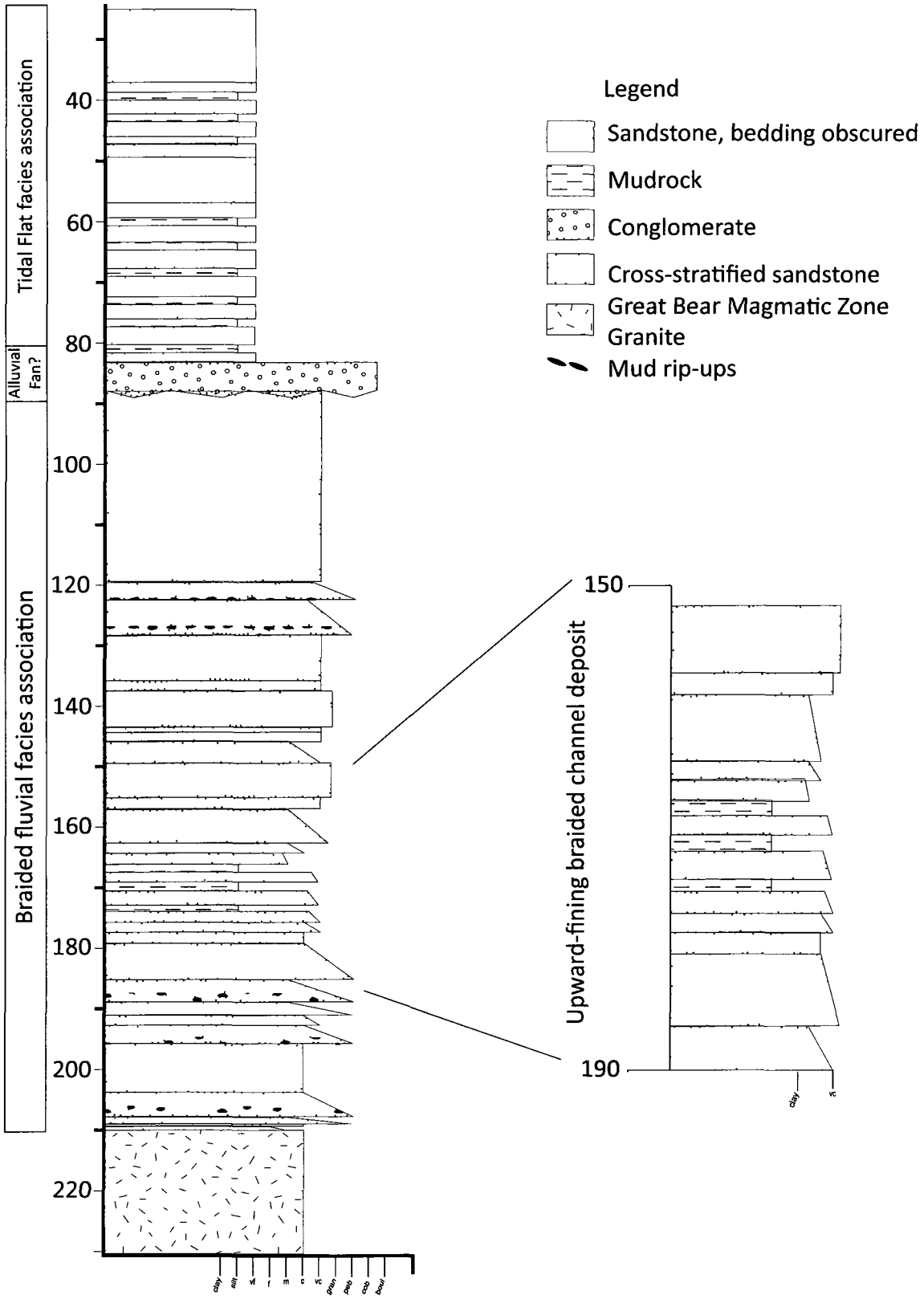

Figure 8: Stratigraphic section from drill hole 78Y-90, within the vicinity of the Mountain Lake uranium deposit, displaying facies successions from the braided stream facies association.

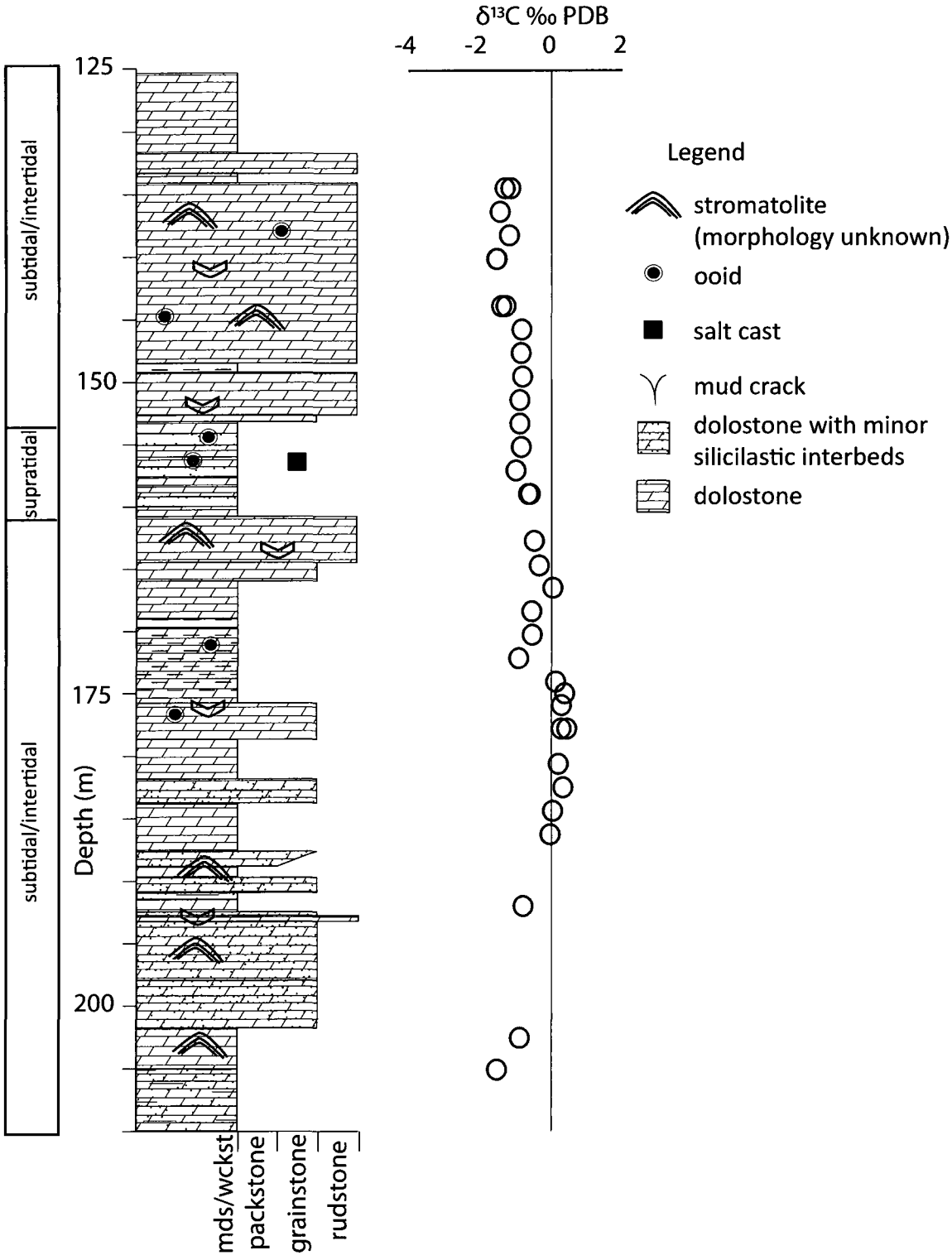

Figure 9: Stratigraphic section from drill hole ML06-019 illustrating the platformal carbonate facies association.

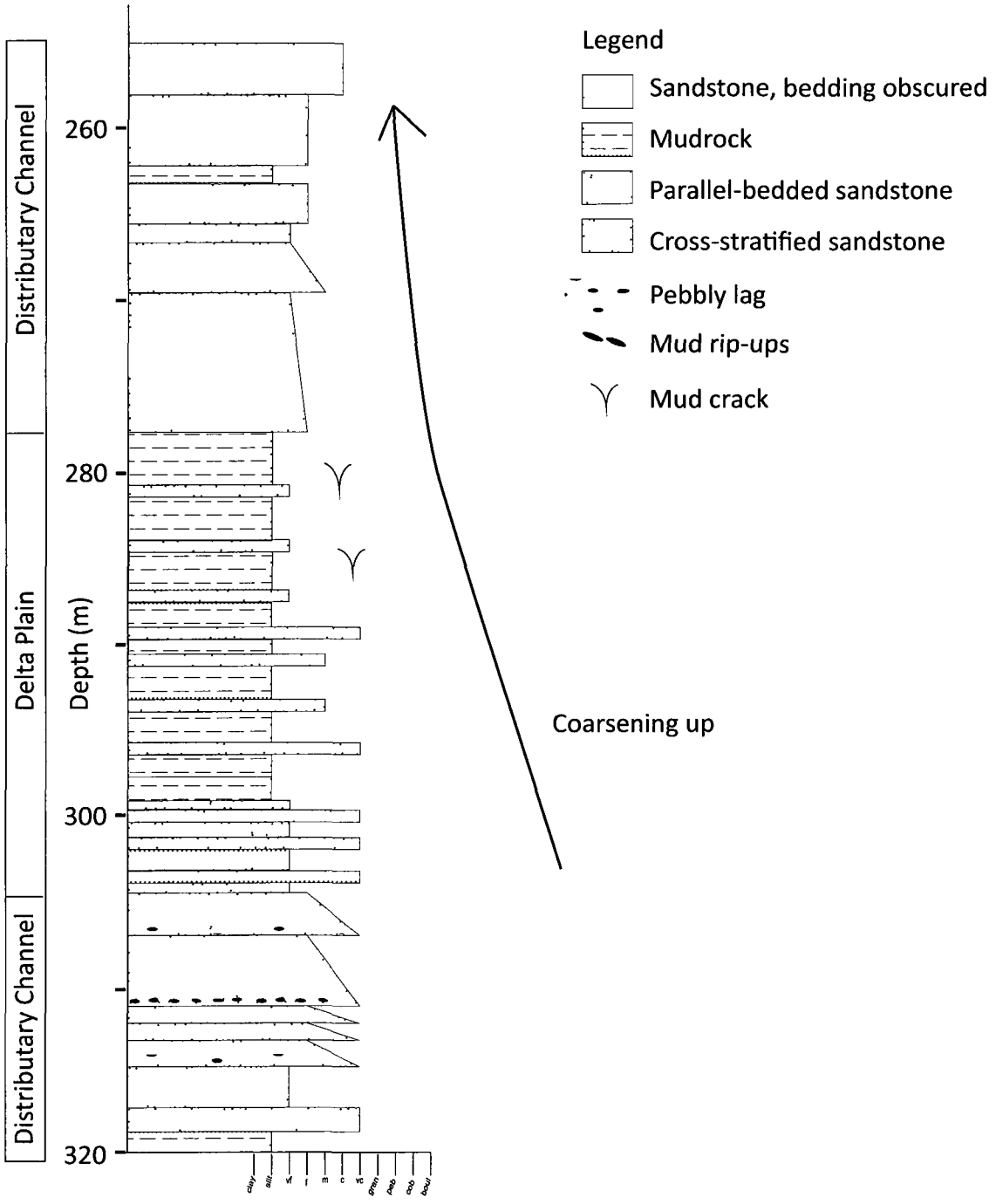

Figure 10: Stratigraphic section from drill hole DL07-007 displaying one complete coarsening upwards package from the deltaic facies association.

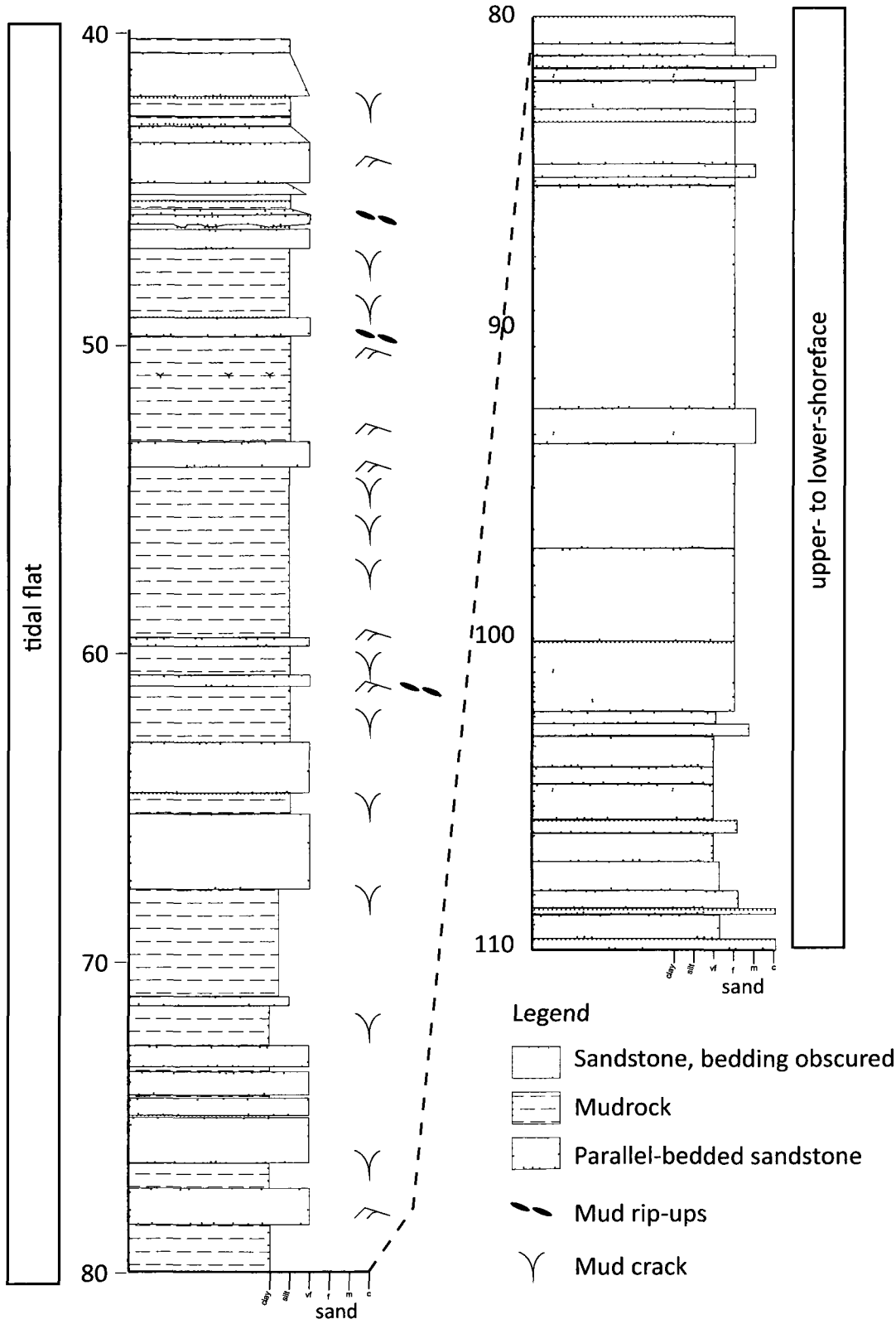

Figure 11: Stratigraphic section from drill hole DL07-004 showing tidal flat and upper- to lower-shoreface facies associations

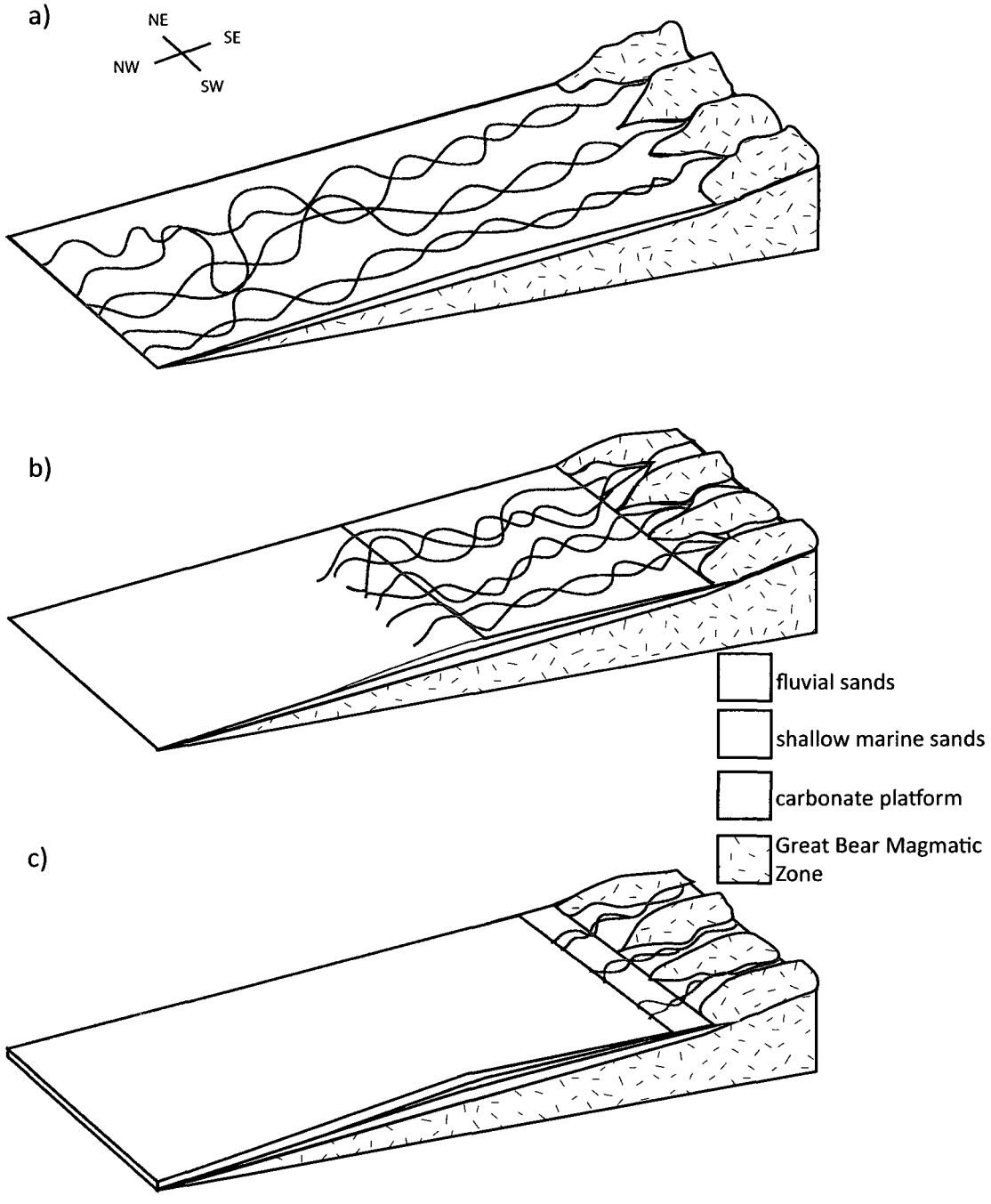

Figure 12: Schematic block diagram of sand-bed braided fluvial and carbonate platform facies associations throughout deposition during of the Hornby Bay Group. a) Sand-bed braided fluvial facies association, northwest-directed paleocurrent predominate. b) Sand-bed braided fluvial facies association emptying into shallow marine basin during sea-level rise (shallow marine facies not observed in this study but is reported in literature). c) Development of carbonate platform facies association

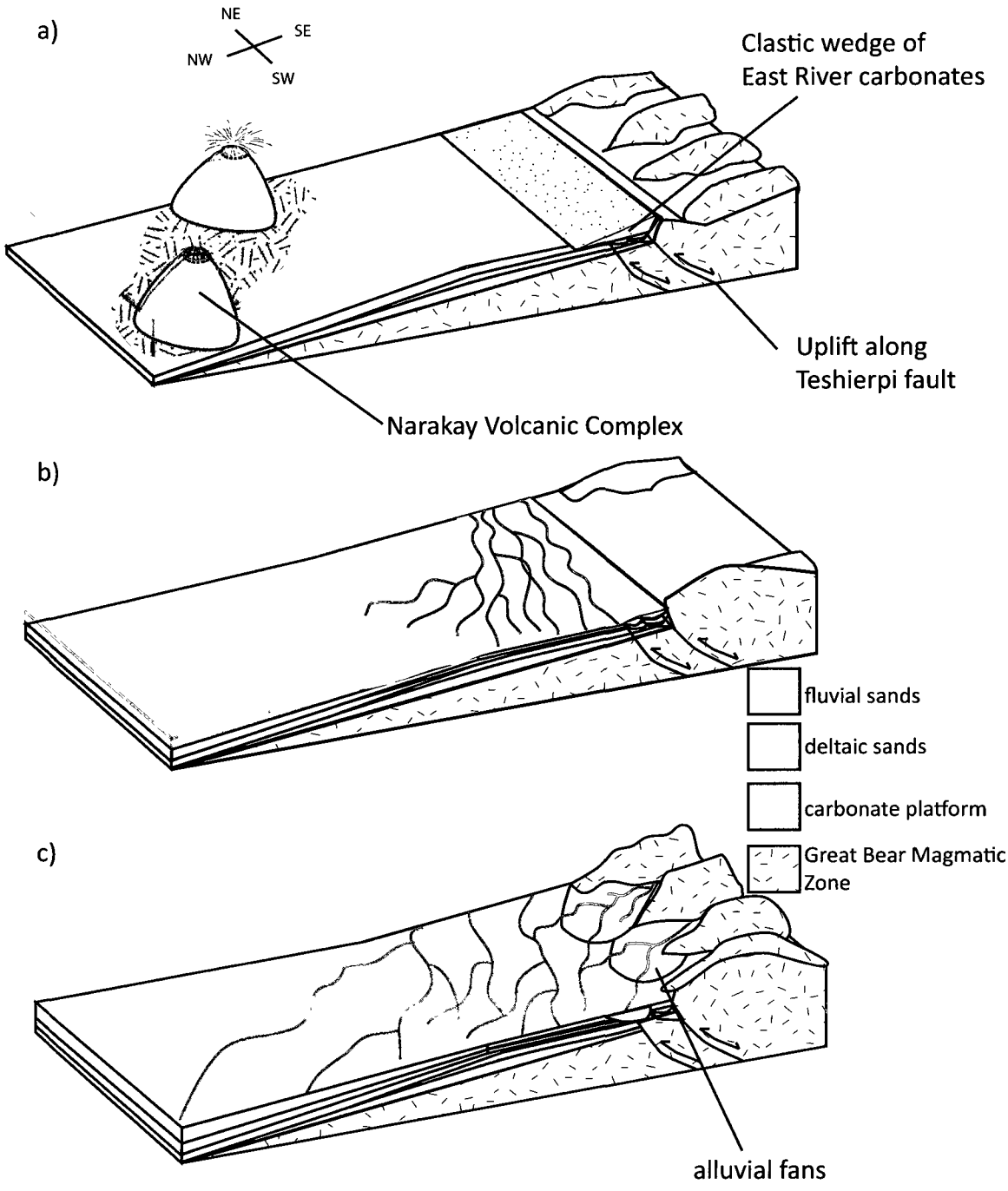

Figure 13: Schematic block diagram of carbonate platform and deltaic facies associations during deposition of the Upper Hornby Bay Group. a) Platformal carbonate facies association showing the beginning of uplift along the Teshierpi fault and syntectonic volcanism in of the Narakay Volcanic b) Development of the tide-dominated deltaic facies association, note fluvial channels parallel to fault trace and shift in shoreline. c) Development once again for braided-fluvial facies association and alluvial fan facies association after tectonic uplift has ceased.

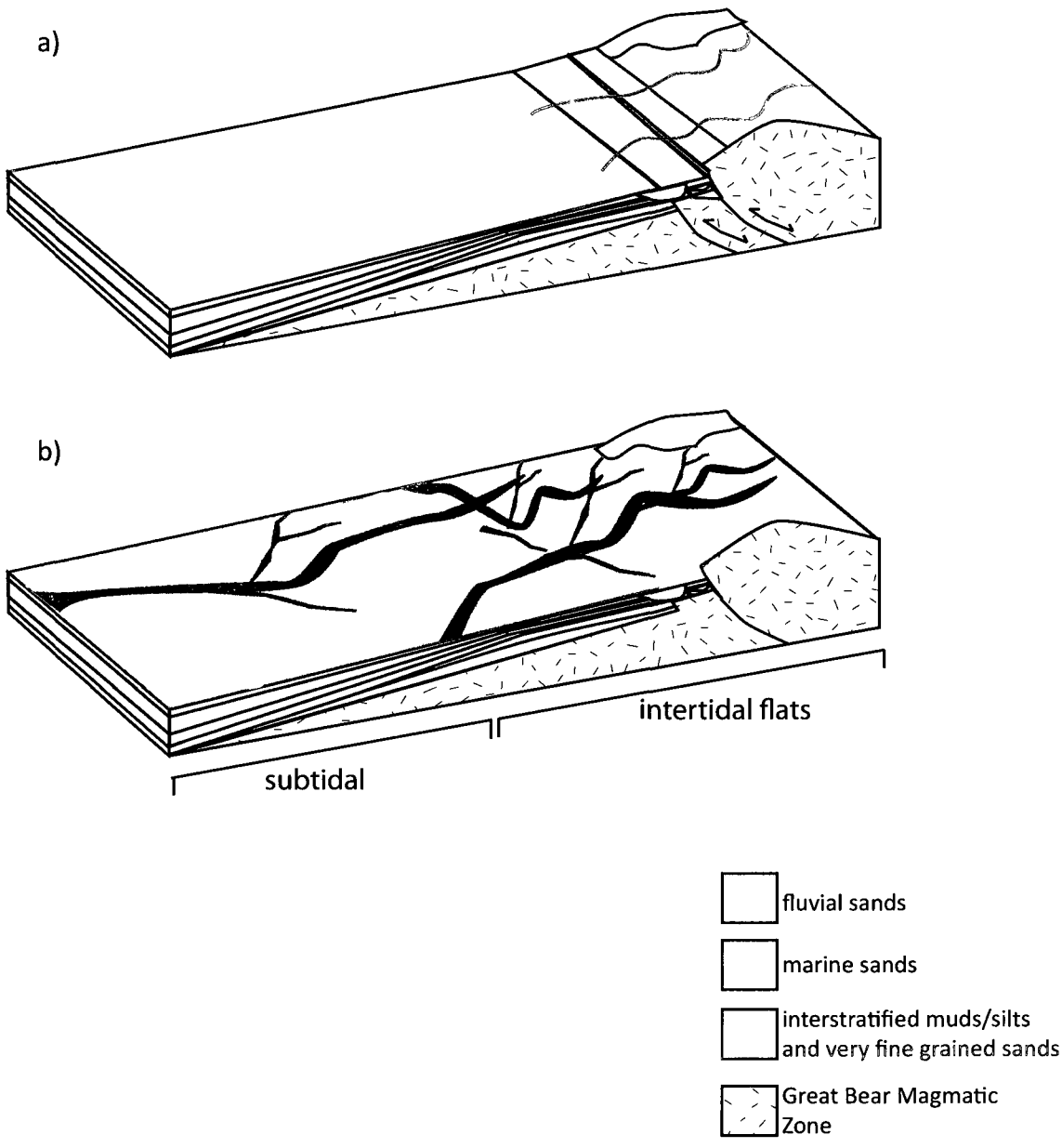

Figure 14: *Schematic block diagrams of lower- to upper-shoreface and tidal flat facies* associations throughout deposition of the lower Dismal Lakes Group. a) Lower- to upper-shoreface facies association deposited on an energetic, sand-dominated shoreline. b) Relative sea-level rise, combined with abundant sediment deposition resulting in development of extensive tidal flats and marine shoreline and channel-fill sands, tidal

shallow nature of the receiving basin (Kerans, 1983). Refer to Figure 14b for schematic block diagram.

6. Sequence Stratigraphy

6.1 Proterozoic Sequence A

Proterozoic supracrustal rocks of western Canada have been subdivided into 3, regionally preserved, unconformity-bounded, sequences (Sequence A, B, and C, of Young et al., 1979) and strata of the Hornby Bay Basin (HBB) are considered to be part of Sequence A (~1.7 Ga to ~1.2 Ga). Sequence A was subdivided into four, unconformity-bounded, sub-sequences (A1, A2, A3, and A4) based on analysis of petroleum industry seismic lines that transect the northern interior plains region, west of the exposed HBB (Maclean and Cook, 2004). Correlations were suggested between Hornby Bay strata and corresponding depositional units within the subsurface. Subsequence A1 comprises the Big Bear and Fault River formations which correlate with the basinal unit and Subsequence A2 consists of a platformal and syntectonic unit in the subsurface, which was correlated with the Lady Nye, East River, Kaertok and LeRoux formations. Maclean and Cook proposed an unconformity between the LeRoux Formation and the Fort Confidence Formation which they considered to be the base of the Dismal Lakes Group. This was based on the mapped relationship, which shows the LeRoux Formation striking into the Fort Confidence Formation (Ross and Kerans, 1989). In this study, the contact between the LeRoux Formation and the Fort Confidence

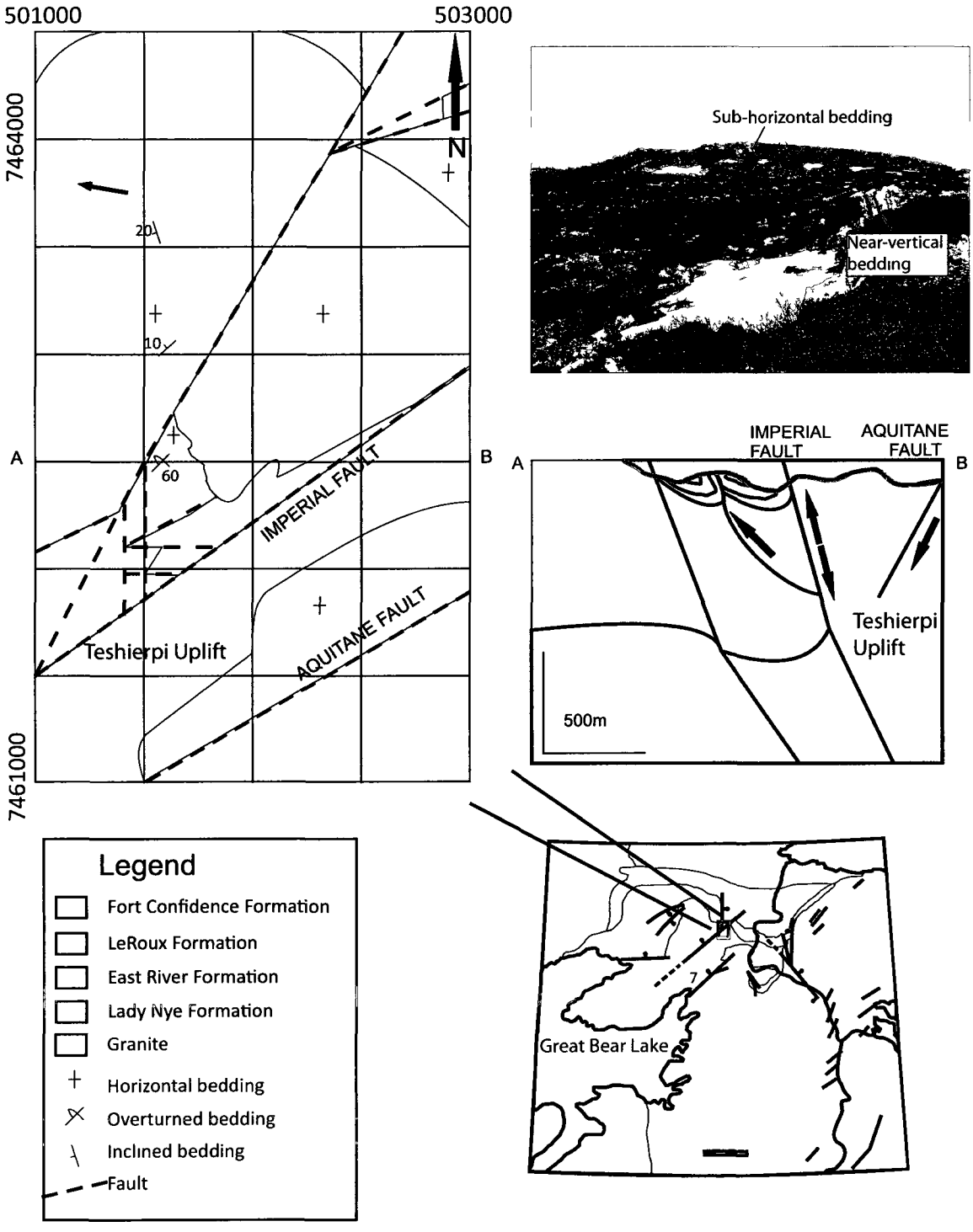

Figure 15: Map of the Teshierpi Fault zone with schematic cross section (Modified from Maclean and Cook, 2004) and outcrop photo of the angular unconformity at the A2-A3 sequence boundary.

Cordillera	Subsurface	Hornby Bay Basin	
Windermere Supergroup			C
Mackenzie Mountains Supergroup 0.78 – 1.0 Ga	Mackenzie/Shaler Assemblage	Shaler Supergroup 0.723 – 1.0 Ga	B
	Tweed Lake Basalt	Coppermine Basalt 1.267 GA	A4
Pinguicula Group	Dismal Lakes Assemblage	Dismal Lakes Group 1.267 – 1.663 Ga	A3
Racklan Orogeny 1.59 – 1.71 Ga	*Forward Orogeny*	*Forward Orogeny 1.663*	A2
	Syntectonic Unit	Kaertok and LeRoux Formations (1.663 Ga)	A2
	Platformal Unit	East River Formation	
	Basinal Unit	Lady Nye Formation	
Wernecke Supergroup	Lower Unit (Seismic sequence A1)	Bigbear and Fault River Formations	A1
	Basement	Wopmay Orogen >1.84 Ga	

Table 2: Correlation chart of Proterozoic strata in northwestern Canada from Maclean and Cook (2004).

Formation was observed to be gradational (Figure 19). The unconformity is present directly below the LeRoux Formation and is described in detail below. The Dismal Lakes Group makes up subsequence A3 and corresponds to the Dismal Lakes assemblage in the subsurface where it is not subdivided into different formations (Maclean and Cook, 2004). Subsequence A4 comprises the Coppermine River Group, which is correlated with the Tweed Lake Basalts in the subsurface (Maclean and Cook, 2004).

6.2 Terminology

Sequence stratigraphy is a useful tool for evaluating depositional history, however the development of a standardized terminology has caused conflicting interpretations of various stratal surfaces. For the purpose of this study the most recent compilation of terminology by Embry (2009) has been used. To satisfy the requirements of sequence stratigraphic interpretation, a combination of lithologic and gamma ray logs were studied. Depositional sequences were evaluated using a material-based surface method, rather than using time-equivalent surfaces. Time-based depositional surfaces require the identification of correlative conformities, which are defined as a time surface commonly located at the start of base-level rise (Embry, 2009). As described by Embry (2009), problems arise with the time-based method because correlative conformities generally lack the defining physical characteristics that are needed for regional correlation. The lack of age-constraints from markers such as

Formation	Maclean and Cook, 2004	This Study
Coppermine River Group	A4	A4
Greenhorn Lakes	A3	A3
Sulky		
Kendall River		
Dease Lake		
Fort Confidence		
LeRoux	A2	
Kaertok		A2
East River		
Lady Nye		
Fault River	A1	A1
Big Bear		

Table 3: Changes to Paleoproterozoic Sequence A in the Hornby Bay Basin

volcanic tuff layers and fossilized beds in the Hornby Bay Basin further complicates any use of time-based surfaces.

A material-based surface is defined by the observable physical characteristics and geometrical relationships of the surface and the overlying and underlying strata (Embry, 2009). Material-based surfaces can often also be picked out in gamma ray profiles due to the correlation between grain size and total gamma counts, and therefore have proven to be most useful in this study.

6.3 Depositional Sequences

In this mainly drill core-based study, the sequence stratigraphy of sequences A2 and A3 were evaluated in greatest detail. The Lady Nye Formation forms the base of sequence A2 and records the first marine incursion within the basin. A broad fluvial braidplain, characterized by the sand-bed braided stream facies association, forms the base of the sequence, which gradually developed into a northwest-directed delta (Ross, 1983) (see Figure 16a and 16b). This is interpreted to record deposition of lowstand systems tract (LST) followed by an early transgressive systems tract (TST). Due to incomplete sections of drill core the contact between the LST and TST is inferred.

Significant shoreline ravinements or transgressive lags were not observed and have not been reported, which indicates that transgression was likely rapid, potentially over a low depositional gradient. The lack of shoreline ravinements or transgressive lags could also be due in part to prolific growth of microbial mats on subaqueous siliciclastic

substrates during the Proterozoic, which would have stabilized bedding planes and restricted shoreline erosion during transgression (Sarkar et al, 2005; Nofke, 2009).

Gradationally overlying the Lady Nye Formation is the platformal carbonate facies association of the East River Formation, which marks the beginning of a highstand systems tract (HST; Figure 16c). Subtidal stromatolites dominate the base of the unit. These were deposited in a deeper water environment than the delta because the presence of mudcracks indicates that the delta was largely intertidal.

Throughout deposition of the HST the carbonate deposits built to sea-level resulting in the deposition of extensive carbonate tidal flats. During late deposition of the East River Formation, uplift was initiated along the Teshierpi fault located at the eastern exposed limit of the East River Formation. Lithified carbonate from the early HST was uplifted and cannibalized, depositing a wedge of mixed siliciclastic and coarse, reworked carbonate sediment onto the platform (Figure 17a).

As uplift continued, fault-controlled fluvial systems began to form west of, and parallel to, the Teshierpi uplift (Figure 17b), causing the fluvial systems to terminate in a tide-dominated delta, characterized by siltstones and cross-bedded sandstones of the Kaertok Formation, that drowned all carbonate production. This deltaic system was deposited throughout the HST as sea level began to fall. Deposition within this systems tract signifies the end of sub-sequence A2. This fall in sea level was largely controlled by tectonic uplift rather than eustacy. Tectonic uplift before deposition of the Dismal Lakes Group (A3) is especially evident near the Mountain Lake deposit (Figure 15) where

movement along the Teshierpi Fault (Figure 15) uplifted and tilted the Lady Nye, East River, and Kaertok formations before deposition of A3 commenced.

Overlying the tide-dominated delta facies association is a laterally extensive sub-aerial disconformity, represented by a variably thick, clay-rich regolith (Figure 19). Close to the Teshierpi uplift, the surface is an angular unconformity that cuts tilted rocks of the Lady Nye, East River, and Kaertok formations, which likely represents a long hiatus this locale (Figure 15). East of the Teshierpi uplift a subaerial disconformity is represented by an oxidized horizon at the top of the Lady Nye Formation, interpreted to represent reworked sediment from the top of the Lady Nye Formation. Different parts of the sequence boundary represent differing magnitudes of a period of non-deposition. The extent of the period of non-deposition is potentially quite large where significant erosion has occurred, forming an angular unconformity, and less significant west of the Teshierpi uplift where the section is more completely preserved.

Directly overlying the unconformity are variable deposits, up to 100m thick, of the alluvial fan, braided fluvial, and shallow marine sandstone facies associations of the LeRoux Formation. In the vicinity of the Teshierpi uplift, thin deposits of the alluvial fan facies association and braided fluvial deposits are present (Figure 17c). West of this region, sandy fluvial deposits prevail. These facies associations represent deposition within the LST. Overlying the fluvial facies association are shallow marine sandstones of the lower- to upper-shoreface facies association (Figure 18a), the transition of which is marked by a pebble-rich bed with a characteristic small gamma peak (Figures 19 and 20). The gamma peak was observed in three drill holes within the study region over a

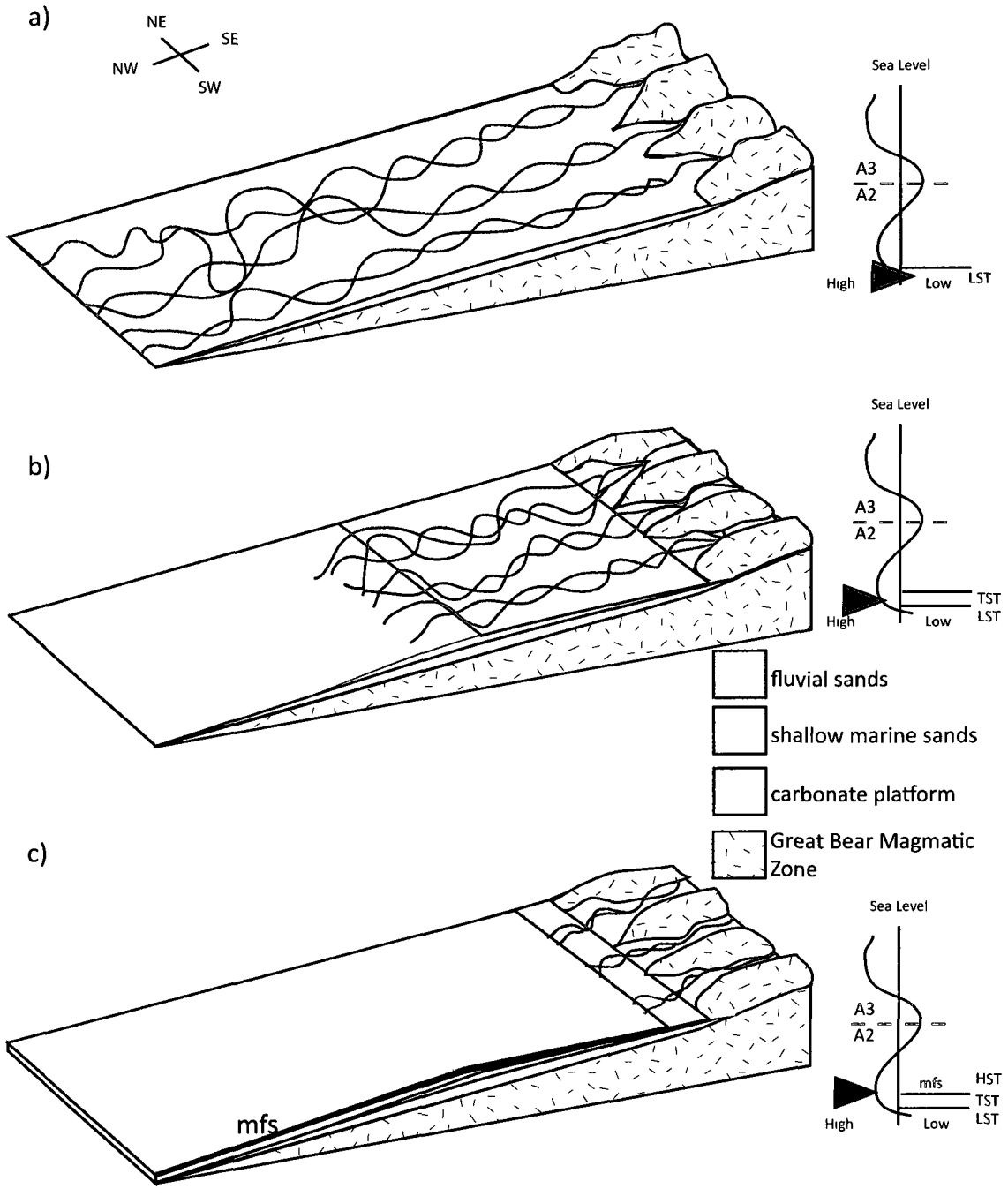

Figure 16: Schematic block diagram illustrating systems tracts and major sequence stratigraphic surfaces of A2. a) Lowstand systems tract (LST) during begining of A2 b) Transgressive systems tract (TST), first appearance in A2 of shallow marine facies associations c) Maximum flooding surface (mfs) recording maximum incursion during A2, transition to highstand systems tract (HST)

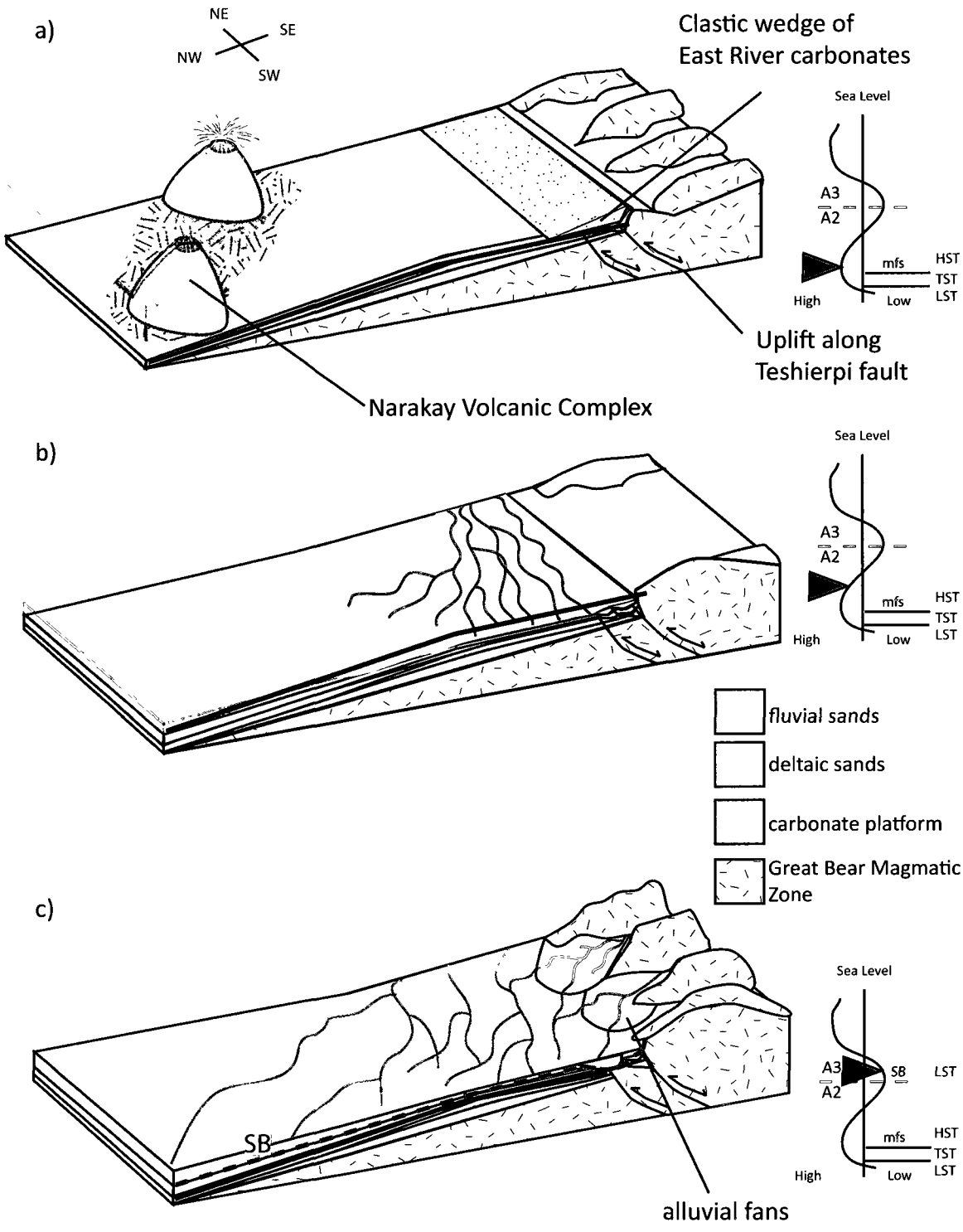

Figure 17: Schematic block diagram illustrating systems tracts and major sequence stratigraphic surfaces of late A2 and early A3. a) Continued deposition during the HST of A2, begining of deformation associated with Forward Orogeny b) Continued deposition during the late HST of A2, continued deformation due to Forward Orogeny c) LST of A3, after deformation associated with Forward Orogeny.

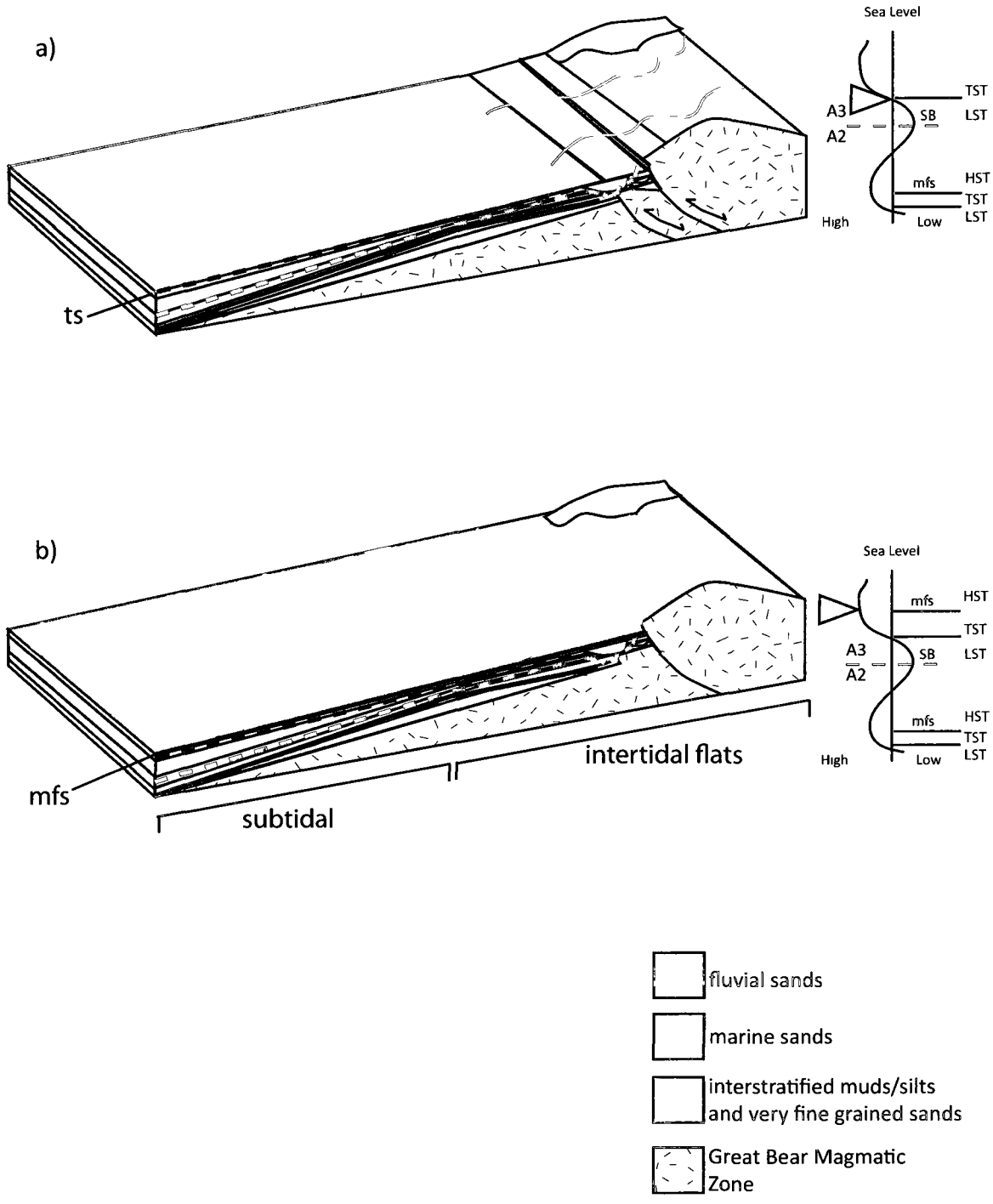

Figure 18: Schematic block diagram illustrating systems tracts and major sequence stratigraphic surfaces of early A3. a) Deposition during the TST showing a transgressive surface (ts) during early A3 b) Deposition during the HST of early A3 showing maximum flooding surface (mfs)

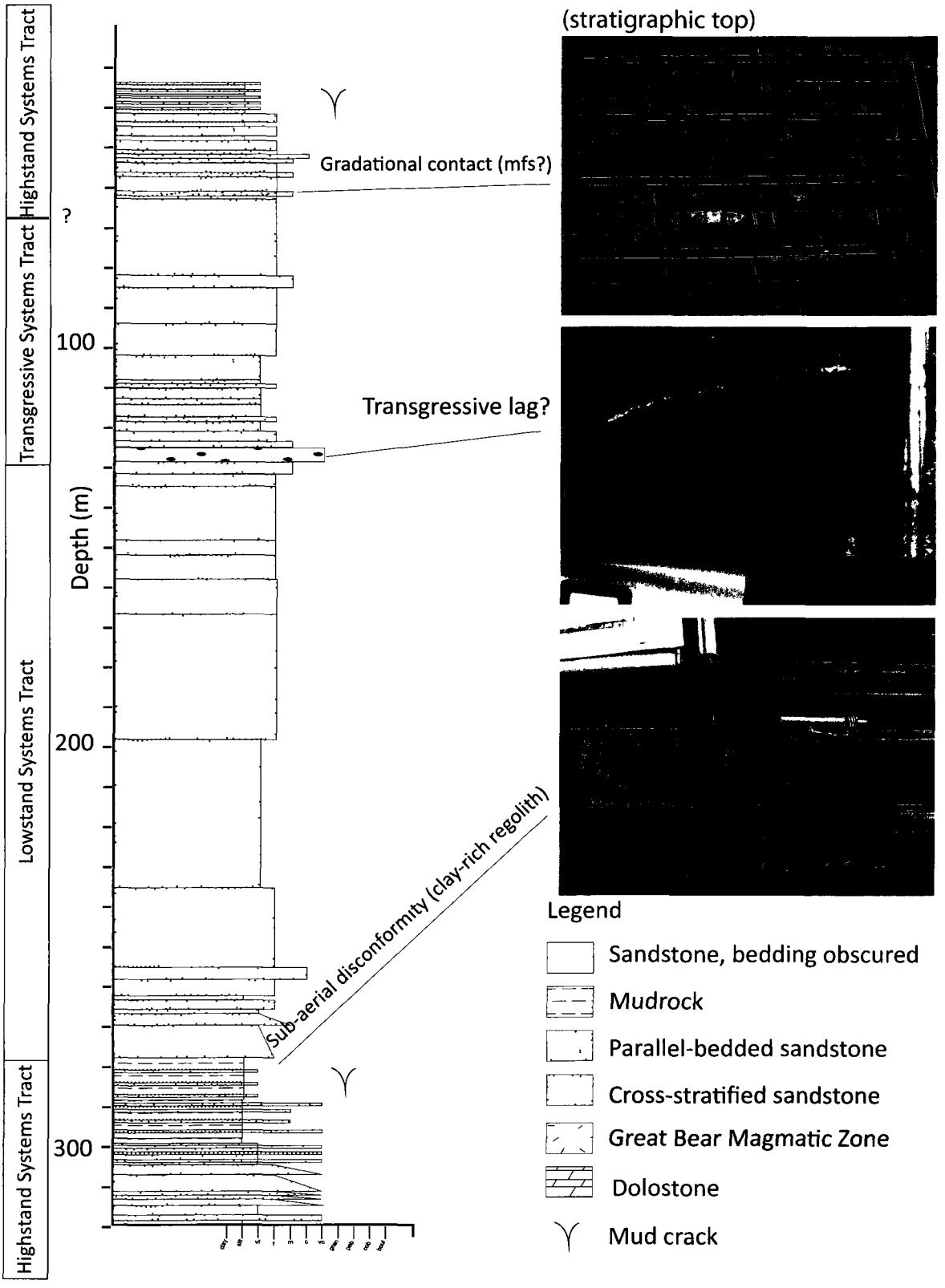

Figure 19: Stratigraphic section from drill hole DL07-007 with major material-based sequence stratigraphic surfaces and corresponding photos.

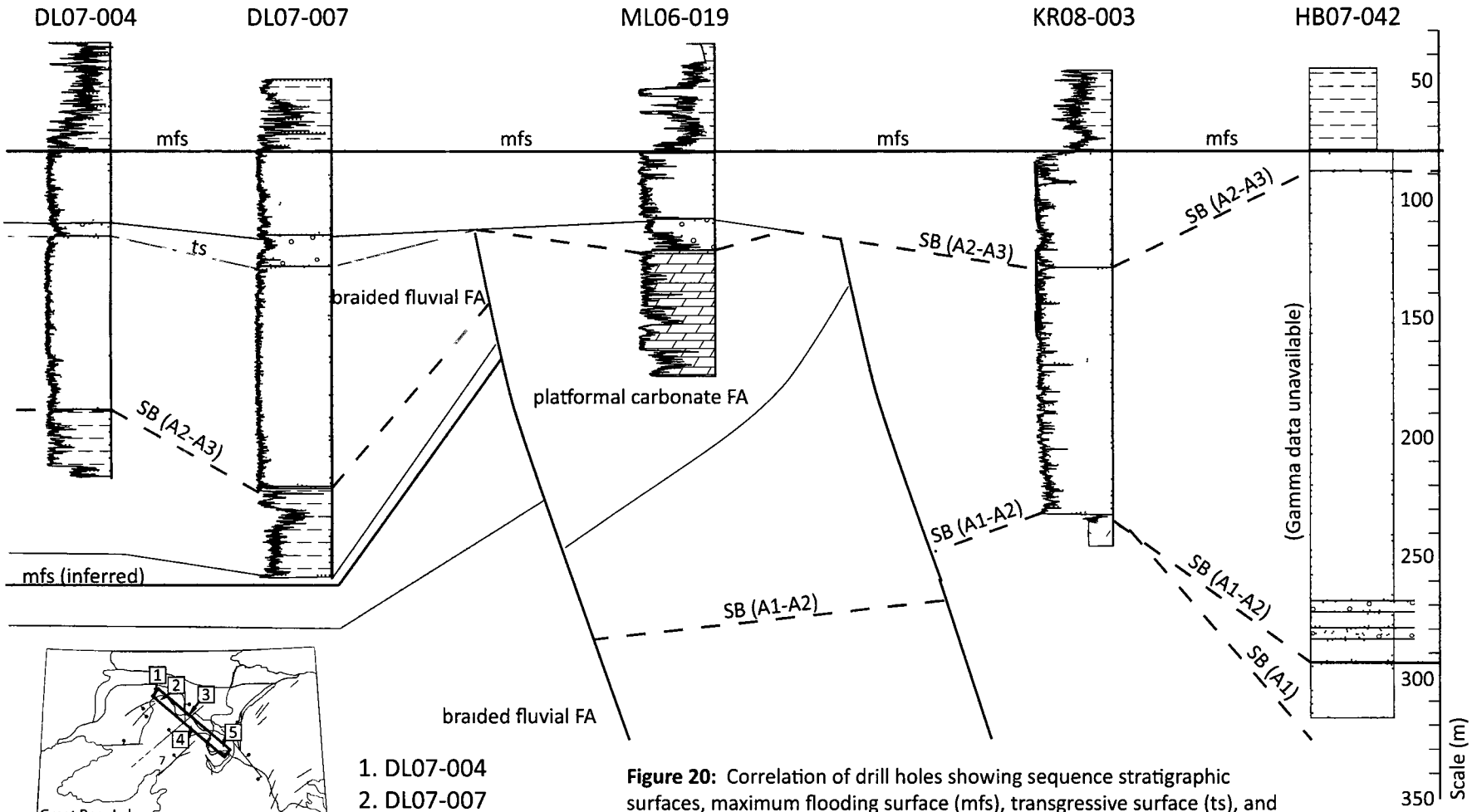

Figure 20: Correlation of drill holes showing sequence stratigraphic surfaces, maximum flooding surface (mfs), transgressive surface (ts), and sequence boundaries (SB). Horizontal distance across correlation is approximately 70 km. Refer to Figure 19 for lithologic legend.

distance of approximately 6 kms and is interpreted as a shoreline ravinement-diastem (SR-D) (Embry, 2009) and represents the change from LST conditions to TST conditions. Possible sources for the gamma peak may include a concentration of phosphate-rich clasts reworked from underlying sub-aerially exposed sandstones, or a higher concentration of feldspathic grains than the overlying quartz-rich mature sandstones.

Gradationally overlying the LeRoux Formation is the subtidal to intertidal flat facies association of the Fort Confidence Formation (Figure 18b). The tidal flat facies association is extensive and covers a much broader region than the underlying shallow marine and fluvial facies associations. The maximum extent of the tidal flats represent maximum marine incursion and marks the transition from a TST to a HST.

These siliciclastic tidal flats pass up-section into the rest of the Dismal Lakes Group, dominated largely by carbonates (see to Kah et al., (2006), for a detailed description of sequence stratigraphy).

7.0 Sm-Nd Analysis

7.1 Introduction and Justification of Method

U-Pb dating of detrital zircon combined with paleocurrent data is a standard technique used in identifying sedimentary provenance. Results from these studies, although useful, are heavily biased towards the felsic component of detritus. Sm is incorporated more easily into mafic minerals and therefore the Sm-Nd isotopic system is

complementary to the U-Pb detrital zircon system and provides important provenance information on the mafic component of clastic sediment (eg. Satkoski et al, 2010; Rainbird et al, 1997).

This method of examining sediment provenance has been vigorously tested (Nelson and DePaolo, 1988 and references therein). Sm-Nd values between fine- and coarse-grained sediment remain consistent, and isotopic fractionation during sedimentary transport, diagenesis, and low grade metamorphism is negligible (Nelson and DePaolo, 1988 and references therein). This is due largely to the low solubility of Sm and Nd in river and ocean water. As sediment is a mechanical disintegration of the source rock, the Sm-Nd isotopic composition and model age of the sediment is perfectly preserved from the source rock. Because of the low solubility of Sm and Nd under surface conditions, chemical weathering to produce clay minerals does not affect the isotopic composition or model age. The isotopic ratio of $^{143}Nd/^{144}Nd$ is expressed in ε_{Nd} notation. This notation represents the deviation in units 0.1 per mil from the isotopic ratio expected in the "bulk earth", or model chondritic reference reservoir, at time T. Sm-Nd model ages can be calculated relative to a curve describing ε_{Nd} in the upper mantle and represent the time at which the sample and upper mantle could have had the same ε_{Nd} value, referred to as the depleted-mantle derivation age (T_{DM}). Isotopic fractionation between individual minerals does occur; however, when bulk samples are taken at the hand sample scale, results reflect the average composition of the source region (Nelson and DePaolo, 1988 and references therein.).

For the purpose of this study, samples were taken from siliciclastic mudstones within the East River, Kaertok, and Fort Confidence formations (Figure 3). This study concentrated on the A2-A3 sequence boundary (refer to Chapter 6) to compare provenance across the unconformity. Results from the upper Hornby Bay Group (A2) will also test correlation with the Wernecke Supergroup by comparing the sedimentary provenance of the two successions. These data were compared to previously determined U-Pb detrital zircon ages from the upper Hornby Bay Group and lower Dismal Lakes Group and several source regions were determined.

7.2 Analytical Methods

Samples of fresh drill core were collected at 20 m intervals through a 100 m-thick section of the Fort Confidence Formation (see Figure 11 for representative section). From the East River Formation, samples were taken where siliciclastic intervals were present in drill core (Figure 9). Samples from the Kaertok Formation were taken from several different drill holes below the A2-A3 sequence boundary, where drill core appeared least altered.

Samples were cleaned, crushed and pulverized using a chipmunk jaw crusher and agate ring mill. Machines were pre-contaminated with small amounts of sample before crushing and grinding. One vial was produced for each sample which provided enough powdered sample to complete XRF and Sm-Nd isotopic analysis.

X-ray fluorescence spectrometry (XRF) was completed on fused glass discs. Discs were created through reacting 1 g of sample with approximately 4 g of flux (lithium

tetraborate/lithium metaborate mixture). The mixture was reacted in platinum alloy crucibles at 1000°C and cooled to produce 35mm diameter glass discs. The discs were run on a Phillips PW2400 Wavelength Dispersive XRF with a Rh source housed at the University of Ottawa. Data were collected using an automated computer system and major elemental concentrations of SiO_2, TiO_2, Al_2O_3, Fe_2O_3, MnO, P_2O_5, MgO, Na_2O, K_2O, CaO, Zn, Ba, Co, Ga, La, Ni, Pb, Rb, Sr, Th, U, V, Y, Zr, Nb, Cr, Ce, and Nd were determined (Appendix 1).

Isotopic variations between Sm and Nd were measured on a ThermoFinnigan TRITON thermal ionization multicollector mass spectrometer equipped with an electron multiplier housed at Carleton University. Between 100 and 200 mg of sample were spiked with $^{149}Sm/^{148}Nd$ and dissolved with HF in teflon bombs using standard procedures outlined by Cousens et al (2000). Samples were run manually on the mass spectrometer at a voltage of 0.3 V due to low initial Nd concentrations. Not every sample produced full length runs on the mass spectrometer however, if results were still within a low limit of error ($< \pm 10^{-5}$) they were deemed to be acceptable. All results with corresponding error are presented in Table 3. Standards were analyzed in every run to maintain quality control.

Two samples of Narakay basalts were analyzed. At the time of analysis, major and trace element data for the samples were unavailable. For this reason, a split and spike method was used to determine isotopic abundances rather than the traditional method of using Nd concentrations in calculating isotopic ratios. For each sample, an unspiked split (IC) and a split spiked with $^{149}Sm/^{148}Nd$ (ID) were analyzed. $^{143}Nd/^{144}Nd$

were compared between the IC and ID samples. One sample had equal $^{143}Nd/^{144}Nd$ ratios and was therefore properly spiked. One sample had significantly different $^{143}Nd/^{144}Nd$ ratios because it was overspiked, so in calculation of ε_{Nd} the value for $^{143}Nd/^{144}Nd$ of the IC sample was used in the ID run.

7.3 Results

7.3.1 Sedimentary Rocks

The absolute age of deposition of the East River, Kaertok, and Fort Confidence formations is uncertain, therefore ε_{Nd} values were calculated at two different ages.

The age of the East River Formation is the most tightly constrained, as it is interpreted to be coeval with the Narakay Volcanic complex, which has a U-Pb (zircon) age of 1663 ± 8 Ma (Bowring and Ross, 1985). Detrital zircon from the ERF provide a maximum age of deposition at 1631 ± 28 Ma (Rainbird et al, 2009). For this reason ε_{Nd} was calculated at both 1700 Ma and 1600 Ma. Measured present day values of ε_{Nd} range broadly from -26.75 to -16.92. Calculated ε_{Nd} values at 1700 Ma and 1600 Ma range from -3.98 to -0.87 and-4.75 to -2.34, respectively. Model ages, or $T_{DM,}$ were calculated to range from 2059 to 2657 Ma.

ε_{Nd} for the Kaertok Formation was calculated using the same age constraints as the East River Formation. The Kaertok Formation gradationally overlies the East River Formation and no other age constraints are available. Measured present day ε_{Nd} values lie in a narrow range between -26.37 and -22.77. Calculated ε_{Nd} at 1700 Ma and 1600

Ma ranges from -7.32 to -6.58 and -8.24 to -7.73, respectively. T_{DM} was calculated to range from 2563 to 2822 Ma (Table 3, Figure 21).

The age of the Fort Confidence Formation is only loosely constrained, with a maximum age defined by a detrital zircon measurement of 1599 Ma from the LeRoux Formation and a minimum age of ~1370 Ma based on correlation of C/O stable isotope stratigraphy (Frank, 2003). For this reason ε_{Nd} was calculated at 1600 Ma and 1400 Ma. The present day value of ε_{Nd} ranges from -25.81 to -17.07. Calculated ε_{Nd} at 1600 Ma and 1400 Ma ranges from -7.37 to -3.71 and -9.78 to -6.42, respectively. T_{DM} was calculated to range from 2186 to 2554 Ma.

7.3.2 Narakay Volcanic Complex

A U-Pb zircon age of 1663 ± 8 Ma (Bowring and Ross, 1985) was reported for the Narakay Volcanic complex, however euhedral detrital zircons from epiclastic sandstones from the East River Formation interpreted to be coeval with the Narakay Volcanic Complex, have yielded younger ages, 1631 ± 28 Ma (Rainbird et al, 2009). For this reason, ε_{Nd} was calculated at 1650 Ma. Two samples of basalt were analyzed and yielded ε_{Nd} values of +3.49 and +2.13, and corresponding T_{DM} values of 1807 Ma and 2175 Ma.

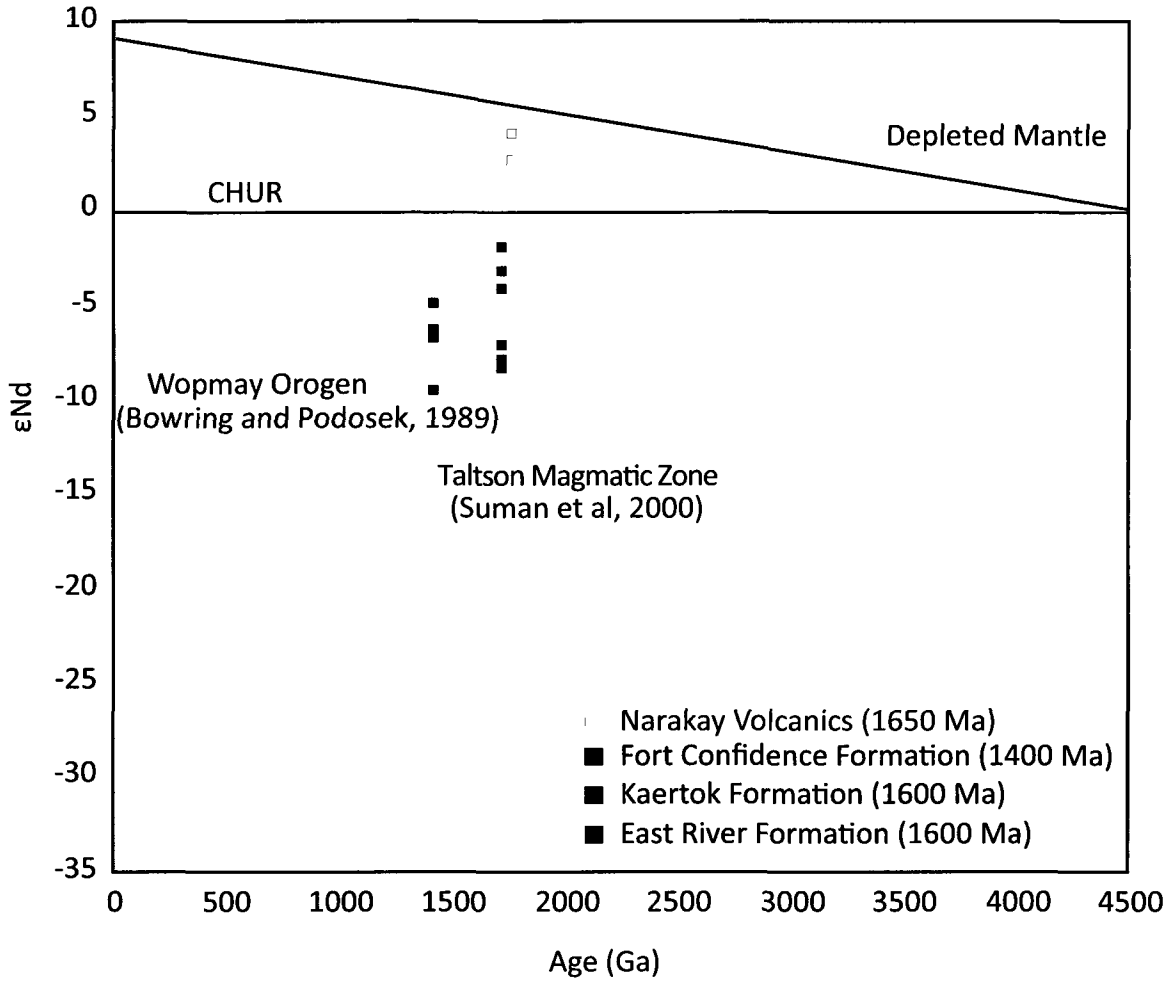

Figure 21: Isotopic evolution fields for different sediment source regions for the Hornby Bay Basin with data points from the East River Formation, Kaertok Formation, Fort Confidence Formation, and Narakay Volcanic Complex.

7.4 Discussion of Results

7.4.1 Sedimentary Provenance

The ε_{Nd} values are highly variable and point to several potential sediment sources. The best way to compare ε_{Nd} values to potential sources for provenance is to plot the data on an ε_{Nd} vs Time graph, and plot a range of known ε_{Nd} values for hypothetical source regions (Figure 21). Plotting a range of isotopic values for a source region creates a large isotopic evolution field that gives a range of different measured ε_{Nd} values from isotopically heterogeneous source regions. T_{DM} values are more difficult to use as an indicator of sedimentary provenance because mineral sorting can complicate interpretations if the source rock has been subjected to metamorphism significantly later than crust formation. Model ages of minerals can also be variable due to differing Sm/Nd ratios; minerals with low Sm/Nd ratios have younger model ages than minerals with high Sm/Nd ratios.

Three potential source regions for Hornby Bay sedimentary rocks were previously hypothesized based on U-Pb detrital zircon ages from Rainbird and Davis (2009); the Trans Hudson Orogen, the Great Bear Magmatic Zone, the Taltson-Thelon Tectonic Zone. The Narakay Volcanic Complex is hypothesized as a fourth source of sediment for the East River Formation. When plotted on an ε_{Nd} vs Time graph (Figure 21), the isotopic evolution field of the Trans-Hudson orogen is wide and encompasses the data sets from the Kaertok, East River, and Fort Confidence formations. Within these data sets two distinct compositional groups are apparent; a more positive group, including the East River Formation, and part of the Fort Confidence Formation, and a

more negative group defined by the Kaertok Formation. Two distinct source regions were identified on the basis of the data sets falling within the isotopic evolution fields of the Great Bear Magmatic Zone and the Taltson-Thelon Magmatic Zone (Figure 21).

All values for ε_{Nd} of the East River Formation lie within the isotopic evolution field of the Great Bear Magmatic Zone (GMZ; Figure 21) (Bowring and Podosek, 1989). The corresponding detrital zircon data identifies a prominent peak at 1.85 Ga (Rainbird and Davis, 2009, data unpublished), which is consistent with the age of the GMZ. The detrital zircon data from the East River Formation also identify a significant juvenile component ranging in age from ~1680-1620 Ma (Rainbird and Davis, unpublished), which indicates possible sourcing from the coeval Narakay Volcanic complex (1663±8Ma). This juvenile component may be reflected in the ε_{Nd} values, however, because the values are based on an average of Nd contributed from two or more sources, the GMZ influence is more dominant. A significant component of Archean aged sediment present in the detrital zircon data is not apparent in the ε_{Nd}, however this could be attributed to the analysis of bulk samples for Sm-Nd, which produce a value that represents a mixture of source material. In this case, the GMZ component is dominant. The Archean component, present in the detrital zircon from the East River Formation, was likely derived from the Slave Province, which lies to the east and has a highly variable ε_{Nd} (eg. Moorbath et al, 1997; Yamashita et al, 1998). This likely is present in siliciclastic mudstones of the East River Formation, however the isotopic evolution fields of the Great Bear Magmatic Zone (Figure 21), and a broad field for the Slave Province (not illustrated) overlap.

The range of ε_{Nd} values in the Kaertok Formation plot entirely within the isotopic evolution field of the Taltson-Thelon Magmatic Zone (TMZ) (Theriault and Ross, 1990). Detrital zircons from the KF identify a strong peak at 1.9 Ga, the age of the TMZ (Rainbird and Davis, unpublished), thereby supporting the hypothesis that the TMZ contributed significant detritus to the Hornby Bay Basin. No influence from the Narakay Volcanic complex was observed in ε_{Nd} values. Some influence was expected based on the similarity in age to the Narakay Volcanic Complex (Ross, 1983, 1986). The Narakay Volcanic Complex is located significantly west of the study area, deeper in the basin, and if sediment transport was dominantly in an offshore direction this could contribute to the lack of Narakay influence in the Kaertok Formation.

ε_{Nd} of the Fort Confidence Formation plots within both the isotopic evolution fields of the GMZ and the TMZ (Figure 21). This suggests that there was no significant change in sedimentary provenance across the sequence A2-A3 boundary, that is, no new source for sediment was identified. The Nd data suggest a provenance more enriched in GMZ material for the Fort Confidence Formation, but the detrital zircon data suggests a composition that is very similar to the Kaertok Formation. This variation could be attributed to sampling bias of detrital zircons; zircons primarily reflect the ages of felsic source rocks, whereas Sm-Nd isotopic studies provide an average composition of source rocks. One significant source for sediment is uplifted and eroded material from the Hornby Bay Group (sequence A2), which given the mix of material similar to both the East River and Kaertok formations present in the Fort Confidence Formation is a viable mechanism for providing sediment.

7.4.2 Linking provenance to the Forward Orogeny

As discussed above, the East River Formation is dominated by sedimentary input from the GMZ. Siliciclastic input at the time of deposition was relatively low, allowing the development of a carbonate platform. The siliciclastic mudstone units revealed the GMZ as the most dominant source for sediment, which provided detritus to the carbonate platform through the weathering of paleotopographic highs within the GMZ. A clastic wedge of lower East River Formation carbonates is present at the top of the unit, which is interpreted to represent a syn-tectonic unit which was formed during initial uplift along the Teshierpi Fault (Ross, 1983).

Uplift continued during deposition of the Kaertok Formation and caused a significant increase in siliciclastic input, blanketing the carbonate platform. The Sm-Nd isotopic data for the Kaertok Formation suggest significant provenance from the TMZ. Although Sm-Nd data are not available for the lower Hornby Bay Group, U-Pb detrital zircon results from the Big Bear and Fault River formations compare well with U-Pb detrital zircon ages from the Kaertok Formation, showing abundant zircon grains sourced from the TMZ. Based on how well Sm-Nd sedimentary provenance and U-Pb detrital zircon provenance compare it is assumed that the Kaertok Formation has a similar provenance to the lower Hornby Bay Group. Sediment from the TMZ was transported and deposited within the once extensive Kilohigok Basin (~1.9 Ga), uplifted, and then recycled into Hornby Bay Group sediment (eg. Grotzinger et al. 1988; McCormick et al, 1989; Rainbird et al, 2009).

The Fort Confidence Formation has a mixed provenance produced by a mechanism similar to that of the Kaertok Formation. Deposition is dominated by sediment that was mobilized during the Forward Orogeny. Locally, extensive amounts of strata were removed and transported at the end of sequence A2, as shown by the angular unconformity and missing strata in the Mountain Lake study area (Figure 15).

7.5 Conclusions

Several conclusions can be drawn about sedimentary provenance based on Sm-Nd analyses which provide an average composition of sedimentary source regions.

1. Two important source regions based on Sm-Nd analysis of mudrocks from the upper Hornby Bay Group (A2) are the Taltson-Thelon Tectonic Zone, and the Great Bear Magmatic Zone.
2. Sedimentary provenance was strongly influenced by the Forward Orogeny. The East River Formation is pre- to syn-orogenic and is dominated by local input from paleotopographic highs within the GMZ. The Kaertok Formation is syn-orogenic and received most detritus from the TMZ, probably recycled from the lower Hornby Bay Group. The Fort Confidence Formation is post-orogenic and reflects a mixed provenance from the GMZ and recycled upper Hornby Bay Group sediments from the TMZ.
3. There was no significant change in sedimentary provenance before and after the Forward Orogeny.

Table 4: Results from Sm-Nd analysis with calculations based ε_{Nd}(1600 Ma) for East River and Kaertok formations, ε_{Nd}(1400 Ma) for Fort Confidence Formation.

Sample	Formation	[Nd] ppm	$^{147}Sm/^{144}Nd$	$^{143}Nd/^{144}Nd$	$\varepsilon_{Nd}(0)$	$\varepsilon_{Nd}(T)$	T_{DM}(Ma)
K100	East River	26	0.1373	0.512279	-16.9 ± 0.5	-4.8± 0.5	2657
K101	East River	22	0.1216	0.512033	-18.7 ± 0.5	-3.3± 0.5	2358
K104	East River	52	0.0777	0.511661	-26.8 ± 0.5	-2.3± 0.5	2059
K119	Kaertok	19	0.1058	0.511559	-26.4 ± 0.5	-7.8± 0.5	2563
K120	Kaertok	40	0.1098	0.511731	-25.5 ± 0.5	-7.7± 0.5	2598
K121	Kaertok	38	0.1257	0.511833	-22.8 ± 0.5	-8.2± 0.5	2822
K106	Fort Confidence	72	0.1006	0.511425	-23.7 ± 0.5	-6.4± 0.5	2262
K110	Fort Confidence	105	0.1298	0.512213	-17.0 ± 0.5	-5.0± 0.5	2435
K112	Fort Confidence	66	0.0899	0.511693	-25.6 ± 0.5	-6.4± 0.5	2186
K114	Fort Confidence	48	0.1071	0.511766	-25.8 ± 0.5	-9.8± 0.5	2554
G80-239	Narakay	N/A	0.1069	0.51225914	N/A	3.49± 0.5	1807
679-299b	Narakay	N/A	0.1620	0.512370	N/A	2.13± 0.5	2175

8.0 Stable C and O Isotope Analysis

8.1 Introduction and justification of method

Carbon from atmospheric CO_2 is fixed during photosynthesis as organic matter and in turn, large fractionations occur between the stable isotopes ^{12}C and ^{13}C. ^{12}C is preferentially incorporated into plant tissues, known as the organic carbon reservoir (Arthur et al, 1983). The other major carbon reservoir is held in carbonate minerals precipitated from a solution (hydrothermal fluids, sea water etc.). The initial isotopic ratio of a solution is preserved in carbonate minerals during precipitation because little fractionation of ^{12}C and ^{13}C occurs during precipitation (Arthur et al, 1983). The ratio between ^{12}C and ^{13}C, expressed as $\delta^{13}C$ relative to the standard PDB, is relatively constant throughout surface waters of the ocean and therefore carbonates precipitated at a given point in time from the global ocean should exhibit similar $\delta^{13}C$ values. This has proven a useful tool for correlation in sedimentary geology. Significant excursions (>4‰ $\delta^{13}C$) occur in the geologic record, and when tight chronostratigraphic data are available, these excursions can be used as markers across significant distances (~1000s kms) (Arthur et al, 1983).

Since carbonates are sensitive to diagenesis, and isotopic exchange may occur during recrystallization, the extent of diagenesis must be evaluated when considering whether or not the data represent a primary seawater signal. This can be done in a number of ways, including petrographic and cathodoluminescence microscopy and analysis of major elements. Elements such as Mn and Sr are particularly sensitive to

diagenetic alteration and can provide a good indication of diagenesis (Kaufman et al, 1991).

8.2 Analytical Methods

Samples were taken at one meter intervals through a 75m thick section of drill core (Figure 25) from the East River Formation. Samples were taken from split NQ drill core and used to produce thin sections for microscopic observations.

The extent of diagenesis was evaluated through microscopy, an analysis of major elements, and a comparison of stable isotopic data to global sea-level curves for the time of deposition. After petrographic examination, only least-altered samples were selected for analysis.

Standard petrographic and cathodoluminescence (CL) microscopy was completed on polished thin sections using an ELM-2 Luminoscope set at 12V running at a current of 50 mA under a vacuum of approximately of 50 millitor. Least-altered zones were identified following Kaufman et al. (1991) and selectively sampled from polished slabs corresponding to thin sections using a MicroMill microscope mounted drill and hand-held dremmel with a 500 μm bit. Micrite and micritic intraclasts were specifically drilled with care taken to avoid cross-cutting veins, late-stage meteoric cement, and recrystallized ooids.

Samples for stable isotopes of approximately 0.5 mg were weighed into glass vials followed by the addition of 0.1 ml of pure phosphoric acid to the side of the container. The containers were then capped and Helium-flushed while horizontal to

ensure no premature reaction of sample and acid. Samples were reacted at 50°C for 24 hours, followed by extraction from sample vials in continuous flow. Measurements were completed at the G.G. Hatch Stable Isotope Lab at the University of Ottawa using a Delta XP mass spectrometer and Gas Bench II, both from Thermo Finnigan.

Major elements (Fe, Mg, Mn, Ca, Sr) were analyzed through inductively coupled plasma atomic emission spectroscopy (ICP-AES) at the University of Ottawa. Samples were analyzed at approximately 10 m intervals. Samples were microdrilled from the same locations as samples that were taken for stable isotopes. Samples are equivalent geochemically to those measured for stable isotopes assuming homogeneity within individual intraclasts and beds. 10-20 mg samples were dissolved in nitric acid and run on the ICP-AES housed at the University of Ottawa. In a few samples, small amounts of undissolved residue remained after dissolution in nitric acid. This residue was dissolved in HF and then redissolved in nitric acid and run separately on the ICP-AES to ensure all material was measured.

8.3 Results

8.3.1 Petrography and cathodoluminescence (CL)

Massive mudstone

Massive dolomudstones are typified by heterogeneous degrees of recrystallization ranging from dolomicrite (<4 μm) containing little to no dolomicrospar (5-30 μm) to dolomicrospar with no micrite containing up to 30% sparry dolomite (>30 μm). Potassium ferricyanide stain reveals a very pale blue stain indicating a slight

enrichment in iron. Post-depositional silicification in many mudstones is present as cherty replacements in (up to 5% in some samples). Detrital siliciclastic grains (quartz, muscovite) comprise up to 10% of most mudstones. Authigenic quartz is common as overgrowths on relict detrital grains. Many samples show evidence of partial dissolution in the form of dissolution seams and stylolites; these were not sampled for stable isotopes. Varying degrees of alteration to hematite and an iron-rich clay mineral is present in the form of concentrations of opaque material and a mottled texture in hand sample. Barite is rarely present as nodules in some samples. Cathodoluminescence of massive mudstones is heterogeneous and ranges from non-luminescent to brightly luminescent but they are otherwise indistinguishable petrographically (Figure 22a and 22b).

Microbially laminated mudstone

Microbially laminated mudstones are generally composed of >70% dolomicrite with varying degrees of recrystallization to sparry dolomite. Laminae are defined by alternating irregular beds of micrite and cement. Silicification is common, preferentially forming as replacements of laminae by chert or as up to 2cm-sized nodules. Discontinuous beds of green clay (glauconite??) and dark organic rich lamina(?) are present in most samples. Staining reveals a slight enrichment in iron. Shrinkage cracks and salt casts filled with secondary dolomite are present in some samples. Luminescence of micritic material is heterogeneous as described above. Cement-rich beds of sparry dolomite are brightly luminescent and chert is non-luminescent.

Secondary calcite veins are non-luminescent and appear much larger under cathodoluminescence than when viewed under regular transmitted light (Figure 22c and 22d).

Peloidal packstone

Peloidal dolo-packstones are not abundant and, where present, commonly form cm-scale beds within massive mudstones. Cathodolouminescence is bright to dull in peloids and heterogeneous in the matrix component. Staining reveals a very slight enrichment in iron in dolomite, and Fe-rich calcite veining (Figure 22e and 22f).

Ooid/Peloidal grainstone

Ooid dolo-grainstones are moderately well preserved with well preserved concentric lamination, but no radial crystals intact. Ooids are commonly replaced by chert. Sparry dolomite is present as coarse cement. In cathodoluminescence ooids are typically dull luminescent with a fine-grained bright luminescent isopachous cement. Sparry dolomite is non-luminescent. Peloidal dolo-grainstones are very similar to ooid grainstone with the exception that peloids are heavily recrystallized and may be altered ooids. Peloids are brightly luminescent with fine-grained cement also brightly luminescent. Sparry dolomite in larger voids is coarser grained and non-luminescent (Figure 23a and 23b).

Intraclastic floatsone/rudstone with grainstone matrix

Intraclastic floatstone ranges from framework to matrix supported with the matrix composed of ooids, intraclasts and terrigenous detritus. Intraclasts are micritic, sporadically re-crystallized to microspar. Ooids are commonly partially silicified, collapsed, sheared, or amalgamated. Variable chemical compaction has occurred with some samples displaying abundant stylolites and sutured grain contacts, and others exhibiting little evidence of compaction. Only samples exhibiting little to no evidence of chemical compaction or dissolution were sampled for stable isotopes. In general, cement is composed of sparry dolomite and is commonly replaced by chert or barite. Under CL, two distinct generations of cement are apparent; a fine-grained brightly luminescent variety that surrounds grains and a coarse-grained, blocky, non-luminescent variety that fills void spaces between grains (Figure 23c and 23d). Micritic intraclasts display heterogeneous luminescence as described above. Ooids commonly show concentrically zoned, alternating, bright and dull luminescence due in part to partial silica replacement.

8.3.2 Stable Isotopes

Values of $\delta^{13}C$ range between -1.5 ‰ and 0.5 ‰ VPDB with an average of -0.63 ‰. Error for both $\delta^{13}C$ and $\delta^{18}O$ is +/- 0.1 ‰. When plotted on a graph versus depth below surface a slight trend becomes apparent (Figure 25). $\delta^{13}C$ increases from -1.52 ‰ to a maximum of 0.4 ‰ from 210 m to 175 m below surface. Samples for this interval were from micritic intraclasts. A slight decrease is observed beginning at 175 m down to

approximately -1.40 ‰ at 145 m where it stabilizes upwards to a depth of 125 m below surface. Samples in this invertal were from microspar, microbial lamination, void-fill cement, ooids, and micrite. No direct link between isotopic values and lithology of sample was observed.

$\delta^{18}O$ ranges between -12.55 ‰ and -6.68 ‰VPDB with an average of -8.76 ‰. Overall, there is a gradual up-section increase in $\delta^{18}O$. The trend of increasing values from 210 m to 175 m is the same as the trend for $\delta^{13}C$, but opposite to the $\delta^{13}C$ trend from 175 m upwards. In a cross-plot of $\delta^{13}C$ vs. $\delta^{18}O$ most $\delta^{13}C$ values cluster tightly close to -0.6 ‰. $\delta^{18}O$ shows more variance with a loose cluster around the mean of -8.7 ‰.

8.3.3 Major Elements

The major elements Ca, Mg, Fe, Mn, and Sr were analyzed in seven samples at approximately 10 m intervals. Strontium values throughout the samples are low, <50 ppm in all samples. Manganese values are very high, ranging between 500-7000 ppm. Ratios of Mn/Sr show two distinct groupings, Mn/Sr ratios of <100 and Mn/Sr ratios of >200. A cross-plot of Fe/Sr and Mn/Sr show a distinct cluster of samples with lower ratios, with a few outlying samples. It should be noted however, that anomalous Fe/Sr and Mn/Sr ratios are not associated with anomalous $\delta^{13}C$ or $\delta^{18}O$ values. A cross-plot of Mn/Sr and $\delta^{18}O$ shows that higher Mn/Sr ratios are more strongly associated with more negative $\delta^{18}O$ values.

Table 5: Stable isotope and major element results

Sample	Depth (m)	Component	$\delta^{13}C$ (‰VPDB)	$\delta^{18}O$ (‰VPDB)	Mg/Ca	Sr (ppm)	Mn (ppm)	Fe (ppm)	Mn/Sr	Fe/Sr
K001	210.0	microspar	-1.52	-12.55	0.55	31	7700	9659	246	308
K003	207.3	microspar	-0.88	-12.1						
K013	196.1	microspar	-0.79	-11.67						
K019	190.0	microspar	-0.03	-10.5	0.56	16	2392	6826	154	440
K021	188.0	microspar	0.04	-10.62						
K023	186.0	microspar	0.33	-8.8						
K025	184.0	microspar	0.20	-9.79						
K027	181.0	microspar	0.28	-8.12						
*K027-D	181.0	microspar	0.44	-8.3						
K029	179.0	microbial lamination	0.29	-9.57	0.56	18	905	4025	51	229
K030-B	178.0	void-fill cement	0.38	-7.82						
K031	177.0	ooid	0.13	-9.10						
***K033	175.0	microspar	-0.92	-10.55	0.58	43	1246	7689	29	179
K035	173.0	micritic intraclast	-0.54	-9.96						
K037	171.0	micritic intraclast	-0.55	-9.29						
K039	169.0	micritic intraclast	0.04	-9.11						
K041	167.1	micrite	-0.34	-8.64						
K043	165.0	microspar	-0.48	-9.91						
K047	161.0	micritic intraclast	-0.59	-7.35	0.58	27	498	2638	18	96
K047-D	161.0	micritic intraclast	-0.64	-7.31						
K049	159.0	micritic intraclast	-0.99	-10.19						
K051	157.0	micritic intraclast	-0.84	-6.82						
K053	155.0	micritic intraclast	-0.88	-7.96						
K055	153.0	micritic intraclast	-0.88	-6.97						
K057	151.0	micritic intraclast	-0.8	-7.59						

Sample	Depth (m)	Component	$\delta^{13}C$ (‰VPDB)	$\delta^{18}O$ (‰VPDB)	Mg/Ca	Sr (ppm)	Mn (ppm)	Fe (ppm)	Mn/Sr	Fe/Sr
K059	149.0	micritic intraclast	-0.84	-7.73						
K061	147.0	micritic intraclast	-0.82	-7.24	0.57	109	1166	6496	11	60
**K063-A	145.0	micritic intraclast	-1.4	-10.16						
**K063-B	145.0	void-fill cement	-1.28	-6.68						
K067	141.0	micritic intraclast	-1.53	-6.92						
K067-D	141.0	micritic intraclast	-1.54	-6.99						
K069	139.0	micritic intraclast	-1.18	-8.31						
K071	137.0	microspar	-1.44	-7.08	0.57	42	627	2805	15	66
**K073-A	135.0	micritic intraclast	-1.3	-6.9						
**K073-B	135.0	void-fill cement	-1.14	-7.85						

* - duplicate sample
** - multiple components from same sample
***-very small, interpret with caution

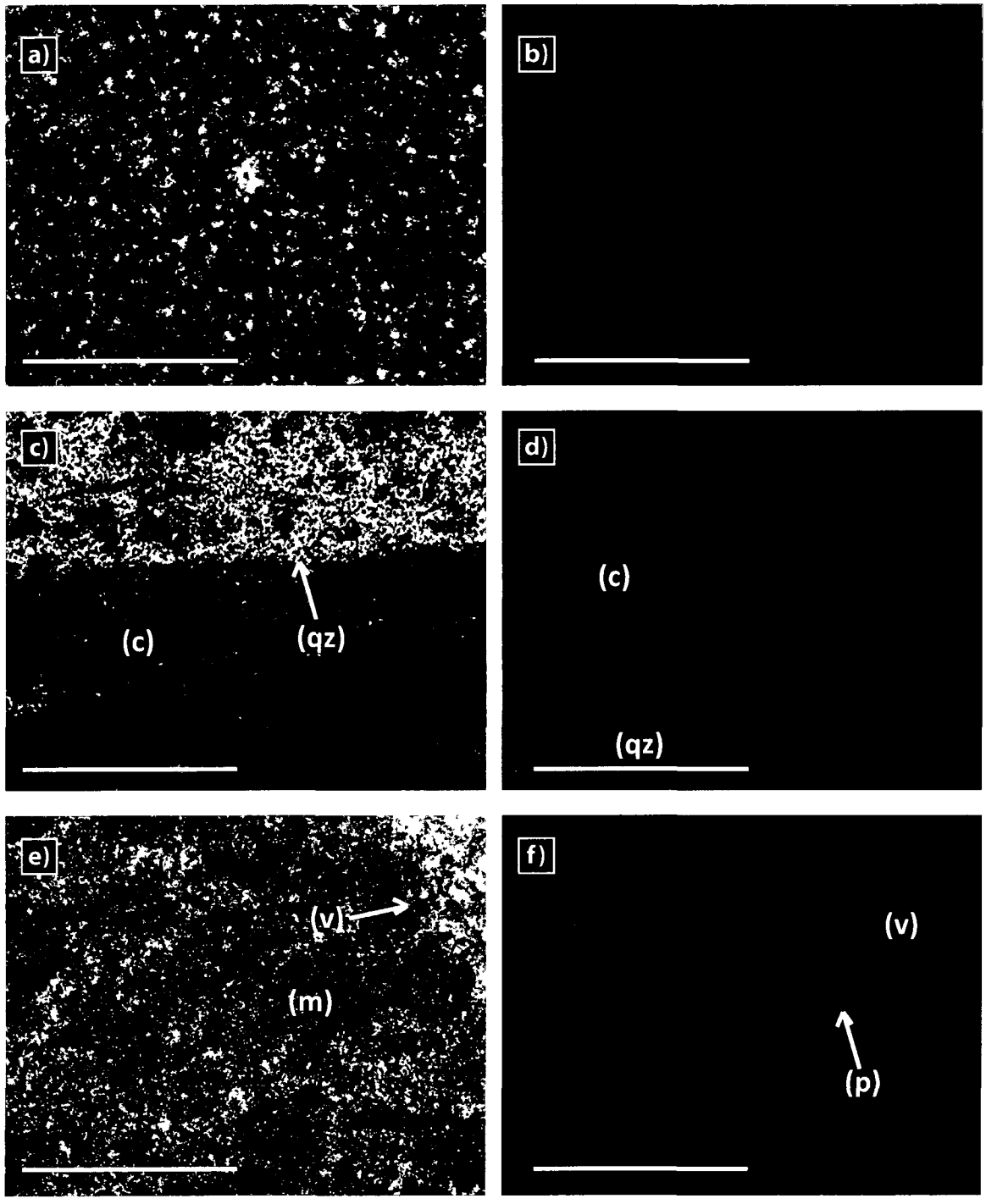

Figure 22: Photomicrographs of several thin sections in plane polarized light, and corresponding image under CL. a) Massive dolomudstone b) Heterogeneous texture of massive dolomudstone in CL c) Microbially laminated mudstone showing cement (c) rich layers and silicification (qz) d) Bright luminescent cement and non-luminescent chert e) Peloidal packstone showing micrite (m) and calcite vein (v) f) Peloids (p) and non-luminescent calcite vein (v) in peloidal packstone. Scale bar 1 mm.

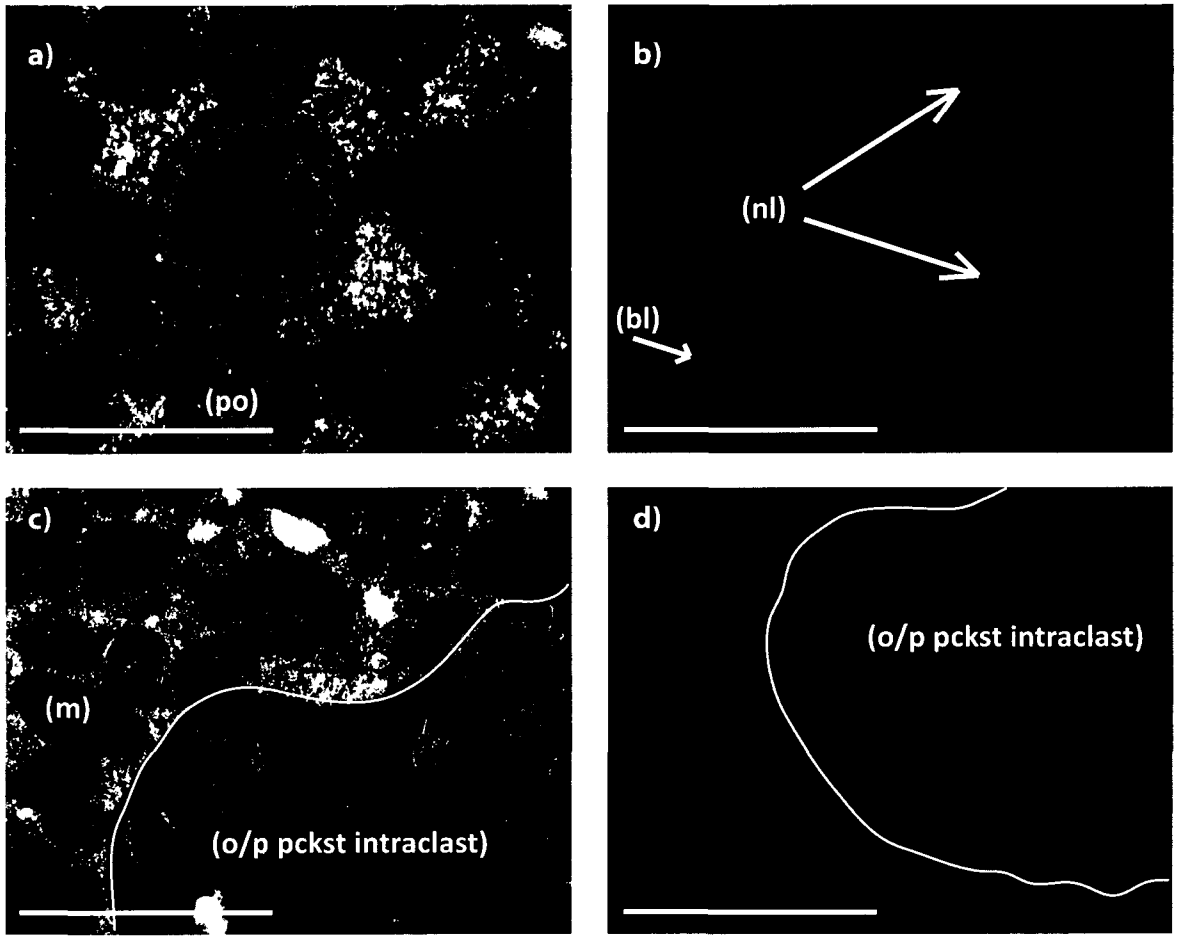

Figure 23: Photomicrographs of thin sections in plane polarized light, and corresponding image under CL. a) Ooid grainstone showing ooids which have been phosphotized (po) b) Two generations of cement, fine-grained bright luminescencent spar (bl) and non-luminescent coarse dolo-spar (nl) c) Intraclastic floatstone showing intraclasts of micrite (m) and ooid/peloid packstone (o/p pckst) d) Bright luminescent cement on grain boundaries, non-luminescent void-fill cement. Scale bar 1 mm.

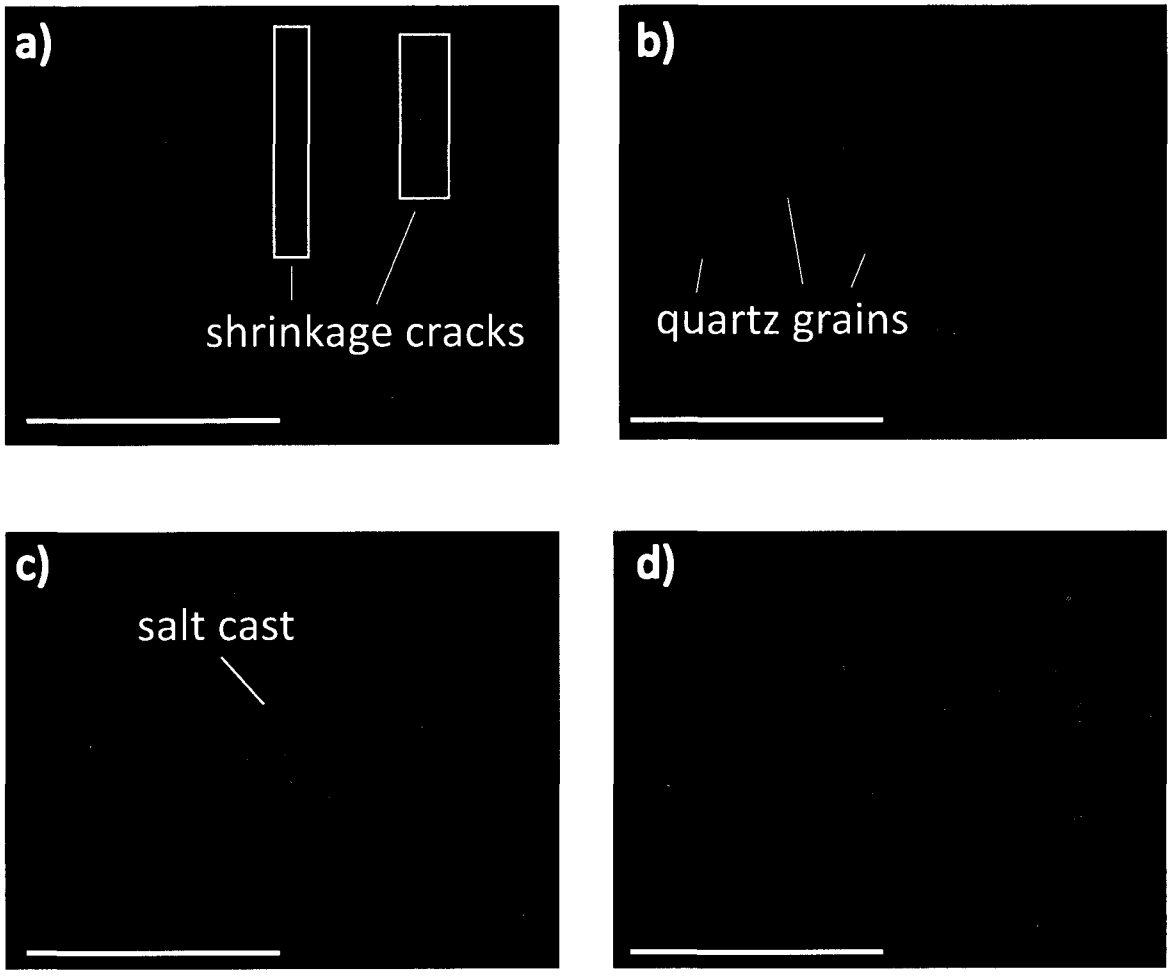

Figure 24: Sedimentologic features of the East River Formation. All photos at 10x mag under CL. a) Non-luminescent (NL) shrinkage cracks in micrite b) Rounded, detrital quartz grains (NL) in dolo-microspar c) NL salt cast in dull luminescent (DL) micrite d) Partially silicified (NL) coated grains with bright luminescent (BL) dolomite cement Scale bar 1 mm

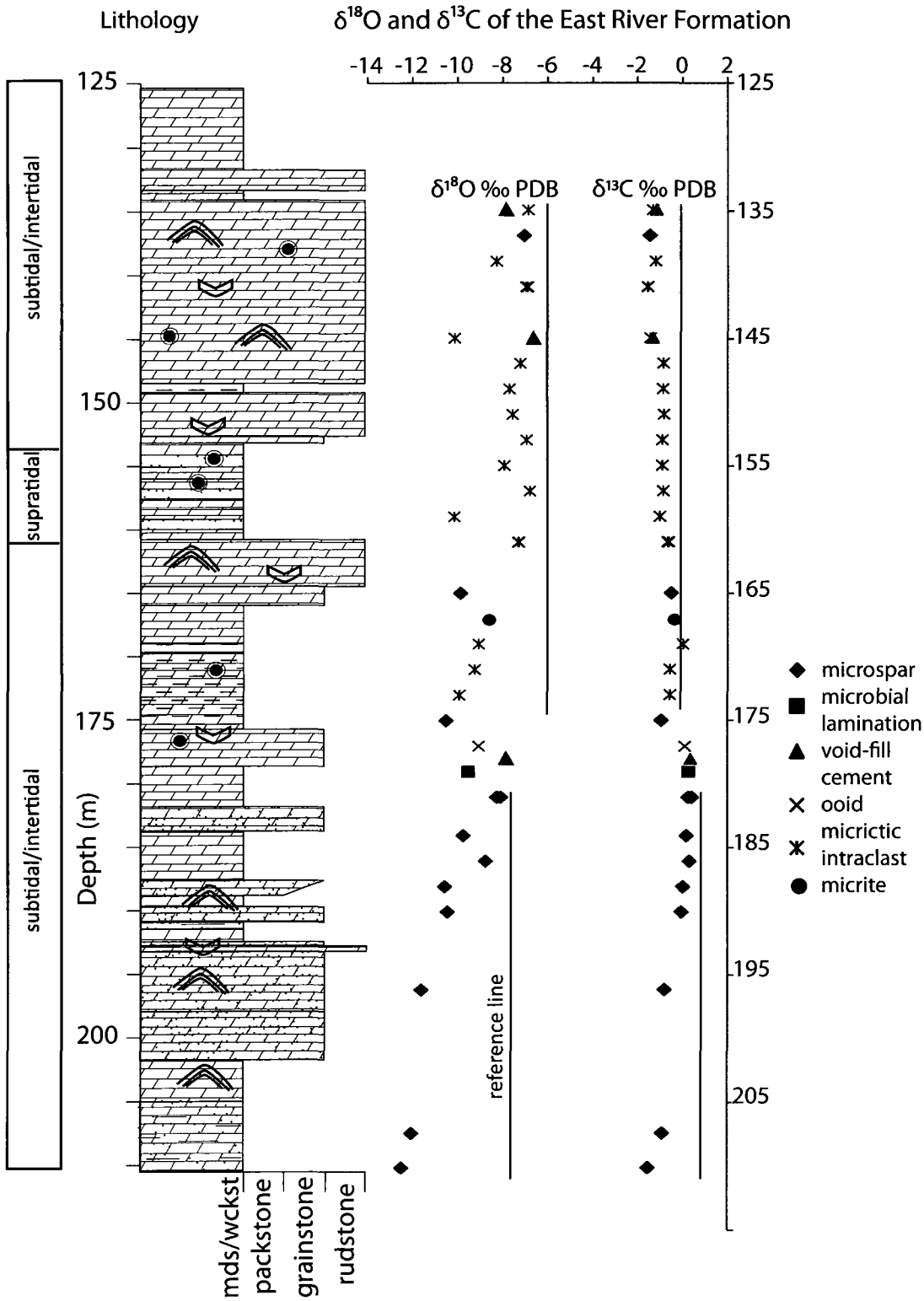

Figure 25: Stratigraphic section from drill hole ML06-019 illustrating stable isotope results. Reference lines present for comparison of isotopic trends. Refer to Figure 9 for lithologic legend.

a)

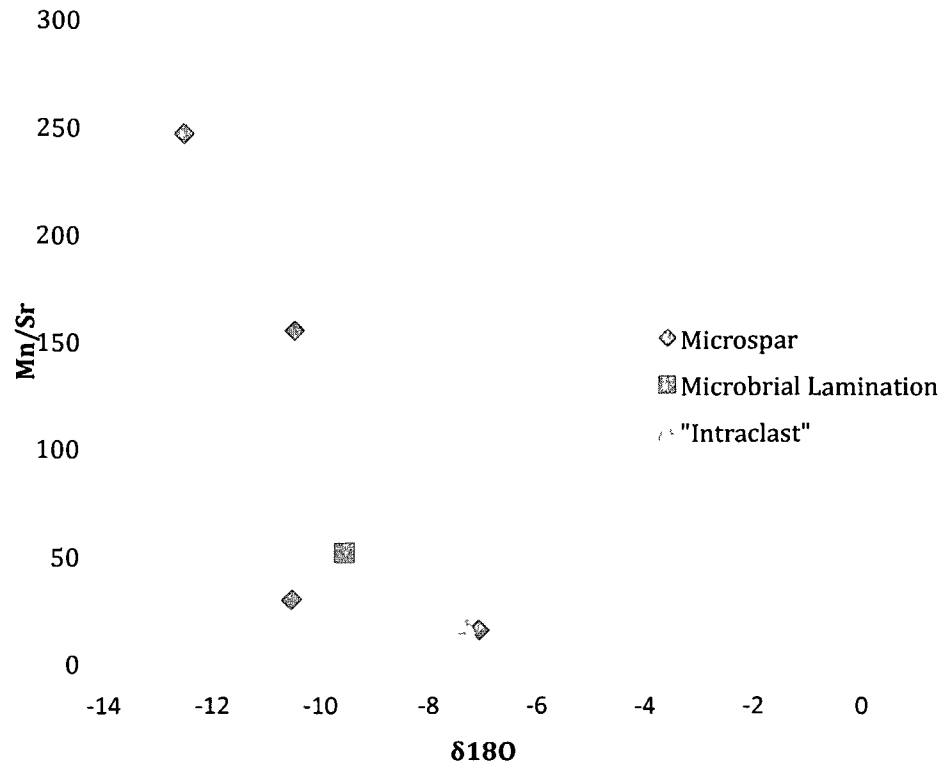

b)

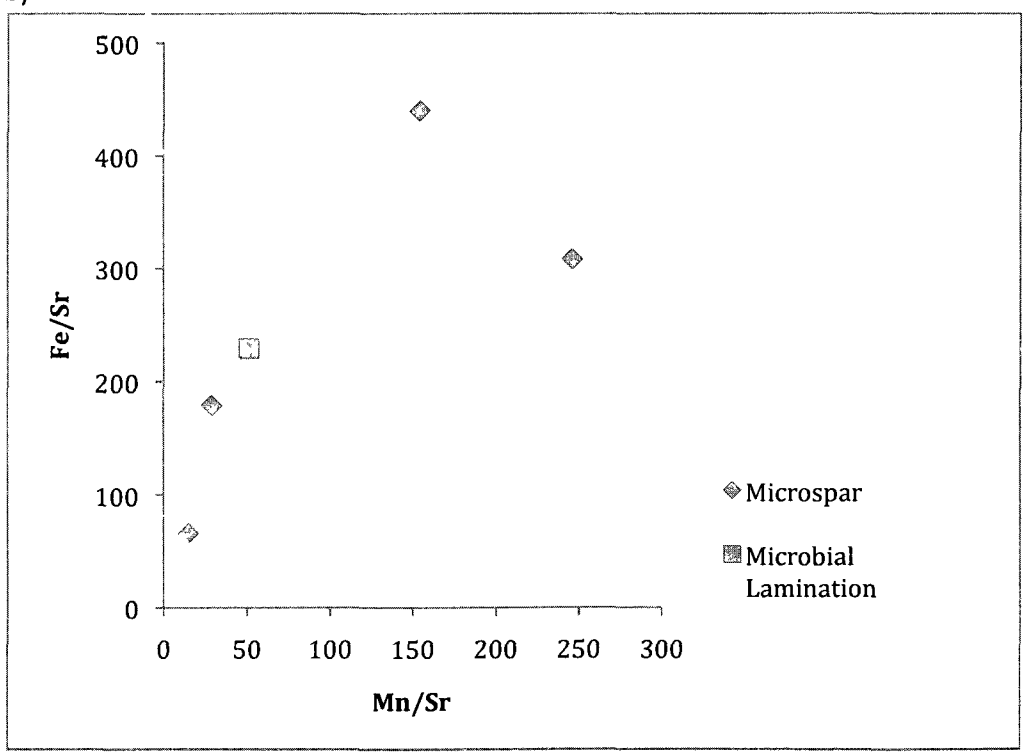

Figure 26: Major element plots of the East River carbonates used for alteration documentation. a) Mn/Sr vs $\delta^{18}O$ b) Fe/Sr vs Mn/Sr.

Mg/Ca ratios are all >0.5, indicating extensive dolomitization, described above. Calcite is present only in very few late-stage veins, which were not analyzed.

8.4 Discussion of Results

No study of stable isotopes is complete without a full evaluation of post-depositional alteration. Work by Knoll et al (1995a) suggests that samples retaining a Mn/Sr ratio as high as 10, much higher than the ratio of 2 originally suggested by Brand and Veizer (1980), can produce a reliable primary carbon isotope signature. Samples within our data set are much higher, with the lowest ratio being 18, and the highest ratio being 436. Strontium loss in carbonates has been reported to occur during early dolomitization, which may partially explain the extreme Mn/Sr values in our study (Veizer, 1983). In general, high Mn concentrations (Mn/Sr ratio >10) are indicative of reducing pore-waters during late-stage diagenesis, while low values are characteristic of initial sea-water values (Brand and Veizer, 1980). These assumptions however are based on a data set from the Phanerozoic, where sea-water is more oxygenated and bioturbation is a significant factor in controlling chemical conditions at the sediment-water interface which (Lindsay and Brasier, 2000).

In a cross-plot of Mn/Sr versus $\delta^{18}O$, a negative correlation is observed (Figure 26). Mn/Sr ratios decrease as $\delta^{18}O$ increases. There is a small cluster of samples with low Mn/Sr ratios and high $\delta^{18}O$ values, which likely represent the least altered samples. These samples with low Mn/Sr ratios are dominantly from micritic intraclasts, wheres high Mn/Sr ratios are samples from microspar. Petrographically microspar is

recrystallized so there may be a correlation between high Mn contents and extent of recrystillization. Mn/Sr ratios in these samples however still exceeds what is normally understood to represent primary ratios and therefore the $\delta^{18}O$ values associated with these values may not represent primary values and should be interpreted with caution. $\delta^{13}C$ therefore should also be interpreted with caution. Variations in $\delta^{13}C$ are may be due to a diagenetic overprint rather than a primary signal. It should be noted that many studies conclude that it is possible that carbonates of Precambrian age can retain near primary values (Knoll et al., 1995). $\delta^{18}O$ is understood to undergo isotopic exchange more readily than $\delta^{13}C$ during diagenetic reactions and therefore is less likely to preserve a primary signal. The effects of diagenesis are often reflected in carbonates as a trend of sharply decreasing $\delta^{18}O$ with slightly decreasing $\delta^{13}C$ (Frank, 2003). Our data is interpreted to follow this trend.

Lindsay and Brasier (2000) conducted a detailed study to define a carbon isotope reference curve for the ca. 1700-1575 Ma McArthur and Mt. Isa basins, where they concluded that global sea-water values were relatively monotonic, within 0.5‰ of a mean of -0.5 ‰ within that time interval. Their study included a detailed screening process of selecting least altered samples, thin section evaluation, analysis of trace and major element composition, and assement of the isotopic data in order to confirm that the preserved $\delta^{13}C$ values were primary. Values for $\delta^{13}C$ in the East River Formation (~1630 Ma) are within the range of data determined from strata of similar age in the Mount Isa and McArthur basins indicating that the East River Formation may have retained its primary isotopic composition. The retention of some primary fabrics also

gives good indication that East River carbonates have not been extensively recrystallized.

The preservation of rare microfossils in chert observed by Horodyski et al. (1985) within the East River Formation indicates that silicification in at least some parts of the basin occurred during early diagenesis. Since the organic walls on bacteria can decay in a matter of days to months, silicification must have occurred very early (Knoll and Swett, 1990; Kaufman et al. 1991). It is also evident that lithification occurred shortly after deposition by the abundant intraclasts of micrite observed petrographically. Most intraclasts are angular to sub-rounded, indicating that they were not transported far, and likely originated locally on the sea-floor and were re-worked by wave action in the subtidal environment. Mud cracks and mud rip-ups along these horizons indicate that lithification occurred quickly in the peritidal environment as well.

Because cementation (lithification) was operating at the surface, or just below the sediment-water interface, primary porosity was significantly reduced before diagenetic processes became dominant causing low water-rock ratios (Frank, 2003). This process, along with early dolomitization and early silicification may have been responsible for sealing carbonates from flow of later stage diagenetic fluids (Frank, 2003). In the East River Formation, this may have occurred, but only locally due to the diagenetic alteration of at least some samples.

Our data set is very similar to interpreted global values from Lindsay and Brasier (2000) which may support the hypothesis that East River Formation carbonates have partially retained initial $\delta^{13}C$ values. Although samples have been somewhat

diagenetically altered, most diagenesis likely occurred shortly after deposition. Isotopic exchange reactions during recrystallization of carbonates are less pervasive for carbon due to the low concentration of carbon and the high concentration of oxygen in water. $\delta^{18}O$ is a good tracer for diagenetic alteration as isotopic exchange occurs more easily. The stratigraphic trend of $\delta^{13}C$ is slightly variable, with the overall pattern being a less exaggerated version of the $\delta^{18}O$ trend. Thus, variations in $\delta^{13}C$ can likely be attributed to diagenesis, rather than a primary signal. The preferred interpretation is that the East River Formation may have retained a near-primary signal. The similarity of our data to other published C isotope curves for the late Paleoproterozoic supports that the shift was likely minor, but individual excursions within our data should not be used as a correlation tool. In summary, the East River Formation has retained a relatively monotonic $\delta^{13}C$ curve, which is characteristic of other Paleoproterozoic carbonates.

8.5 Conclusions

1. Lithification and silicification occurred near the time of deposition of the East River Formation, possibly "locking in" the $\delta^{13}C$ signature, similar to the process described by Frank et al. (2003) from the overlying Dismal Lakes Group.
2. The East River Formation was subjected to some diagenetic alteration as shown by petrographic and CL studies. This is corroborated by major element geochemical anaylsis of selected samples, which have high Mn and Fe concentrations, and low Sr concentrations.

3. The $\delta^{13}C$ signature of the East River Formation is monotonic with an average of -0.5 ‰ PDB, which is consistent with other carbonates of late Paleoproterozoic age. Because the $\delta^{13}C$ values are so similar to global Paleoproterozoic values, they may represent a primary sea-water value, or may have experienced a slight shift to more negative values due to diagenesis, which would account for their high Mn values and low Sr values.
4. $\delta^{18}O$ values are much more susceptible to isotopic exchange during diagenesis and due to the higher variability likely do not represent a primary value.

9.0 Discussion

New stratigraphic and geochemical information from the Hornby Bay Basin supports correlation of deep-water marine sedimentary rocks of the Wernecke Supergroup, of the Wernecke Mountains of the northern Canadian Cordillera, with shallow-water sedimentary rocks of sequence A2 of the Hornby Bay Group.

9.1 Linking deformation of A2 to the Forward Orogeny

The Forward Orogeny is interpreted to be a compressional deformation event that generated basement anticlinal and thrust-block uplifts in northwestern Canada during the late Paleoproterozoic (Cook and Maclean, 1995). Structures associated with this deformation have been identified in outcrop and the subsurface in sub-sequence A2 (eg. Maclean and Cook, 2004). An example of these structures was observed in the vicinity of the Mountain Lake uranium deposit where uplift occurred along the Teshierpi

fault generating fold and overturned beds within the Hornby Bay Group (A2), but not in the overlying Dismal Lakes Group (A3). A westward-tapering wedge of intraformational fragmental dolostones of canabilized East River dolostones indicates that uplift was initiated during late deposition of the East River Formation (Ross, 1983). Based on the age of the Narakay Volcanic Complex (~1663 Ma), which is contemporaneous with the East River Formation, an approximate maximum age can be assigned to the Forward Orogeny (Cook and Maclean, 1995). The age of the termination of the Forward Orogeny is more poorly constrained. In the study area, clasts of locally derived fault breccia were recognized within alluvial fan deposits of the basal LeRoux Formation (A3), indicating that faults were reactivated during early deposition of the Dismal Lakes Group. The LeRoux Formation is younger than 1590 Ma based on U-Pb detrital zircon geochronology (Rainbird et al. 2009, unpublished) and the Western Channel Diabase (~1590 Ma) that cuts sequence A2 but has not been observed in A3 (Hamilton and Buchan, 2010). This puts an end to the Forward Orogeny somewhere around 1590 Ma.

9.2 Paleogeography of the Hornby Bay Basin

The Wernecke Supergroup is a thick (>13km) succession of metasedimentary rocks exposed in central Yukon (Delaney, 1981). Strata were deformed by the ~1.6 Ga Racklan orogeny and intruded by the Wernecke Breccia (Thorkelson et al., 2005). The Wernecke Supergroup is unconformably overlain by the Pinguicula Group (Figure 28). The Wernecke Supergroup is ~500 km west of the Hornby Bay Group and is characterized by thick deposits of deep-water turbidites that pass

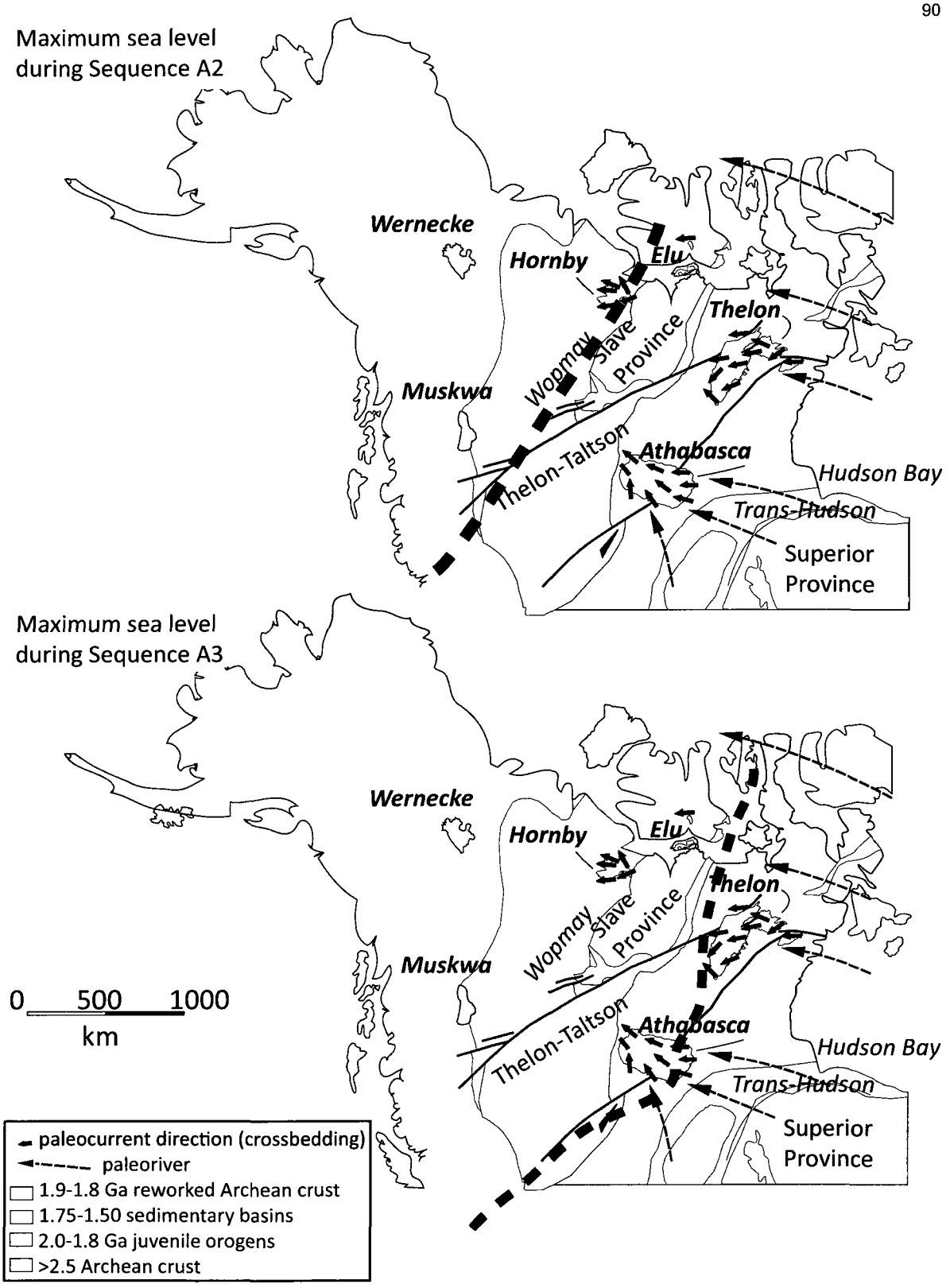

Figure 27: Generalized map of present day North America illustrating approximate extent of intracratonic sea at ~1650 Ma (A2) and ~1400 Ma (A3).
Modified from Rainbird and Young (2009).

gradationally up-section into shallow marine carbonates. The age of the Wernecke Supergroup, and its deep-water sedimentary rocks led Young et al. (1979) to propose that it was a distal equivalent to the Hornby Bay Group. Correlating Sequence A2 of the Hornby Bay Group to the Wernecke Supergroup provides a good model of a westward-deepening basin. Turbidites at the base of the Wernecke Supergroup correlate well to the proximal Lady Nye fluvial/deltaic system. The carbonates which overlie turbidites in the Wernecke Supergroup correlate well with the dolomitic East River Formation of the Hornby Bay Group.

Deposition during late A2 was observed in the Hornby Bay Basin as a marginal marine basin which deepened to the west. This is reflected in thicker sediment packages and deeper-water facies west of the Leith Line. The Leith Line was interpreted to represent a structural hinge underlying Hornby Bay strata that may have been a suture zone within the Wopmay Orogen. Subsidence is interpreted to have been greater west of the Leith Line (Ross, 1983). Strata dramatically thin to the east in the HBG and some pinch out. The East River carbonates and the Kaertok deltaic deposits are not present east of the Teshierpi fault-zone, implying that this may have been the most eastern extent of marine facies deposited during A2. If this westward-deepening and stratigraphic thickening trend is continuous, then the Wernecke Supergroup may represent a distal equivalent to the Hornby Bay Group (Young et al., 1979).

This interpretation suggests that the Hornby Bay Group was part of a broad epicontental sea that reached to the shelf-margin (Wernecke Supergroup), and potentially to the open ocean. Intertidal and terrestrial facies associations observed in

the Hornby Bay Group indicate that the Hornby Bay Basin represents the approximate location of a westward sloping shoreline (Figure 27). It is unknown how far south this basin extended. Deep-water deposits of the Muskwa assemblage, located in British Columbia, may have been part of the same basin (Ross, Villeneuve et al. 2001). Sediments of sequence 3 of the Athabasca Group are of the same age but reflect lacustrine and terrestrial depositional environments, and so the extent of the shoreline was unlikely to have reached that far southeast (see below for more detailed discussion of correlation).

Sequence A3 (Dismal Lakes Group) of the Hornby Bay Basin records the gradual development of a much deeper marine environment. Strata at the base of A3 are characterized by terrestrial and shoreline depositional environments. These terrestrial sedimentary rocks pass up-section into deep-water shelf-carbonates. This basin was much more extensive than in A2 and marine sediments can be correlated east to the Elu basin and southeast to the Athabasca basin (Figure 1). The Pinguicula Group in the Wernecke Mountains may represent a distal equivalent of the Dismal Lakes Group of the Hornby Bay Basin (Figure 27).

9.3 Potential Correlation with the WSG – The Forward and Racklan Orogenies

The Racklan orogeny is defined as a Proterozoic deformational event that affected strata in the Rackla River area of the Wernecke Mountains, Yukon Territory (Gabrielse, 1967; Young et al. 1979; Cook, 1992), including the Wernecke Supergroup, but not the overlying Pinguicula Group. The Racklan orogeny comprises three phases of

deformation that produced east-verging overturned folds and a schistose fabric, followed by south-verging folds, crenulations, and kink bands. This event caused partial exhumation and erosion of Wernecke strata, prior to deposition of the Pinguicula Group. A maximum age constraint on the event is based on the 1663 Ma age of the Narakay Volcanic Complex constrained by the presence of Narakay-aged detrital zircons (Furlanetto et al., 2008). The upper age of the event is constrained by the Wernecke Breccia, which intrudes the deformed Wernecke strata. The Wernecke Breccia is considered to be approximately 1600 Ma in age based on one U-Pb titanite age (Thorkelson et al, 2005).

Based on the similarity in age of the Racklan and Forward orogenies they can be considered one and the same event (Cook, 1992; Laughton et al, 2005; Thorkelson et al, 2005). This helps refine the correlation between the Wernecke Supergroup and the Hornby Bay group, originally suggested by Young et al. (1979).

The correlation between the two basins was further refined by Maclean and Cook (2004), who linked the Wernecke Supergroup to sub-sequence A1 of the Hornby Bay Basin, which was based on the previous assumption that the Wernecke Supergroup was >1710 Ma is age. This presumption was made based on the age of the Bonnet River Plume intrusions, which were considered to intrude the Wernecke Supergroup (Thorkelson et al, 2005; Laughton et al, 2005). Problems exist with this correlation because A1 in the Hornby Bay Group is composed of dominantly fault-controlled fluvial and eolian sub-basins, whereas the Wernecke deposits are deep water turbidites that pass gradationally up-section to marine carbonates, making direct facies correlation

difficult. New U-Pb detrital zircon ages require the Wernecke Supergroup to be younger than originally hypothesized (Furlanetto et al, 2008), and the Bonnet River Plume intrusions do not intrude the Wernecke Supergroup. Rainbird et al. (2009) refined the correlation by specifically correlating the Wernecke Supergroup with A2 of the Hornby Bay Group (Figure 28), based primarily on the new detrital zircon data, and on the relative stratigraphic position of similar platformal carbonates within each basin. In order to test this correlation a comparison between Sm-Nd isotopic signature on mudrocks and stable C isotopes from carbonates is discussed below.

9.4 Linking sedimentary provenance to the Wernecke Supergroup

U-Pb detrital zircon geochronology has revealed the maximum age for the Wernecke Supergroup to be nearly 100 million years younger than the minimum age that was previously hypothesized. The presence of abundant detrital zircons with ages between 1600-1700 Ma constrains the age of the Wernecke Supergroup to be similar to sequence A2 of the Hornby Bay Group. As well, the age distribution profiles of detrital zircons in the Wernecke Supergroup (Furlanetto et al, 2008) bear a striking similarity to those in the Hornby Bay Group (Rainbird et al., 2009). Both groups show strong abundances at 1900 Ma and 2200 Ma, which indicate both basins likely received detritus from common sources. Most notable in the Wernecke Supergroup is the presence of zircons approximately 1660-1610 M in age (Furlanetto et al, 2008), which are in the same age range as detrital zircons from the East River Formation of the Hornby Bay Basin (Rainbird et al., 2009, unpublished)

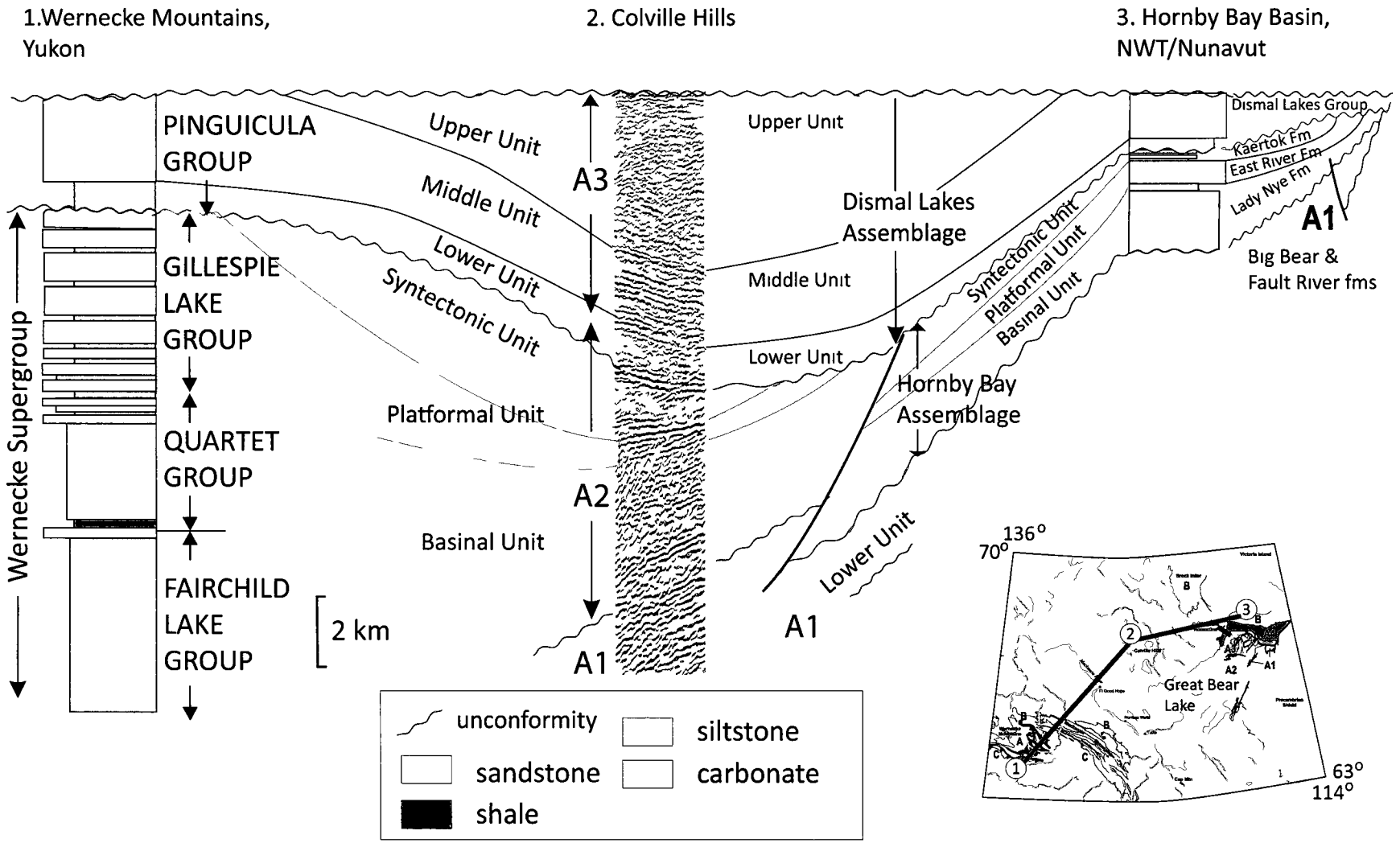

Figure 28: Stratigraphy of the Wernecke Supergroup between the Hornby Bay Basin and Wernecke Mountains, from Rainbird et al., 2008

Preliminary results from Sm-Nd analyses on mudrocks in the Wernecke Supergroup show good correspondence with Hornby Bay those presenting in this study, although a much wider range of values was noted (Furlanetto, pers. com.).

9.5 Carbon isotope stratigraphy of the Hornby Bay Group and Wernecke Supergroup

Rainbird et al (2009) suggested that carbonates of the Gillespie Lake Group (upper Wernecke Supergroup) represent the distal equivalent of the East River Formation carbonates (Figure 28). Recent work by Furlanetto (pers. com.) has established a low-resolution C- isotope curve through a complete section, approximately 20 samples over 4 km of stratigraphic section, for the Gillespie Lake Group. While the resolution of this curve is too low to make precise correlations, it provides a broad-scale data trend for purposes of comparison.

Both data sets fall within a range in $\delta^{13}C$ from -2‰ to +0.5‰ VPDB. These data sets also fall within range of proposed global isotopic values during the Late Paleoproterozoic (Lindsay and Brasier, 2000; Kah et al, 2003). This supports the interpretation of a near-primary $\delta^{13}C$ signal within the Gillespie Lake Group. One caveat to this interpretation is that cross-cutting carbonate veins within the Gillespie Lake carbonates were analyzed and exhibited C values similar to the interpreted primary carbonate. Higher resolution sampling, a major element analysis, and detailed petrography is needed to state with confidence whether the Gillespie Lake Group carbonates have preserved a primary sea-water C value.

9.6 Paleoproterozoic basins – Implications for paleogeography – Canadian Basins

Broad correlations between Late Paleoproterozoic basins in Canada can be made with reasonable confidence. These correlations are based on similarities in age, sediment provenance, sequence stratigraphy, and paleocurrents (eg. Fraser et al., 1970; Young et al. 1979; Maclean and Cook, 2005; Rainbird et al., 2009). More specific correlations can be made based using the sub-sequences of the Hornby Bay Basin (Figure 30).

Sub-sequence A1 (~>1740 to <1726 Ma) of the Hornby Bay Basin is correlative to: (i) Sequences 1 and 2 of the Athabasca Basin, (ii) potentially the Wharton Group (1760-1740 Ma) of the Thelon Basin, and (iii) potentially to the base of the Tinney Cove Formation of the Elu Basin (Figure 30). Sedimentation during this period is characterized by broad fluvial and eolian systems with generally west-directed paleocurrents. Fault-controlled, rift-related sub-basins were common. In the Hornby Bay Basin, the Big Bear and Fault River formations are rift-related, fault-controlled sub-basins and may actually be precursors to the Hornby Bay Basin which was dominated by broad thermal subsidence (Ramaekers, 2010).

Sub-sequence A2 (~<1726 - ~1600 Ma) of the Hornby Bay Basin is correlative to: (i) Sequence 3 of the Athabasca Group, (ii) potentially the upper Tinney Cove Formation, (iii) the Wernecke Supergroup (see discussion above), and (iv) potentially the Muskwa assemblage (Fraser et al., 1970). This sequence records a broad marine-incursion, related to sag-phase sedimentation, throughout the craton with the development of carbonate platforms in the Hornby Bay Basin and Wernecke Supergroup. All of these

sequences, with the exception of the Muskwa assemblage, are bounded by an unconformity at the top at ca. 1600 Ma.

Sub-sequence A3 (~<1600 -1270 Ma) of the Hornby Bay Basin is correlative to: (i) sequence 4 of the Athabasca Basin, (ii) the Parry Bay and Ellice formations of the Elu Basin, (iii) the Thelon Basin, (iv) potentially the Pinguicula Group of the Wernecke Mountains, and (v) the upper Muskwa assemblage. Sedimentation during this sequence records a much broader marine incursion than during sub-sequence A2, reflected in a laterally extensive carbonate platform from the Wernecke Mountains, through the Hornby Bay, Elu, Thelon, and Athabasca basins.

9.7 Paleoproterozoic basins – Implications for paleogeography – Global Connections

Late Paleoproterozoic to early Mesoproterozoic intracratonic sedimentary basins within the north and west Australian cratons, such as the McArthur and Mount Isa basins, record a very similar evolution to those in Canada (Figure 31), and comparable large-scale sequence stratigraphy shows that Australia and Laurentia may have undergone very similar processes and tectonic events. Stable isotopes from the Hornby Bay Group and Wernecke Supergroup (this study) fall into the same isotopic range as an isotopic curve established across Australia that was interpreted as a primary, open ocean signal (Lindsay and Brasier, 2000). If these basins have all preserved primary $\delta^{13}C$ values, then our data supports the hypothesis that these basins were all part of a connected global ocean. Broad correlations have been suggested between several orogenic events along the southern margins of each continent (Laurentia and Australia),

and have been used in paleogeographic reconstructions, summarized in Betts et al (2008).

The sub-sequences of Laurentia (A1-A4) can be loosely correlated to several phases of sedimentary deposition on the west Australian craton. The first phase of deposition on the west Australian craton was in rift basins dominated by fluvial and eolian deposition. This initial phase of deposition lasted from ~1785-1750 Ma, which is approximately the same age as the earliest rift-related deposits of the Wharton Basin in Laurentia (Rainbird and Davis 2007). A second phase of extensional, rift-related, deposition occurred on the west Australian craton from ~1730-1670 Ma (Jackson et al, 2000),which may be loosely correlated to sub-sequence A1 (<1740 Ma) of Laurentia. Between 1670 and 1600 Ma, deposition on the West Australian craton was characterized by sag-phase sedimentation and the marine Isa Superbasin, characterized by a broad carbonate platform, developed (Scott et al, 1998; Krassay et al, 2000). A2 of Laurentia ended around 1600 Ma and is also characterized by sag-phase sedimentation and carbonate platform development. Although the lower age constraint for A2 of Laurentia is unknown, the similarity in types of sedimentation and upper age constraints suggest that A2 was contemporaneous with sag-phase deposition on the west Australian craton. Sedimentation and basin evolution patterns on both continents diverge after ~1590 Ma.

9.8 Paleoproterozoic basins – Implications for paleogeography – Assembly of Nuna (Columbia)

Linking deposition in Laurentia to deposition on the west Australian craton holds implications for paleogeographic reconstructions. There has been speculation about the

existence of the supercontinent Nuna (Columbia), for which several different configurations have been hypothesized (eg. Buchan et al., 2000; Betts et al., 2008; Hou et al, 2008; Zhao et al., 2004). In reconstructions by Betts et al (2008) the western margin of Laurentia is proximal to the North and West Australian cratons (Figure 31). This reconstruction places the intracratonic basins of Laurentia and Australia in proximity and can account for many of the similarities in sedimentation patterns and depositional histories of the two continents.

There is general agreement that Nuna accreted from ~1.9 to 1.8 Ga, but its break-up, after 1.5 Ga, is less well documented. In Betts et al. (2008), a maximum packing was achieved sometime after 1650 Ma, during the time when the Mazatzal orogen was active on the southern margin of Laurentia, and the Forward Orogeny was active on the western margin of Laurentia. Using new information on the age of the Forward Orogeny, which is interpreted to have ended around 1600 Ma it can be suggested that in Laurentia accretion ended around 1600 Ma.

Drawing from the paleogeographic reconstruction of Betts et al. (2008), the North Australian craton is proximal to the northwestern margin of Laurentia (Figure 31). In this configuration, the Hornby Bay Basin and its counterparts in Laurentia, are part of one large interior basin, which is linked, potentially by an oceanic seaway, to the Isa Superbasin on the North Australian craton during deposition of sub-sequence A2. A westward deepening trend is observed in Laurentia as shallow water sedimentary rocks of the Hornby Bay Group pass laterally into deep-water sedimentary rocks of the Wernecke Supergroup. This is mirrored in the North Australian craton as deeper water

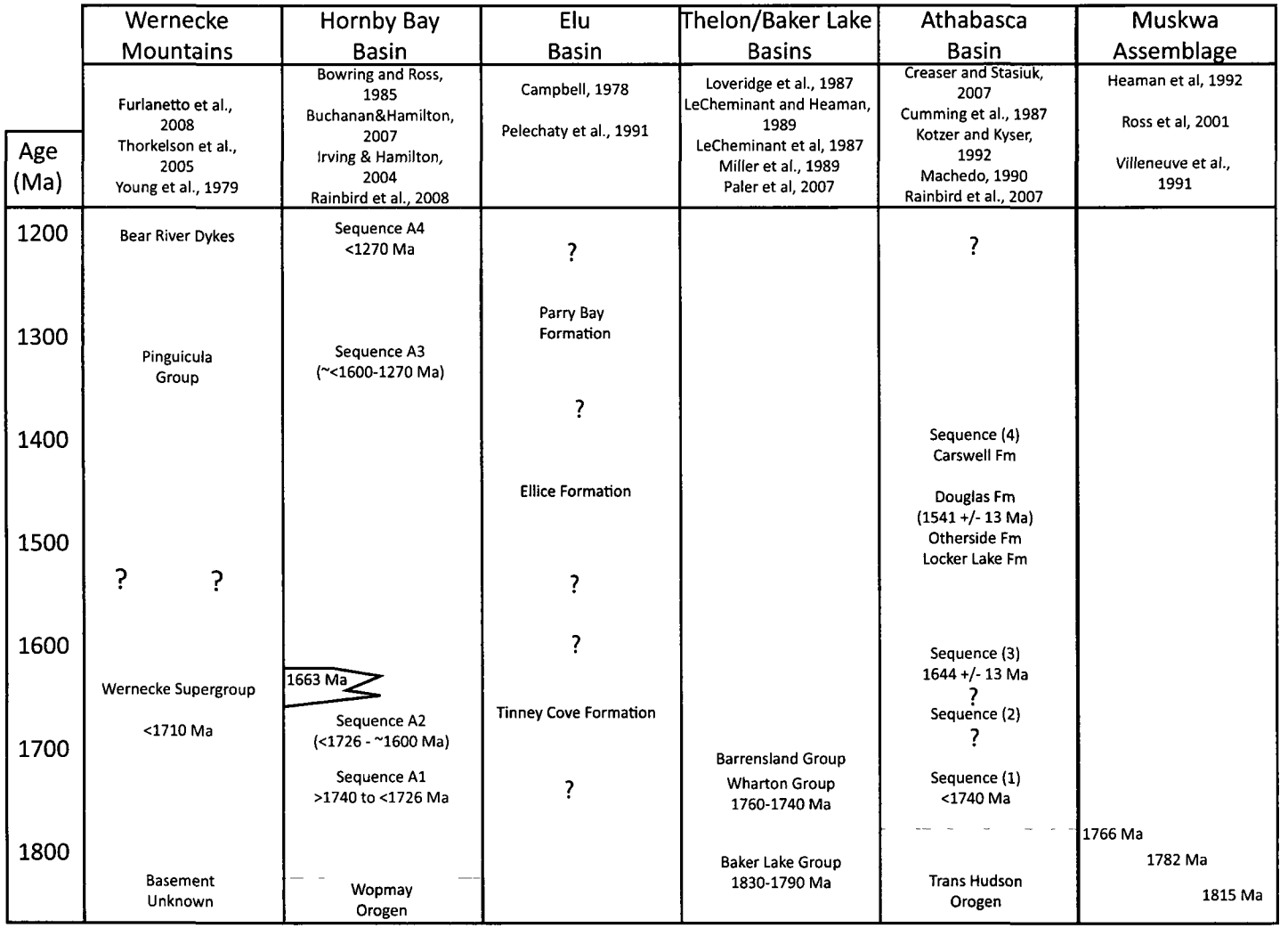

Figure 29: Correlation of Paleoproterozoic basins within Canada showing ages and similar lithologies.

Age (Ma)	Wernecke Mountains	Hornby Bay Basin	Thelon/Baker Lake Basins	Athabasca Basin	Mt. Isa Basin	North Australian Craton
	Furlanetto et al., 2008 Thorkelson et al., 2005 Young et al., 1979	Bowring and Ross, 1985 Buchanan&Hamilton, 2007 Irving & Hamilton, 2004 Rainbird et al., 2008	Loveridge et al., 1987 LeCheminant and Heaman, 1989 LeCheminant et al, 1987 Miller et al., 1989 Palmer et al, 2007	Creaser and Stasiuk, 2007 Cumming et al., 1987 Kotzer and Kyser, 1992 Machedo, 1990 Rainbird et al., 2007	Betts et al, 2008; and references therein	Betts et al, 2008; and references therein
1600	Wernecke Supergroup <1710 Ma	1663 Ma Sequence A2 (<1726 - ~1600 Ma)	Barrensland Group Wharton Group 1760-1740 Ma	Sequence (3) 1644 +/- 13 Ma ? Sequence (2) ?	Isa Superbasin	Upper Willyama Supergroup
1700		Sequence A1 >1740 to <1726 Ma		Sequence (1) >1740 Ma	Calvert Superbasin	Lower Willyama Supergroup
1800	Basement Unknown	Wopmay Orogen	Baker Lake Group 1830-1790 Ma	Trans Hudson Orogen	Leichhardt Superbasin	

Extrusive Igneous
Intrusive Igneous
Carbonate
Siltstone
Sandstone

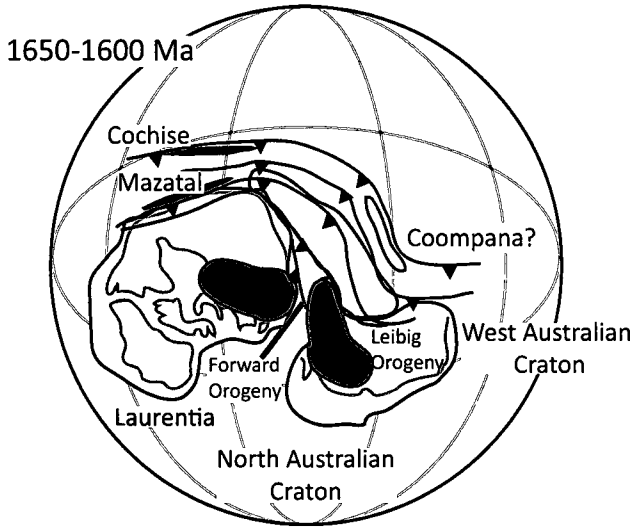

Figure 30: Correlation of North American Paleoproterozoic basins to corresponding Australian basins. Australian correlations modified from Betts et al. (2008). Paleogeographic reconstruction modified from Betts et al., 2008, illustrating extent of intractonic seas.

sedimentation was predominant on its eastern margin. Contrary to Betts et al (2008), who concluded that the interior basins in North Australia and Laurentia shared a similar tectonic evolution between ca. 1800 and 1670 Ma, we are now able to state with confidence, based on new ages from the Wernecke Supergroup and Hornby Bay Group, that this similar tectonic evolution lasted to 1600 Ma, marking the end of accretion in Columbia.

10. Conclusions

1. The Lady Nye Formation conformably to unconformably overlies fluvial and eolian sandstones of the early Hornby Bay Group (Fault River and Big Bear formations). It consists dominantly of arenites with minor conglomerates and siliciclastic mudstones and is up to 500 m thick in some sections. The vertical succession is generally cross-bedded fluvial sandstones at the base to shallow marine deltaic deposits at the top. The conformably overlying East River Formation ranges in thickness from 100 to 200 m and records gradual development of a storm-dominated carbonate platform during marine transgression. Mudstone to cross-bedded arenite of the Kaertok Formation gradationally overlies the East River Formation and ranges in thickness from 0 to >400 m. It records development of a syntectonic delta as indicated by paleocurrents and geometry being largely controlled by movement along the Teshierpi uplift (Cook and Maclean, 1995). The LeRoux Formation (Dismal Lakes

Group) unconformably to disconformably overlies the Kaertok Formation and other strata of the Hornby Bay Group. It ranges in thickness from 10 to >150 m and is dominantly composed of cross-bedded, white quartz arenite. Sedimentology of the LeRoux Formation indicates that it was deposited in fluvial environments at its base and shallow marine settings towards its gradational upper contact with the Fort Confidence Formation. The Fort Confidence Formation (>130 m in thick) is composed of interbedded wavy- and lenticular-bedded sandstone and carbonaceous mudstone, which are interpreted to represent extensive tidal flat deposits.

2. Sequences A2 records a full sequence of systems tracts which is reflected in the development of a LST and potential TST in the Lady Nye Formation, and an HST in the East River and Kaertok formations. The development of systems tracts within A2 were controlled by thermal subsidence and sea level rise during deposition of the Lady Nye Formation and during early deposition of the East River Formation. During last deposition of the East River Formation and the Kaertok Formation systems tract development was controlled by a regional tectonic event (Forward Orogeny).
3. The sequence A2-A3 boundary is reflected in outcrop at the angular unconformity between the flat lying LeRoux Formation and uplifted strata of the Hornby Bay Group. In the subsurface, the unconformity is present as an oxidized horizon of reworked material of the Lady Nye Formation east of the Teshierpi

uplift, as an angular unconformity within the vicinity of the Teshiperpi fault zone, and as a clay-rich regolith west of the Teshierpi fault zone.

4. Deposition during sequence A3 was controlled by eustasy and the development of a broad carbonate platform records the maximum sea-level during late deposition of the Dismal Lakes Group.
5. Sequence A2 of the Hornby Bay Group can been correlated to Wernecke Supergroup based on stratigraphy, age, U-Pb detrital zircon provenance, Sm-Nd and C isotopes, and equivalent depositional facies. Hornby Bay Group strata were deposited at or near the shoreline of a westward-facing ocean basin with the Wernecke Supergroup representing equivalent deep-water strata.
6. Sequence A2 of the Hornby Bay Group correlates in age across Laurentia (Hornby Bay, Wernecke, Elu, Muskwa, Athabasca basins) and into the North Australian craton (Isa Superbasin). Carbonates from A2 in North America correlate well with carbonates from equivalent aged rocks in Australia which may indicate they were all part of the same oceanic basin.
7. The tectonic evolution of sequence A2 in Laurentia is remarkably similar to that of the North Australian craton up to ~1600 Ma. This is the age of the Forward Orogeny and may mark the end of accretion of the supercontinent Columbia.

References

Aitken, J.D., and Cook, D.G., 1970, Geology, Colville Lake and Coppermine, District of Mackenzie, Geological Survey of Canada, Ottawa, ON, Canada.

Arthur, M.A.A., T.F.; Kaplan, I.R.; Veizer, J; Land, L.S., 1983, Stable isotopes in sedimentary geology, Society of Sedimentary Geology, Tulsa, OK, United States.

Ashley, G.M., 1990, Classification of large-scale subaqueous bedforms: a new look at an old problem; SEPM bedforms and bedding structures: Journal of Sedimentary Petrology, v. 60, p. 160-172.

Baragar, W.R.A., Ernst, R.E., Hulbert, L., and Peterson, T., 1996, Longitudinal petrochemical variation in the Mackenzie dyke swarm, northwestern Canadian Shield: Journal of Petrology, v. 37, p. 317-359.

Baragar, W.R.A.D., J.A., 1973, Coppermine and Dismal Lakes map-areas, Geological Survey of Canada, Ottawa, ON, Canada, 20 p.

Betts, P.G., Giles, D., and Schaefer, B.F., 2008, Comparing 1800-1600 Ma accretionary and basin processes in Australia and Laurentia; possible geographic connections in Columbia: Precambrian Research, v. 166, p. 81-92.

Blair, T.C., 1999a, Sedimentary processes and facies of the waterlaid Anvil Spring Canyon alluvial fan, Death Valley, California: Sedimentology, v. 46, p. 913-940.

Blair, T.C., 1999b, Sedimentology of the debris-flow-dominated Warm Spring Canyon alluvial fan, Death Valley, California: Sedimentology, v. 46, p. 941-965.

Bowring, S.A., and Grotzinger, J.P., 1992, Implications of new chronostratigraphy for tectonic evolution of Wopmay orogen, northwest Canadian Shield: American Journal of Science, v. 292, p. 1-20.

Bowring, S.A., and Podosek, F.A., 1989, Nd isotopic evidence from Wopmay Orogen for 2.0-2.4 Ga crust in western North America: Earth and Planetary Science Letters, v. 94, p. 217-230.

Bowring, S.A., and Ross, G.M., 1985, Geochronology of the Narakay Volcanic Complex - Implications for the Age of the Coppermine Homocline and Mackenzie Igneous Events: Canadian Journal of Earth Sciences, v. 22, p. 774-781.

Brand, U., and Veizer, J., 1980, Chemical diagenesis of a multicomponent carbonate system; 1, Trace elements: Journal of Sedimentary Petrology, v. 50, p. 1219-1236.

Buchan, K.L., Mertanen, S., Park, R.G., Pesonen, L.J., Elming, S.A., Abrahamsen, N., and Bylund, G., 2000, Comparing the drift of Laurentia and Baltica in the Proterozoic; the importance of key palaeomagnetic poles: Tectonophysics, v. 319, p. 167-198.

Cant, D.J.a.W., R.C., 1978, Fluvial processes and facies sequences in the sandy braided South Saskatchewan River, Canada: Sedimentology, v. 25, p. 625-646.

Cook, D.G., and MacLean, B.C., 1992, Proterozoic thick-skinned intracratonic deformation, Colville Hills region, Northwest Territories, Canada: Geology (Boulder), v. 20, p. 67-70.

Cook, D.G.a.M., B.C., 1995, The intracratonic Paleoproterozoic Forward orogeny, and implications for regional correlations, Northwest Territories, Canada: Canadian Journal of Earth Science, v. 32, p. 1991-2008.

Cousens, B.L., 2000, Geochemistry of the Archean Kam Group, Yellowknife greenstone belt, Slave Province, Canada: Journal of Geology, v. 108, p. 181-197.

Dalrymple, R.W., Knight, R.J., Zaitlin, B.A., and Middleton, G.V., 1990, Dynamics and facies model of a macrotidal sand-bar complex, Cobequid Bay-Salmon River estuary (Bay of Fundy): Sedimentology, v. 37, p. 577-612.

Delaney, G.D., 1981, The Mid-Proterozoic Wernecke Supergroup, Wernecke Mountains, Yukon Territory: Paper - Geological Survey of Canada, v. 81-10, p. 1-23.

Donaldson, J.A., 1969, Stratigraphy and sedimentology of the Hornby Bay Group, District of Mackenzie, parts of 86J, K, L, M, N, and O: Paper - Geological Survey of Canada, v. 69-1, p. 154-157.

Embry, A., 2009a, Practical sequence stratigraphy; IX, The units of sequence stratigraphy; Part 1, Material-based sequences: Reservoir, v. 36, p. 23-27, 29.

Embry, A., 2009b, Practical sequence stratigraphy; X, The units of sequence stratigraphy; Part 2, Time-based depositional sequences: Reservoir, v. 36, p. 21-24.

Embry, A., 2009c, Practical sequence stratigraphy; XI, The units of sequence stratigraphy; Part 3, Systems tracts: Reservoir, v. 36, p. 24-29.

Embry, A., 2009d, Practical sequence stratigraphy; XII, The units of sequence stratigraphy; Part 4, Parasequences: Reservoir, v. 36, p. 25-26, 28-29.

Embry, A., 2009e, Practical sequence stratigraphy; XIV, Correlation: Reservoir, v. 36, p. 14-19.

Embry, A., 2009f, Practical sequence stratigraphy; XV, Tectonics versus eustasy and applications to petroleum exploration: Reservoir, v. 36, p. 17-23.

Frank, T.D., Kah, L.C., and Lyons, T.W., 2003, Changes in organic matter production and accumulation as a mechanism for isotopic evolution in the Mesoproterozoic ocean: Geological Magazine, v. 140, p. 397-420.

Fraser, J.A., Donaldson, J.A., Fahrig, W.F., and Tremblay, L.P., 1970, Helikian basins and geosynclines of the northwestern Canadian shield: Paper - Geological Survey of Canada, v. 70-40, p. 213-238.

Furlanetto, F., Thorkelson, D.J., Davis, W., Gibson, H.D., Rainbird, R.H., and Marshall, D.D., 2008, Preliminary results of detrital zircon geochronology, Wernecke Supergroup, Yukon: Yukon Exploration and Geology 2008, p. 125-135.

Gabrielse, H., 1967, Tectonic evolution of the northern Canadian Cordillera: Canadian Journal of Earth Sciences = Journal Canadien des Sciences de la Terre, v. 4, p. 271-298.

Galloway, W.E., 1975, Process framework for describing the morphologic and stratigraphic evolution of deltaic depositional systems, *in* Broussard, M.L., ed., Deltas, models for exploration, Houston Geol. Soc., Houston, United States, p. 87-98.

Gostin, V.A.a.P., P.S., 1981, Shrinkage Cracks: desiccation or syneresis: Journal of Sedimentary Petrology, v. 51, p. 1147-1156.

Grotzinger, J.P., and McCormick, D.S., 1988, Flexure of the early Proterozoic lithosphere and the evolution of Kilohigok Basin (1.9 Ga), Northwest Canadian Shield, *in*

Kleinspehn, K.L., and Paola, C., eds., New perspectives in basin analysis, Springer-Verlag, New York, NY, United States, p. 405-430.

Hadlari, T., Rainbird, R.H., and Donaldson, J.A., 2006, Alluvial, eolian and lacustrine sedimentology of a Paleoproterozoic half-graben, Baker Lake basin, Nunavut, Canada: Sedimentary Geology, v. 190, p. 47-70.

Haines, P.W., 1988, Storm-dominated mixed carbonate/siliciclastic shelf sequence displaying cycles of hummocky cross-stratification, late Proterozoic Wonoka Formation, South Australia: Sedimentary Geology, v. 58, p. 237-254.

Hamilton, M.A., and Buchan, K.L., 2007, Precise 1.59 Ga age for Western Channel Diabase, Wopmay Orogen; implications for Laurentia APWP and reconstructions of Laurentia, Baltica and Gawler Craton: Abstracts with Programs - Geological Society of America, v. 39, p. 285-286.

Horodyski, R.J., Dudek, K.B., Ross, G.M., and Donaldson, J.A., 1985, Microfossils from the Early Proterozoic Hornby Bay Group, District of Mackenzie, Northwest-Territories, Canada: Canadian Journal of Earth Sciences, v. 22, p. 758-767.

Hou, G.T., Santosh, M., Qian, X.L., Lister, G.S., and Li, J.H., 2008, Configuration of the Late Paleoproterozoic supercontinent Columbia: Insights from radiating mafic dyke swarms: Gondwana Research, v. 14, p. 395-409.

Irving, E., Baker, J., Hamilton, M., and Wynne, P.J., 2004, Early Proterozoic geomagnetic field in western Laurentia; implications for paleolatitudes, local rotations and stratigraphy: Precambrian Research, v. 129, p. 251-270.

Jackson, M.J., Scott, D.L., and Rawlings, D.J., 2000, Stratigraphic framework for the Leichhardt and Calvert superbasins; review and correlations of the pre-1700 Ma successions between Mt Isa and McArthur River: Australian Journal of Earth Sciences, v. 47, p. 381-403.

Jefferson, C.W., Davis, W., Ramaekers, P., Rainbird, R., Bosman, S., Chamberlain, K., Peterson, T., and Bleeker, W., 2009, The search for uranium in the Great White North; similarities and differences amongst four Canadian Proterozoic settings: Atlantic Geology, v. 45, p. 88.

Kaufman, A.J., Hayes, J.M., Knoll, A.H., and Germs, G.J.B., 1991, Isotopic compositions of carbonates and organic carbon from upper Proterozoic successions in Namibia; stratigraphic variation and the effects of diagenesis and metamorphism: Precambrian Research, v. 49, p. 301-327.

Kerans, C., 1983, Sedimentology and Stratigraphy of the Dismal Lakes Group, Proterozoic, Northwest Territories Ottawa, Carleton University.

Kerans, C., Ross, G.M., Donaldson, J.A., Geldsetzer, H.J., 1981, Tectonism and deposition of the Helikian Hornby Bay and Dismal Lakes Groups, District of MacKenzie, *in* Campbell, F.H.A., ed., Proterozoic Basins of Canada, Geological Survey of Canada, p. 157-182.

Knoll, A.H., Kaufman, A.J., and Semikhatov, M.A., 1995, The carbon-isotopic composition of Proterozoic carbonates; Riphean successions from northwestern Siberia (Anabar Massif, Turukhansk Uplift): American Journal of Science, v. 295, p. 823-850.

Knoll, A.H., and Swett, K., 1990, Carbonate deposition during the late Proterozoic era; an example from Spitsbergen: American Journal of Science, v. 290-A, p. 104-132.

Krassay, A.A., Bradshaw, B.E., Domagala, J., and Jackson, M.J., 2000, Siliciclastic shoreline to growth-faulted, turbiditic sub-basin; the Proterozoic River Supersequence of the upper McNamara Group on the Lawn Hill Platform, northern Australia: Australian Journal of Earth Sciences, v. 47, p. 533-562.

Laughton, J.R., Thorkelson, D.J., Brideau, M.-A., Hunt, J.A., and Marshall, D.D., 2005, Early Proterozoic orogeny and exhumation of Wernecke Supergroup revealed by vent facies of Wernecke Breccia, Yukon, Canada: Canadian Journal of Earth Sciences = Revue Canadienne des Sciences de la Terre, v. 42, p. 1033-1044.

Lindsay, J.F.B., M.D. , 2000, A carbon isotope reference curve for ca. 1700-1575 Ma, McArthur and Mount Isa Basins, northern Australia: Precambrian Research, v. 99, p. 271-308.

MacLean, B.C., and Cook, D.G., 2004, Revisions to the Paleoproterozoic Sequence A, based on reflection seismic data across the western plains of the Northwest Territories, Canada: Precambrian Research, v. 129, p. 271-289.

Moorbath, S., Whitehouse, M.J., and Kamber, B.S., 1997, Extreme Nd-isotope heterogeneity in the early Archaean; fact or fiction? Case histories from northern Canada and West Greenland: Chemical Geology, v. 135, p. 213-231.

Nelson, B.K., and DePaolo, D.J., 1988, Comparison of isotopic and petrographic provenance indicators in sediments from Tertiary continental basins of New Mexico: Journal of Sedimentary Petrology, v. 58, p. 348-357.

Pratt, B.R., 1998, Syneresis cracks: subaqueous shrinkage in argillaceous sediments caused by earthquake-induced dewatering: Sedimentary Geology, v. 117, p. 1-1.

Quaresma, V.d.S., Bastos, A.C., Amose, C.L., 2007, Sedimentary processes over an intertidal flat: A field investigation at Hythe flats, Southampton Water (UK): Marine Geology, v. 241, p. 117-136.

Rainbird, R., Davis, W., Hahn, K., Furlanetto, F., and Thorkelson, D.J., 2009, Revised correlation of the late Paleoproterozoic sequences in Northwestern Canada and linkage of the Forward and Racklan Orogenies, *in* Jackson, V., and Palmer, E., eds., 37th Annual Yellowknife Geoscience Forum, Volume YKGSF Abstracts Volume 2009: Yellowknife.

Rainbird, R.H., McNicoll, V.J., Theriault, R.J., Heaman, L.M., Abbott, J.G., Long, D.G.F., and Thorkelson, D.J., 1997, Pan-continental river system draining Grenville Orogen recorded by U-Pb and Sm-Nd geochronology of Neoproterozoic quartzarenites and mudrocks, northwestern Canada: Journal of Geology, v. 105, p. 1-17.

Ross, G.M., 1983, Geology and Depositional History of the Hornby Bay Group, Proterozoic, Northwest Territories, Canada: Ottawa, Carleton University.

Ross, G. M. (1986). "Eruptive style and construction of shallow marine mafic tuff cones in the Narakay volcanic complex (Proterozoic, Hornby Bay group, Northwest

Territories, Canada)." Journal of Volcanology & Geothermal Research **27**(GEOBASE): 265-297

Ross, G.M.K., C., 1989, Geology, Hornby Bay and Dismal Lakes groups, Coppermine Homocline, District of Mackenzie, Northwest Territories 1663A, Geological Survey of Canada, "A" Series Map: Ottawa, Geological Survey of Canada, Ottawa, On, Canada.

Ross, G. M., M. E. Villeneuve, et al. (2001). "Isotopic provenance of the lower Muskwa assemblage (Mesoproterozoic, Rocky Mountains, British Columbia); new clues to correlation and source areas." Precambrian Research **111**(1-4): 57-77

Sarkar, S., Banerjee, S., Eriksson, P.G., and Catuneanu, O., 2005, Microbial mat control on siliciclastic Precambrian sequence stratigraphic architecture; examples from India: Sedimentary Geology, v. 176, p. 195-209.

Satkoski, A.M., Barr, S.M., and Samson, S.D., 2010, Provenance of late Neoproterozoic and Cambrian sediments in Avalonia; constraints from detrital zircon ages and Sm-Nd isotopic compositions in southern New Brunswick, Canada: Journal of Geology, v. 118, p. 187-200.

Scholle, P.A., Bebout, D.G., and Moore, C.H., 1983, Carbonate depositional environments, 708 p.

Scott, D.L., Bradshaw, B.E., and Tarlowski, C.Z., 1998, The tectonostratigraphic history of the Proterozoic northern Lawn Hill Platform, Australia; an integrated intracontinental basin analysis: Tectonophysics, v. 300, p. 329-358.

Theriault, R.J., and Ross, G.M., 1991, Nd Isotopic Evidence for Crustal Recycling in the Ca 2.0 Ga Subsurface of Western Canada: Canadian Journal of Earth Sciences, v. 28, p. 1140-1147.

Thorkelson, D.J., Abbott, J.G., Mortensen, J.K., Creaser, R.A., Villeneuve, M.E., McNicoll, V.J., and Layer, P.W., 2005, Early and Middle Proterozoic evolution of Yukon, Canada: Canadian Journal of Earth Sciences = Journal Canadien des Sciences de la Terre, v. 42, p. 1045-1071.

Veizer, J., 1983, Geologic evolution of the Archean-early Proterozoic Earth, *in* Schopf, J.W., ed., Earth's earliest biosphere; its origin and evolution, Princeton Univ. Press, Princeton, NJ, United States, p. 240-259.

Walker, R.G., and Plint, A.G., 1992, Wave- and storm-dominated shallow marine systems, *in* Walker, R.G., and James, N.P., eds., Facies models; response to sea level change, Geological Association of Canada, St. Johns, NL, Canada, p. 219-238.

Yamashita, K., Creaser, R.A., and Heaman, L.M., 1998, Geochemical and isotopic constraints for tectonic evolution of the Slave Province: Lithoprobe Report, p. 11-14.

Young, G.M., Jefferson, C.W., Delaney, G.D., and Yeo, G.M., 1979, Middle and late Proterozoic evolution of the northern Canadian Cordillera and Shield: Geology (Boulder), v. 7, p. 125-128.

Zhao, G., Sun, M., Wilde, S.A., and Li, S., 2004, A Paleo-Mesoproterozoic supercontinent; assembly, growth and breakup: Earth-Science Reviews, v. 67, p. 91-123.

Appendix 1

		Sum of conc. (%)	L.O.I. (%)	CONC. + LOI (%)	SiO2 Si4 (%)	Al2O3 Al3 (%)	CaO Ca4 (%)	K2O K2 (%)	MgO Mg3 (%)
Formation	Sample								
Fort Confidence	K106	95.17	5.22	100.39	57.56	24.19	0.25	8.379	2.04
Fort Confidence	K108	96.287	4.2	100.49	64.40	19.89	0.25	7.325	1.81
Fort Confidence	K117	95.84	5.06	100.90	60.10	25.31	0.15	7.192	0.43
Fort Confidence	K110	95.263	5.29	100.55	58.63	23.09	0.22	7.786	2.08
Fort Confidence	K114	94.993	5.53	100.52	56.65	24.83	0.27	8.423	2.13
Fort Confidence	K116	95.288	5.19	100.48	60.95	22.24	0.18	7.632	1.77
Fort Confidence	K112	95.496	5.16	100.66	58.25	23.70	0.19	7.954	1.92
Kaertok	K120	96.551	4.38	100.93	61.80	17.62	0.14	6.430	2.49
Kaertok	K121	96.567	4.63	101.20	57.55	19.51	0.18	7.302	2.06
Kaertok	K119	97.788	2.73	100.52	73.79	14.07	0.10	4.565	0.72
East River	K105	95.36	5.8	101.16	53.18	20.35	0.22	7.167	2.34
East River	K101	96.258	4.72	100.98	61.33	18.71	0.32	7.457	2.12
East River	K104	91.411	8.22	99.63	49.31	18.57	2.26	7.246	4.14
East River	K102	94.951	5.61	100.56	50.38	19.76	0.25	8.760	3.96
East River	K100	97.509	7.41	104.92	55.58	17.56	2.78	7.682	3.67
East River	K103	94.604	6.01	100.61	53.00	20.45	0.55	8.320	3.45

		MnO Mn3 (%)	Na2O Na3 (%)	P2O5 P2 (%)	Fe2O3(T) Fe6 (%)	Zn Zn4 (ppm)	TiO2 Ti4 (%)	Ba Ba1 (ppm)	Co Co1 (ppm)
Formation	Sample								
Fort Confidence	K106	0.008	0.16	0.083	1.456	13	0.824	655	29
Fort Confidence	K108	0.009	0.10	0.063	1.502	10	0.780	547	<10
Fort Confidence	K117	0.002	0.13	0.061	1.349	<10	0.967	127	30
Fort Confidence	K110	0.009	0.16	0.094	2.167	17	0.841	470	10
Fort Confidence	K114	0.007	0.08	0.100	1.498	12	0.855	372	12
Fort Confidence	K116	0.006	0.13	0.051	1.394	13	0.784	333	11
Fort Confidence	K112	0.006	0.29	0.066	1.986	13	0.945	402	<10
Kaertok	K120	0.021	0.08	0.041	7.063	23	0.730	349	10
Kaertok	K121	0.024	0.13	0.069	8.807	62	0.790	411	10
Kaertok	K119	0.003	0.23	0.038	3.616	12	0.536	162	<10
East River	K105	0.022	0.07	0.078	10.981	96	0.799	200	14
East River	K101	0.006	0.07	0.123	5.579	26	0.414	310	<10
East River	K104	0.03	0.07	0.237	8.515	57	0.902	169	13
East River	K102	0.008	0.05	0.018	11.313	39	0.338	252	12
East River	K100	0.113	0.06	0.165	9.250	61	0.540	158	11
East River	K103	0.010	0.09	0.040	8.058	32	0.503	339	<10

		Ga Ga1 (ppm)	La La1 (ppm)	Ni Ni3 (ppm)	Pb Pb1 (ppm)	Rb Rb1 (ppm)	Sr Sr1 (ppm)	Th Th1 (ppm)	U U1 (ppm)
Formation	Sample								
Fort Confidence	K106	27	123	11	18	240	70	49	19
Fort Confidence	K108	22	103	<10	11	205	66	35	11
Fort Confidence	K117	28	44	<10	33	147	209	32	23
Fort Confidence	K110	27	127	<10	11	245	112	39	12
Fort Confidence	K114	32	70	<10	10	228	58	35	12
Fort Confidence	K116	28	98	<10	15	237	58	38	14
Fort Confidence	K112	29	123	<10	11	244	82	47	16
Kaertok	K120	20	50	29	<10	241	26	30	10
Kaertok	K121	21	35	<10	18	278	19	34	17
Kaertok	K119	13	49	<10	<10	114	20	36	13
East River	K105	33	88	21	18	259	137	36	22
East River	K101	18	<10	<10	19	217	26	40	16
East River	K104	21	85	11	17	274	59	21	10
East River	K102	20	22	<10	30	298	12	38	18
East River	K100	17	29	<10	20	203	27	41	15
East River	K103	20	36	<10	18	231	14	39	17

		V V1 (ppm)	Y Y1 (ppm)	Zr Zr2 (ppm)	Nb Nb3 (ppm)	Cr Cr1 (ppm)	Ce Ce1 (ppm)	Nd Nd1 (ppm)
Formation	Sample							
Fort Confidence	K106	85	62	396	24	61	216	72
Fort Confidence	K108	82	28	276	17	64	172	56
Fort Confidence	K117	68	45	430	20	38	129	55
Fort Confidence	K110	93	48	242	19	83	243	105
Fort Confidence	K114	115	24	226	19	114	150	48
Fort Confidence	K116	96	33	213	19	80	137	51
Fort Confidence	K112	99	42	257	24	83	207	66
Kaertok	K120	86	24	197	18	84	113	40
Kaertok	K121	96	25	247	18	90	92	38
Kaertok	K119	28	<10	570	10	20	69	19
East River	K105	75	60	267	17	65	152	43
East River	K101	38	36	254	21	33	47	22
East River	K104	113	21	145	12	97	147	52
East River	K102	17	32	284	26	<10	<10	<10
East River	K100	37	50	361	20	18	83	26
East River	K103	41	53	407	20	<10	25	14